

# Climate4you update September 2022



1

## Summary of observations until September 2022:

1: Observed average global air temperature change last 40 years is about  $+0.17^{\circ}\text{C}$  per decade. If unchanged, additional average global air temperature increase by year 2100 will be about  $+1.3^{\circ}\text{C}$ . However, part of the apparent temperature increase reported is due to administrative changes, and the real future increase may therefore be smaller.

2: Tide gauges along coasts indicate a typical global sea level increase of about 1-2 mm/yr. Coastal sea level change rate last 100 year has essentially been stable, without recent acceleration. If unchanged, global sea level at coasts will typically increase 8-16 cm by year 2100, although many locations in regions affected by glaciation 20,000 years ago, will experience a relative sea level drop.

3: Since 2004 the global oceans above 1900 m depth on average have warmed about  $0.07^{\circ}\text{C}$ . The maximum warming (about  $0.2^{\circ}\text{C}$ , 0-100 m depth) mainly affects oceans near Equator, where the incoming solar radiation is at maximum.

4: Changes in atmospheric  $\text{CO}_2$  follow changes in global air temperature. Changes in global air temperature follow changes in ocean surface temperature.

5: There was no perceptible effect on atmospheric  $\text{CO}_2$  due to the 2020-21 COVID-related drop in GHG emissions. Thus, natural sinks and sources for atmospheric  $\text{CO}_2$  far outweigh human contributions.

## Contents:

Page 3:	September 2022 global surface air temperature overview
Page 4:	September 2022 global surface air temperature overview versus September last 10 years
Page 5:	September 2022 global surface air temperature compared to September 2021
Page 6:	Temperature quality class 1: Lower troposphere temperature from satellites
Page 7:	Temperature quality class 2: HadCRUT global surface air temperature
Page 8:	Temperature quality class 3: GISS and NCDC global surface air temperature
Page 11:	Comparing global surface air temperature and satellite-based temperatures
Page 12:	Global air temperature linear trends
Page 13:	Global temperatures: All in one, Quality Class 1, 2 and 3
Page 15:	Global sea surface temperature
Page 18:	Ocean temperature in uppermost 100 m
Page 20:	Pacific Decadal Oscillation (PDO)
Page 21:	North Atlantic heat content uppermost 700 m
Page 22:	North Atlantic temperatures 0-800 m depth along 59N, 30-0W
Page 23:	Global ocean temperature 0-1900 m depth summary
Page 24:	Global ocean net temperature change since 2004 at different depths
Page 25:	La Niña and El Niño episodes, Oceanic Niño Index
Page 26:	Zonal lower troposphere temperatures from satellites
Page 27:	Arctic and Antarctic lower troposphere temperatures from satellites
Page 28:	Arctic and Antarctic surface air temperatures
Page 31:	Temperature over land versus over oceans
Page 32:	Troposphere and stratosphere temperatures from satellites
Page 33:	Sea ice; Arctic and Antarctic
Page 37:	Sea level in general
Page 38:	Global sea level from satellite altimetry
Page 39:	Global sea level from tide gauges
Page 40:	Snow cover; Northern Hemisphere weekly and seasonal
Page 42:	Greenland Ice Sheet net surface mass balance
Page 43:	Atmospheric specific humidity
Page 44:	Atmospheric CO <sub>2</sub>
Page 45:	Relation between annual change of atm. CO <sub>2</sub> and La Niña and El Niño episodes
Page 46:	Phase relation between atmospheric CO <sub>2</sub> and global temperature
Page 47:	Global air temperature and atmospheric CO <sub>2</sub>
Page 51:	Latest 20-year QC1 global monthly air temperature change
Page 52:	Sunspot activity and QC1 average satellite global air temperature
Page 53:	Sunspot activity and average neutron counts
Page 54:	Sunspot activity, ONI, and change rates of atmospheric CO <sub>2</sub> and specific humidity
Page 55:	Monthly lower troposphere temperature and global cloud cover
Page 56:	Climate and history: <i>Bridge across the River Danube at the Iron Gate 101-106 AD.</i>

## September 2022 global surface air temperature overview

General: This newsletter contains graphs and diagrams showing a selection of key meteorological variables, if possible updated to the most recent past month. All temperatures are given in degrees Celsius. In the maps on page 4, showing the geographical pattern of surface air temperature anomalies, the last previous 10 years are used as reference period.

The rationale for comparing with this recent period instead of various 'normal' periods defined for parts of the past century, is that such reference periods often will be affected by past cold periods, like, e.g., 1945-1980. Most modern comparisons with such reference periods will inevitably appear as warm, and it will be difficult to decide if modern temperatures are increasing or decreasing. Comparing instead with the last previous 10 years overcomes this problem and clearer displays the modern dynamics of ongoing change. This decadal approach also corresponds well to the typical memory horizon for many people and is also adopted as reference period by other institutions, e.g., the Danish Meteorological Institute (DMI).

In addition, most temperature databases display temporal instability for past data (see, e.g., p. 9). Any comparison with such reference periods will therefore be influenced by ongoing monthly changes apparently of mainly administrative origin. A fluctuating value is clearly not suited as reference value. Simply comparing with the last previous 10 years is more useful as reference for modern changes. Please see also additional reflections on page 48-49. The different air temperature records have been divided into three quality classes, QC1, QC2 and QC3, respectively, as described on page 9.

In many diagrams shown in this newsletter the thin line represents the monthly global average value, and the thick line indicate a simple running average, in most cases a simple moving 37-month average, nearly corresponding to a three-year average. The 37-month average is calculated from values covering a range from 18 months before to 18 months after, with equal weight given to all individual months.

The year 1979 has been chosen as starting point in many diagrams, as this approximately corresponds

to both the beginning of satellite observations and the onset of the late 20<sup>th</sup> century warming period. However, several of the data series have a much longer record length, which may be inspected in greater detail on [www.climate4you.com](http://www.climate4you.com).

### September 2022 surface air temperature

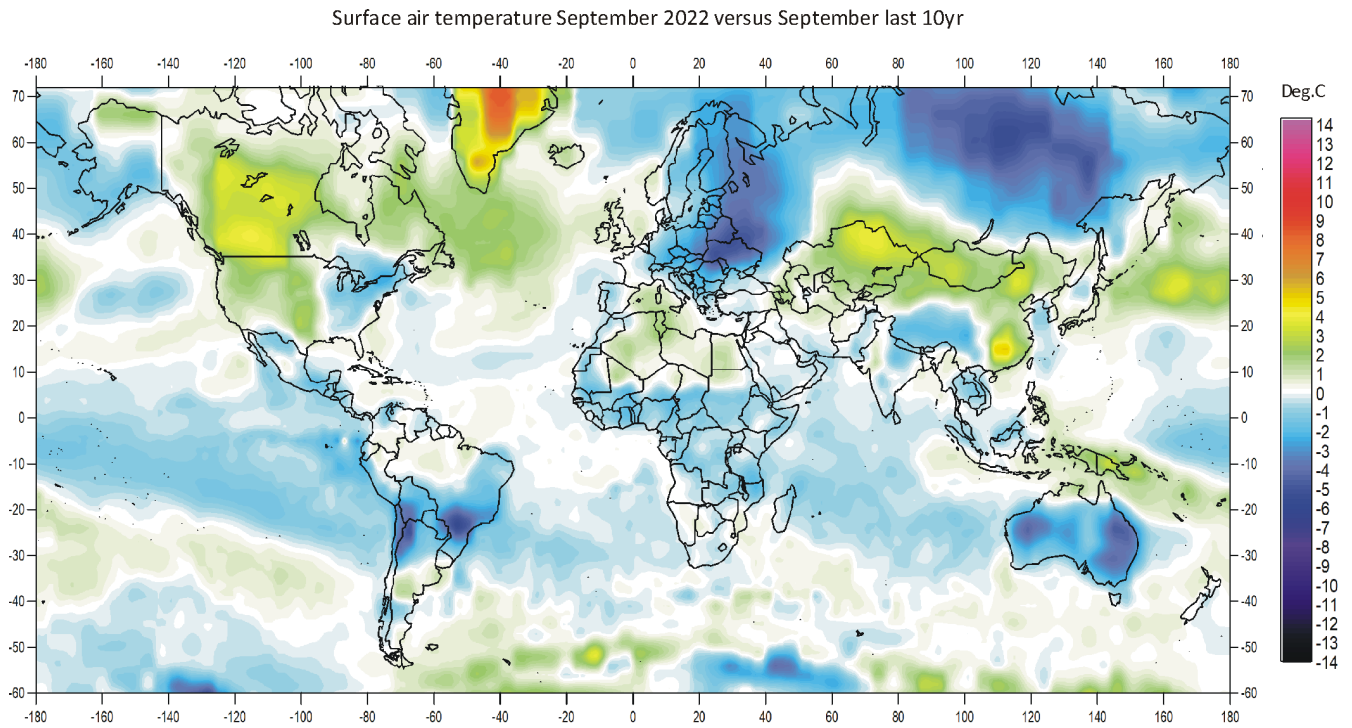
General: For September 2022, the GISS data portal (<https://data.giss.nasa.gov/gistemp/>) provided 16200 AIRS interpolated surface air data points, based on satellite observations, and visualised here on pages 4-5. According to the GISS and NCDC surface air temperature records, the September 2022 global temperature anomaly was a little lower than in the previous month. According to the RSS lower troposphere satellite record the September 2022 temperature anomaly almost unchanged compared to the previous month. The UAH satellite record has not yet been updated beyond August 2022. According to AIRS the September 2022 average surface air temperature was a little lower than the average for the last 10 years.

The Northern Hemisphere surface temperature anomaly pattern (p.4) was characterised by regional contrasts, mainly controlled by the dominant jet stream configuration. Parts of Canada, and especially Greenland was relatively warm, compared to the average for the last 10 years. In contrast, much of Europe, Russia, Siberia, and southern Alaska were relatively cold. Ocean wise, the North Atlantic was relatively warm between 30 and 50°N, while the remaining parts were below or near the 10-yr average. Parts of northern Pacific was relatively warm. Over most of the Arctic Ocean surface air temperatures were near or below the 10-yr average.

Near the Equator temperatures were mostly near or below the 10-year average. Especially a region between 10°N and 30°S in the Pacific Ocean was relatively cold. Below or near average temperatures characterised most land areas.

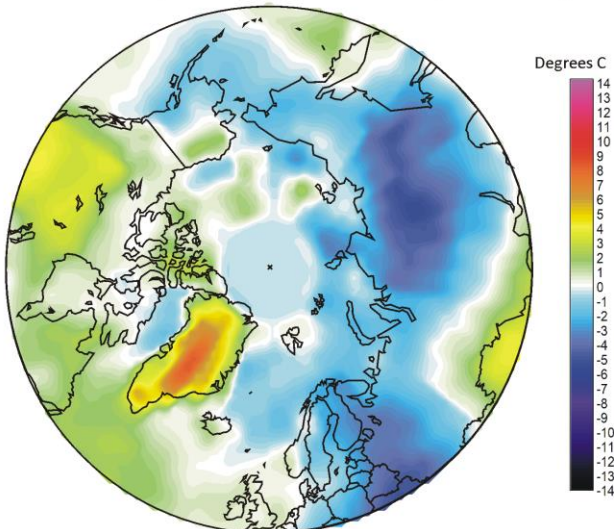
Southern Hemisphere temperatures were generally near or below the average for the previous 10 years. Most land areas had below average temperatures. Antarctic was characterised by a mixture of relatively high and low temperatures.

## September 2022 global surface air temperature overview versus average September last 10 years

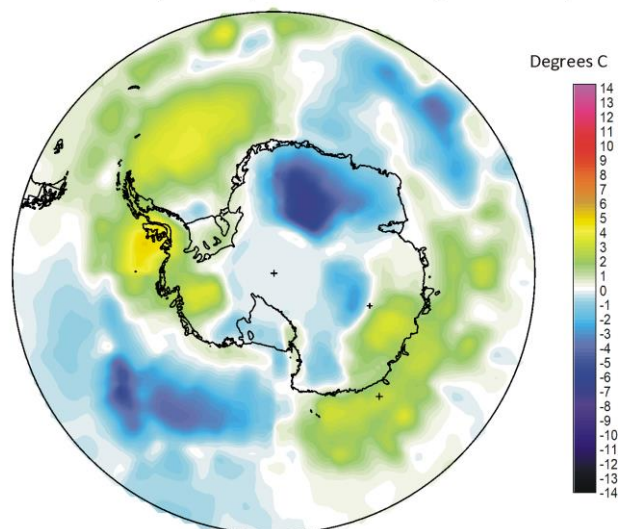


4

Surface air temperature September 2022 versus September last 10 yr

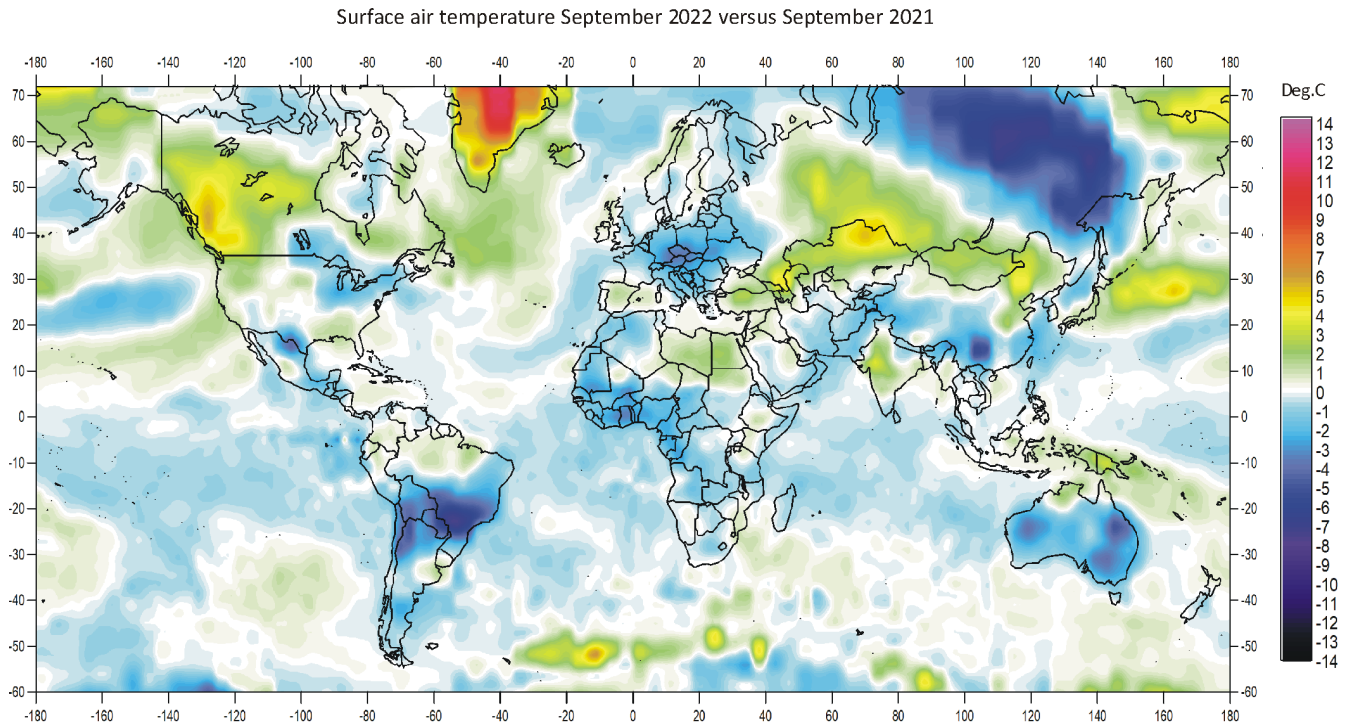


Surface air temperature September 2022 versus September last 10 yr



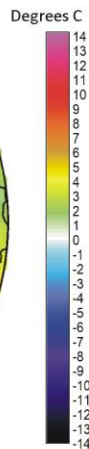
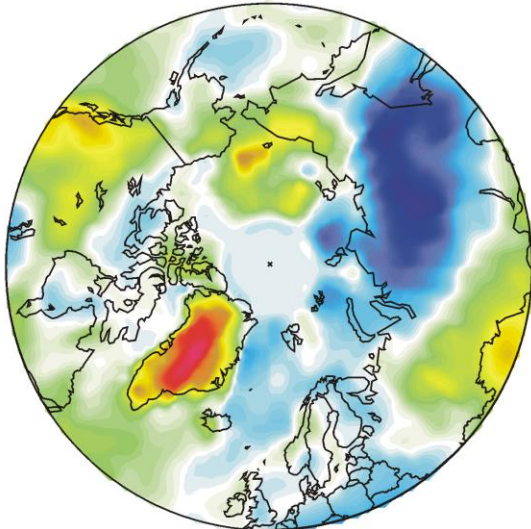
September 2022 surface air temperature compared to the average of September over the last 10 years. Green-yellow-red colours indicate areas with higher temperature than the 10-year average, while blue colours indicate lower than average temperatures. Data source: Remote Sensed Surface Temperature Anomaly, AIRS/Aqua L3 Monthly Standard Physical Retrieval 1-degree x 1-degree V007 (<https://airs.jpl.nasa.gov/>), obtained from the GISS data portal ([https://data.giss.nasa.gov/gistemp/maps/index\\_v4.html](https://data.giss.nasa.gov/gistemp/maps/index_v4.html)).

## September 2022 global surface air temperature compared to September 2021

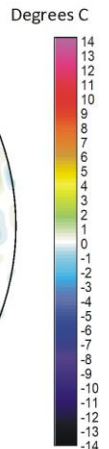
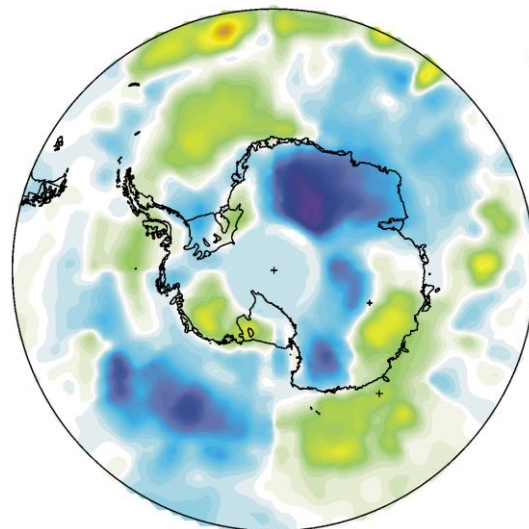


5

Surface air temperature September 2022 versus September 2021

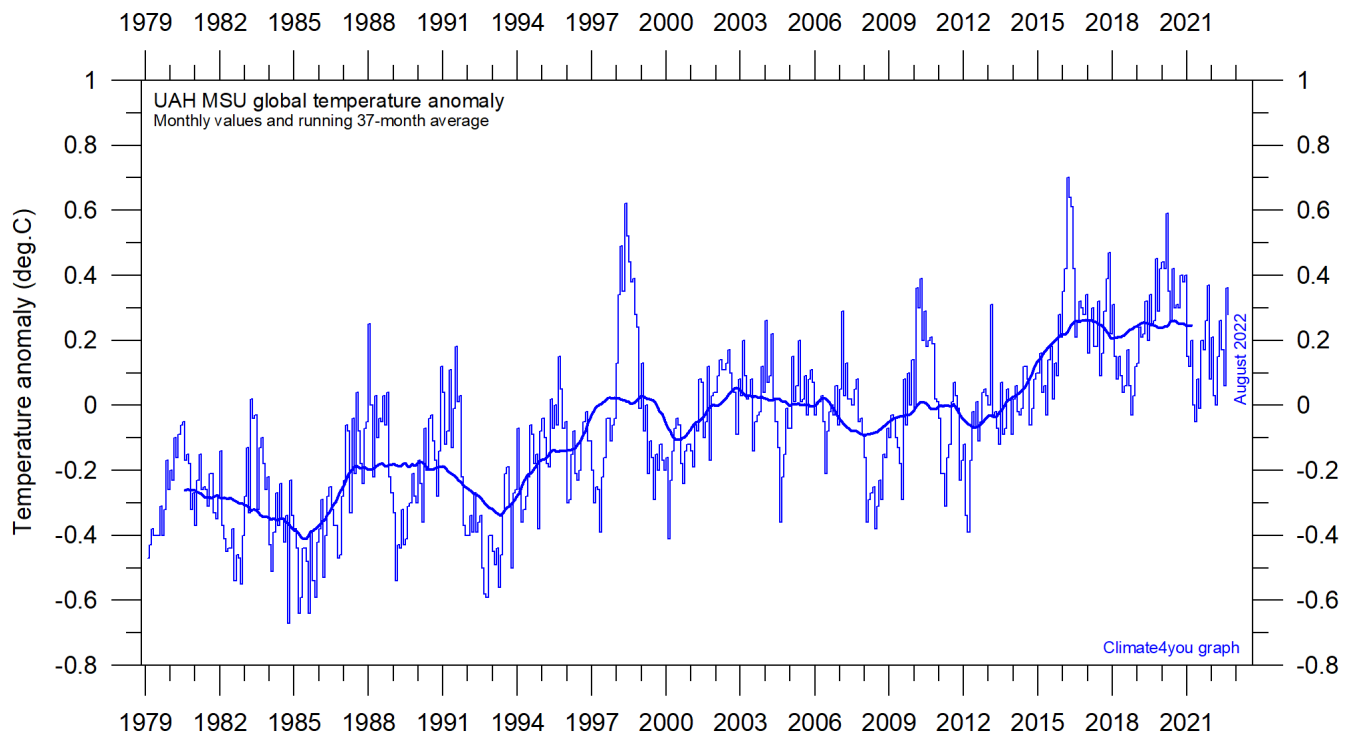


Surface air temperature September 2022 versus September 2021



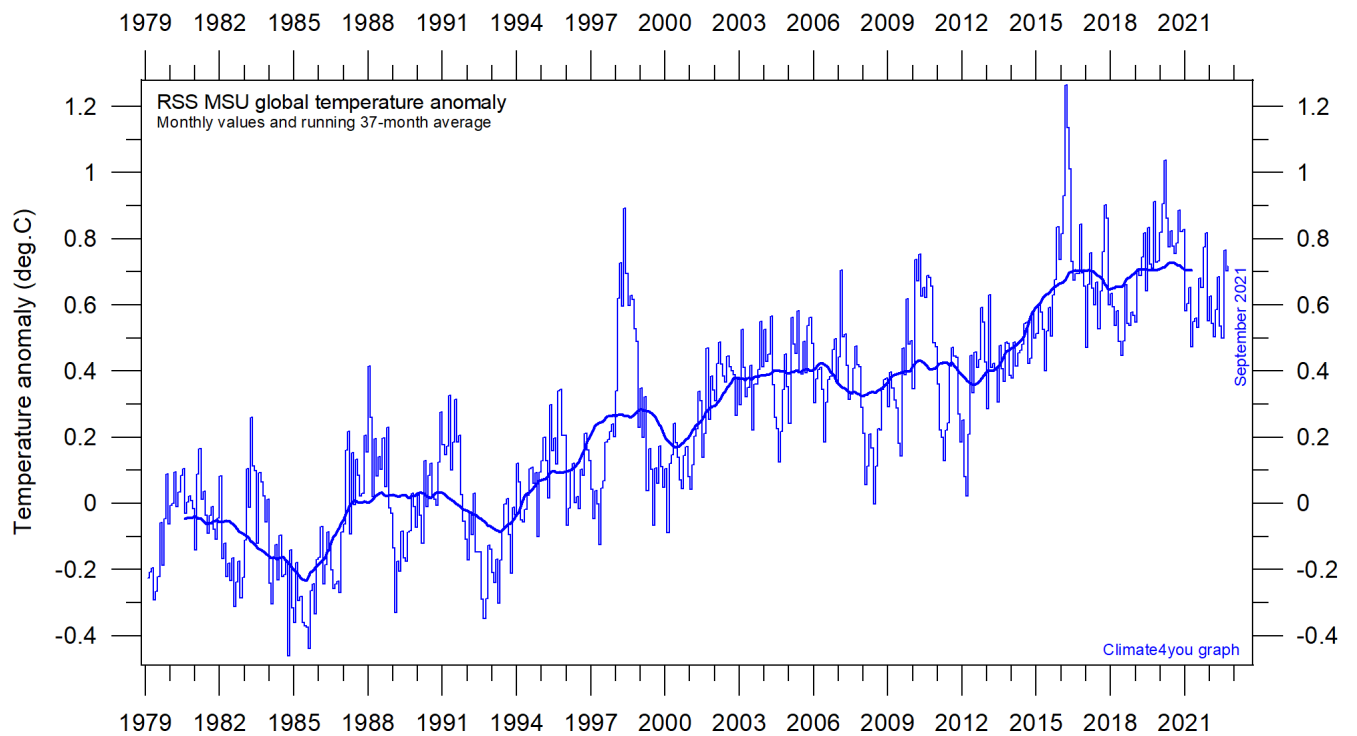
September 2022 surface air temperature compared to September 2021. Green-yellow-red colours indicate regions where the present month was warmer than last year, while blue colours indicate regions where the present month was cooler than last year. Variations in monthly temperature from one year to the next has no tangible climatic importance but may nevertheless be interesting to study. Data source: Remote Sensed Surface Temperature Anomaly, AIRS/Aqua L3 Monthly Standard Physical Retrieval 1-degree x 1-degree V007 (<https://airs.jpl.nasa.gov/>), obtained from the GISS data portal ([https://data.giss.nasa.gov/gistemp/maps/index\\_v4.html](https://data.giss.nasa.gov/gistemp/maps/index_v4.html)).

**Temperature quality class 1: Lower troposphere temperature from satellites, updated to September 2022** (see page 9 for definition of classes)



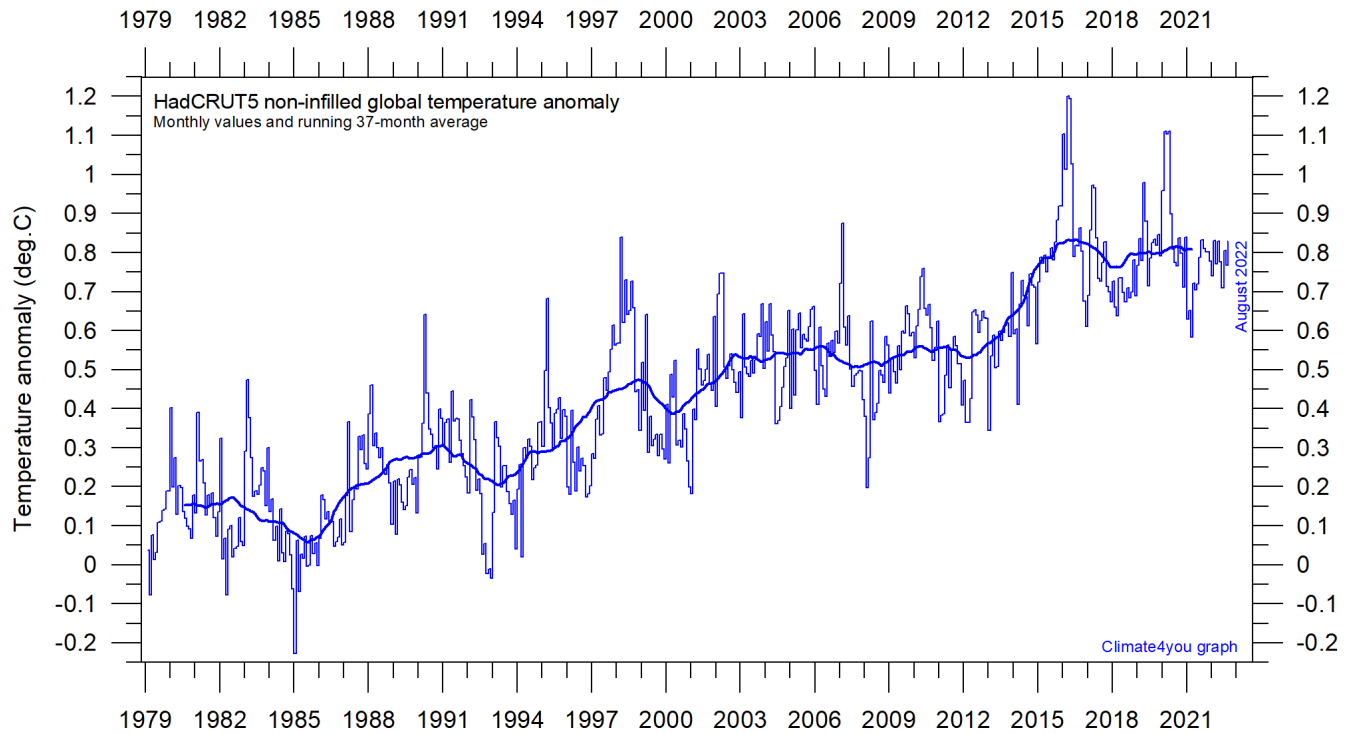
Global monthly average lower troposphere temperature (thin line) since 1979 according to [University of Alabama](#) at Huntsville, USA. The thick line is the simple running 37-month average. Reference period 1991-2020.

6



Global monthly average lower troposphere temperature (thin line) since 1979 according to according to [Remote Sensing Systems](#) (RSS), USA. The thick line is the simple running 37-month average.

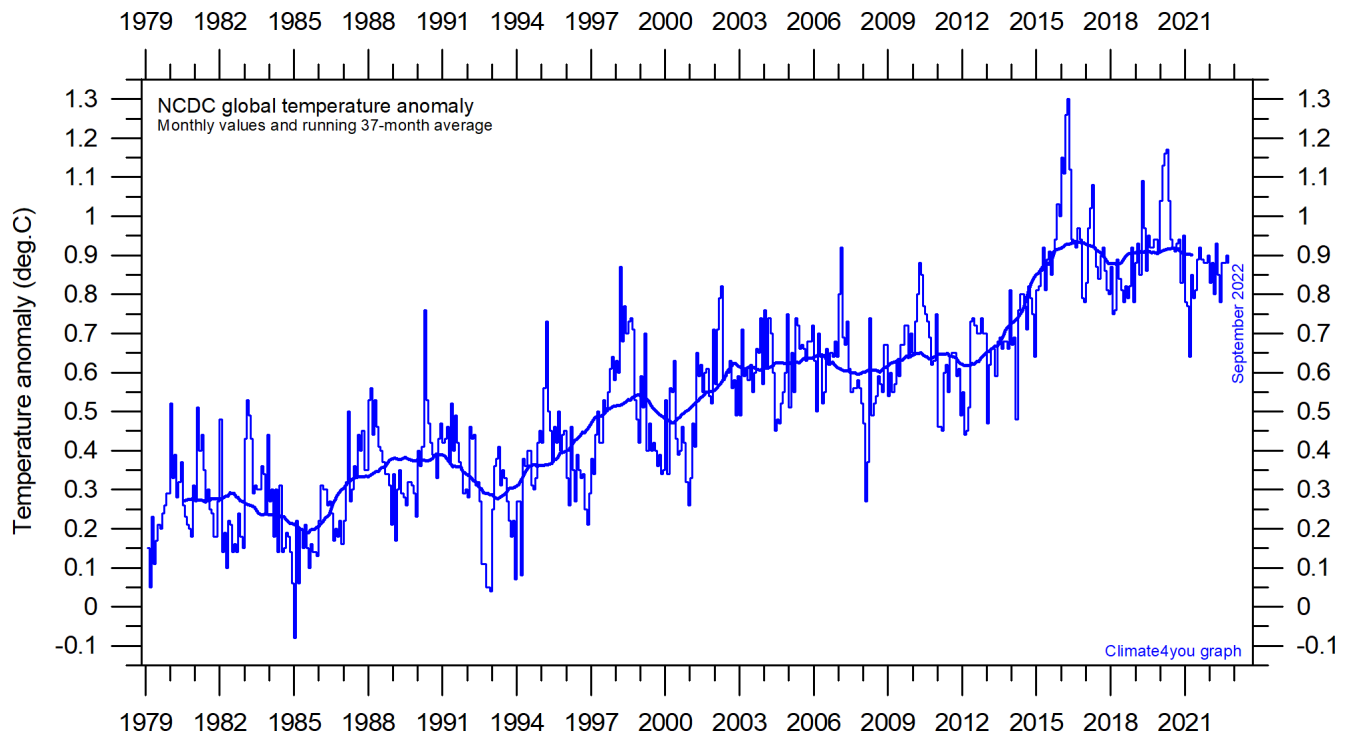
## Temperature quality class 2: HadCRUT global surface air temperature, updated to August 2022



7

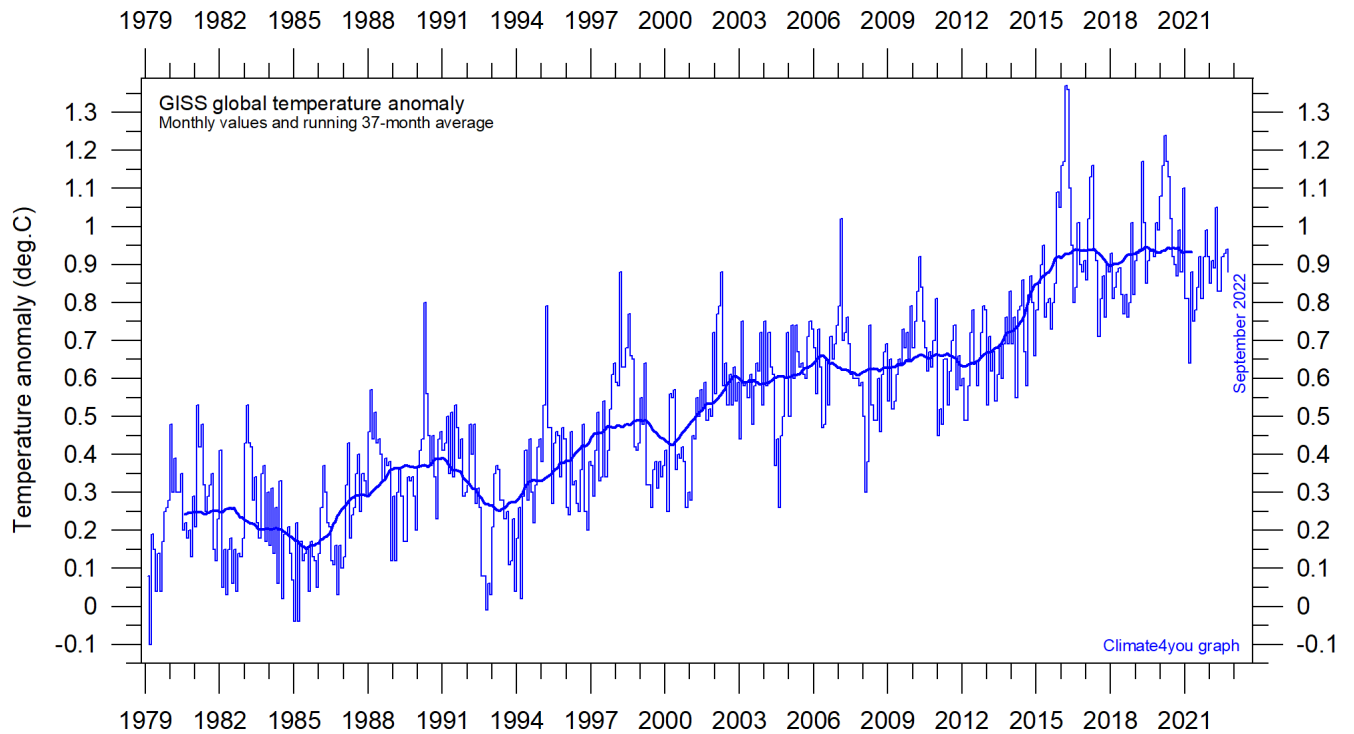
Global monthly average surface air temperature (thin line) since 1979 according to the Hadley Centre for Climate Prediction and Research and the University of East Anglia's [Climatic Research Unit \(CRU\)](#), UK. The thick line is the simple running 37-month average. Please note that HadCRUT5 is not yet updated beyond May 2022.

### Temperature quality class 3: GISS and NCDC global surface air temperature, updated to September 2022



Global monthly average surface air temperature since 1979 according to according to the [National Climatic Data Center \(NCDC\)](#), USA. The thick line is the simple running 37-month average.

8



Global monthly average surface air temperature (thin line) since 1979 according to according to the [Goddard Institute for Space Studies \(GISS\)](#), at Columbia University, New York City, USA, using ERSST\_v4 ocean surface temperatures. The thick line is the simple running 37-month average.



### A note on data record stability and -quality:

The temperature diagrams shown above all have 1979 as starting year. This roughly marks the beginning of the recent episode of global warming, after termination of the previous episode of global cooling from about 1940. In addition, the year 1979 also represents the starting date for the satellite-based global temperature estimates (UAH and RSS). For the three surface air temperature records (HadCRUT, NCDC and GISS), they begin much earlier (in 1850 and 1880, respectively), as can be inspected on [www.climate4you.com](http://www.climate4you.com).

For all three surface air temperature records, but especially NCDC and GISS, administrative changes to anomaly values are quite often introduced, even affecting observations many years back in time. Some changes from the recent past may be due to the delayed addition of new station data or change of station location, while others probably have their origin in changes of the technique implemented to calculate average values from the raw data. It is clearly impossible to evaluate the validity of such administrative changes for the outside user of these records; it is only possible to note that such changes quite often are introduced (see example diagram next page).

In addition, the three surface records represent a blend of sea surface data collected by moving ships or by other means, plus data from land stations of partly unknown quality and unknown degree of representativeness for their region. Many of the land stations also has been moved geographically during their period of operation, instrumentation have been changed, and they are influenced by changes in their near surroundings (vegetation, buildings, etc.). The surface network is inherently heterogeneous (dense over continents but sparse over oceans) and probably contaminated by urbanization surrounding many measurement sites.

The satellite temperature records also have their problems, but these are generally of a more technical nature and probably therefore better correctable. In addition, the temperature sampling by satellites is more regular and complete on a

global basis than that represented by the surface records. It is also important that the sensors on satellites measure temperature directly by microwave radiance (thereby unobstructed by clouds), while most modern surface temperature measurements are indirect, using electronic resistance.

Everybody interested in climate science should gratefully acknowledge the big efforts put into maintaining the different temperature databases referred to in the present newsletter. At the same time, however, it is also important to realise that all temperature records cannot be of equal scientific quality. The simple fact that they to some degree differ shows that they cannot all be correct.

On this background, and for practical reasons, Climate4you therefore operates with three quality classes (1-3) for global temperature records, with 1 representing the highest quality level:

Quality class 1: The satellite records (UAH and RSS).

Quality class 2: The HadCRUT surface record.

Quality class 3: The NCDC and GISS surface records.

The main reason for discriminating between the three surface records is the following:

While both NCDC and GISS often experience quite large administrative changes (see example on p.10), and therefore essentially must be considered as unstable records, the changes introduced to HadCRUT are fewer and smaller. For obvious reasons, as the past does not change, any record undergoing continuing changes cannot describe the past correctly all the time. Frequent and large corrections in a database unavoidably signal a fundamental uncertainty about what is likely to represent the correct values.

You can find more on the issue of lack of temporal stability on [www.climate4you.com](http://www.climate4you.com) (go to: *Global Temperature*, and then proceed to *Temporal Stability*).

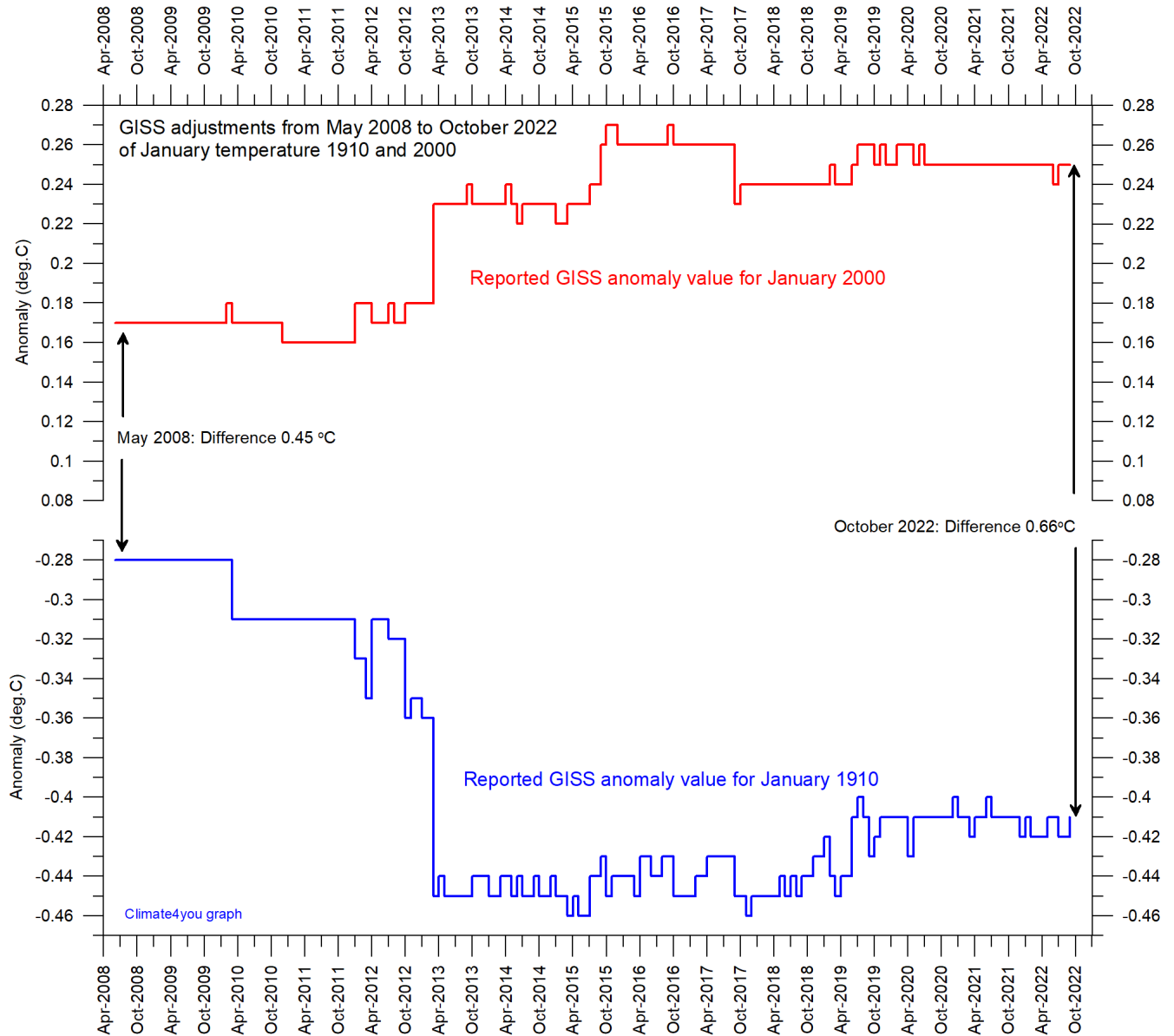
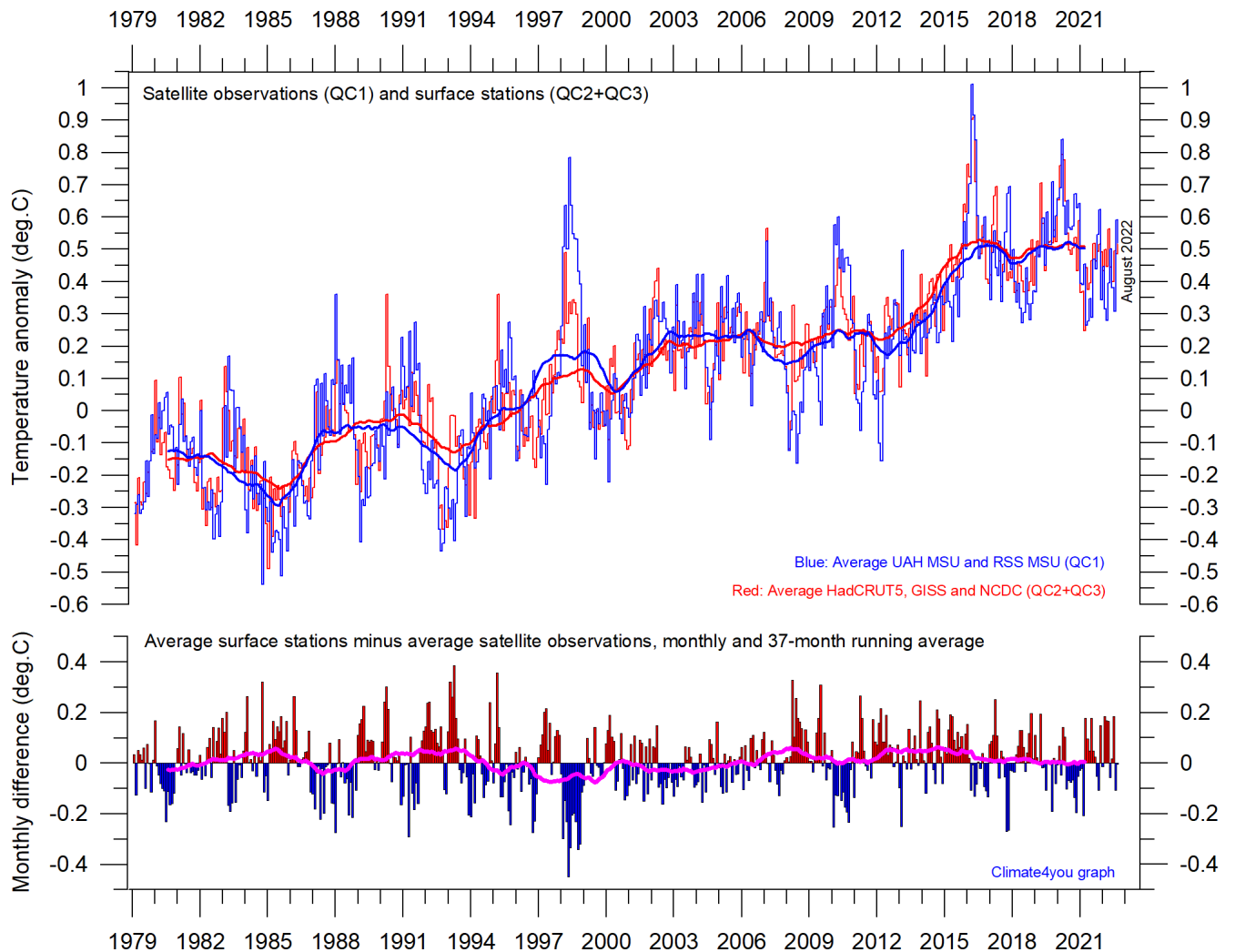


Diagram showing the monthly adjustments made since May 2008 by the [Goddard Institute for Space Studies](#) (GISS), USA, as recorded by published anomaly values for the two months January 1910 and January 2000.

The administrative upsurge of the temperature increase from January 1915 to January 2000 has grown from 0.45 (reported May 2008) to 0.66°C (reported October 2022). This represents an about 47% administrative temperature increase over this

period, meaning that a significant part (almost half) of the apparent global temperature increase from January 1910 to January 2000 (as reported by GISS) is caused by administrative changes of the original data since May 2008.

Comparing global surface air temperature and lower troposphere satellite temperatures; updated to August 2022



Plot showing the average of monthly global surface air temperature estimates (HadCRUT5, GISS and NCDC) and satellite-based temperature estimates (RSS MSU and UAH MSU). The thin lines indicate the monthly value, while the thick lines represent the simple running 37-month average, nearly corresponding to a running 3-yr average. The lower panel shows the monthly difference between average surface air temperature and satellite temperatures. As the base period differs for the different temperature estimates, they have all been normalised by comparing to the average value of 30 years from January 1979 to December 2008.

**Global air temperature linear trends updated to August 2022**

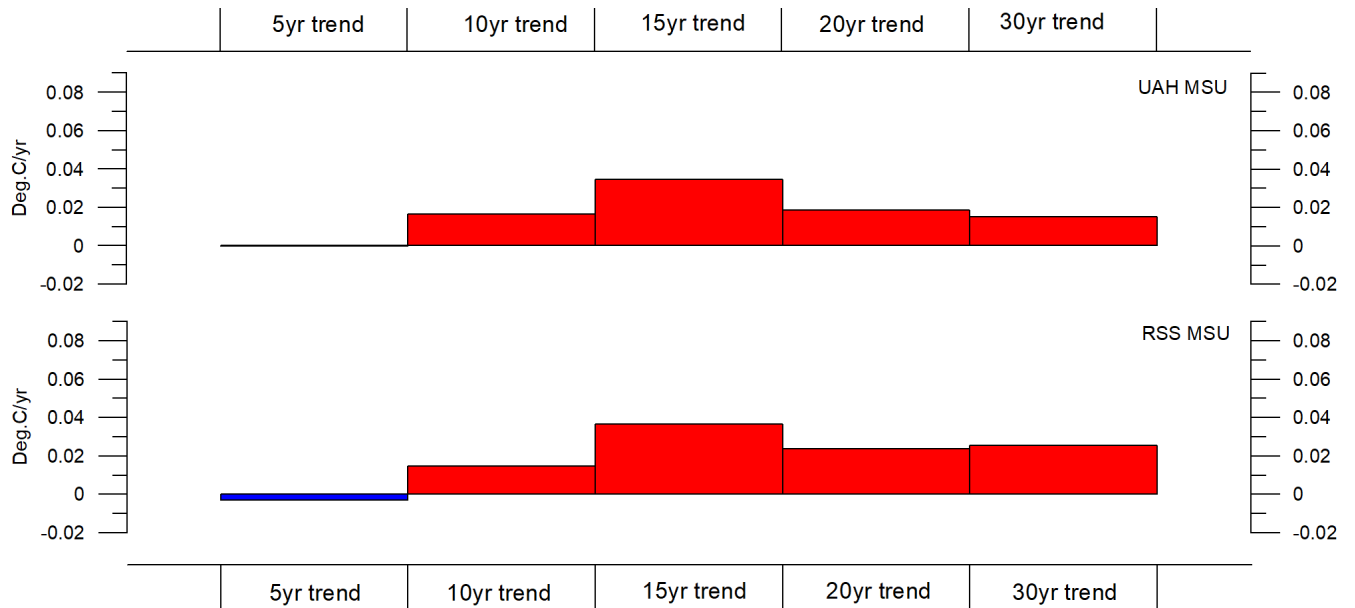


Diagram showing the latest 5, 10, 20 and 30-yr linear annual global temperature trend, calculated as the slope of the linear regression line through the data points, for two satellite-based temperature estimates (UAH MSU and RSS MSU).

12

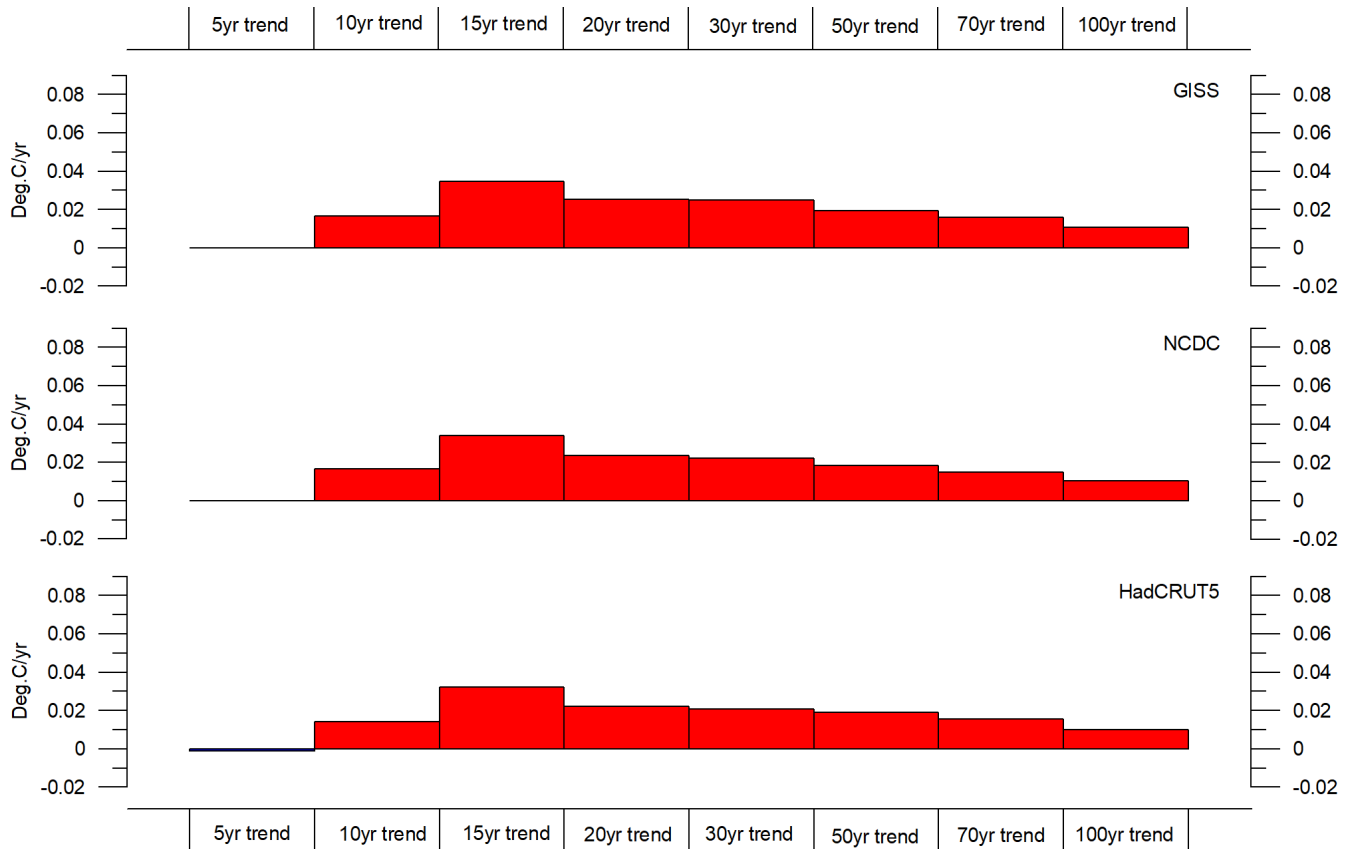
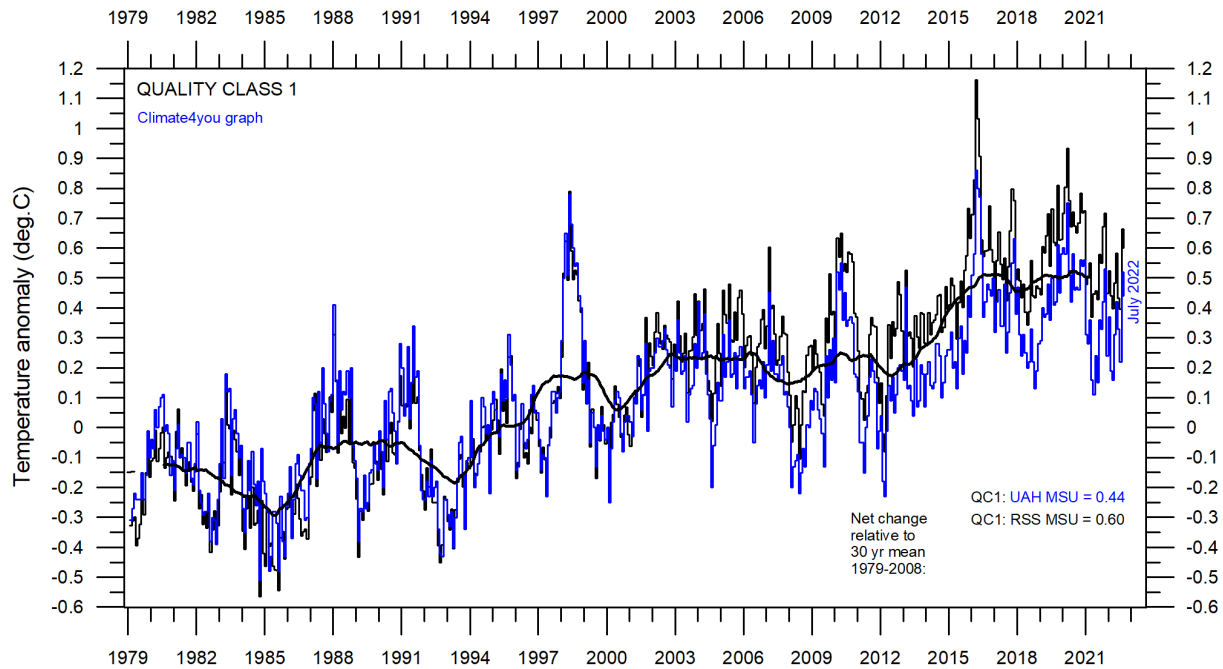


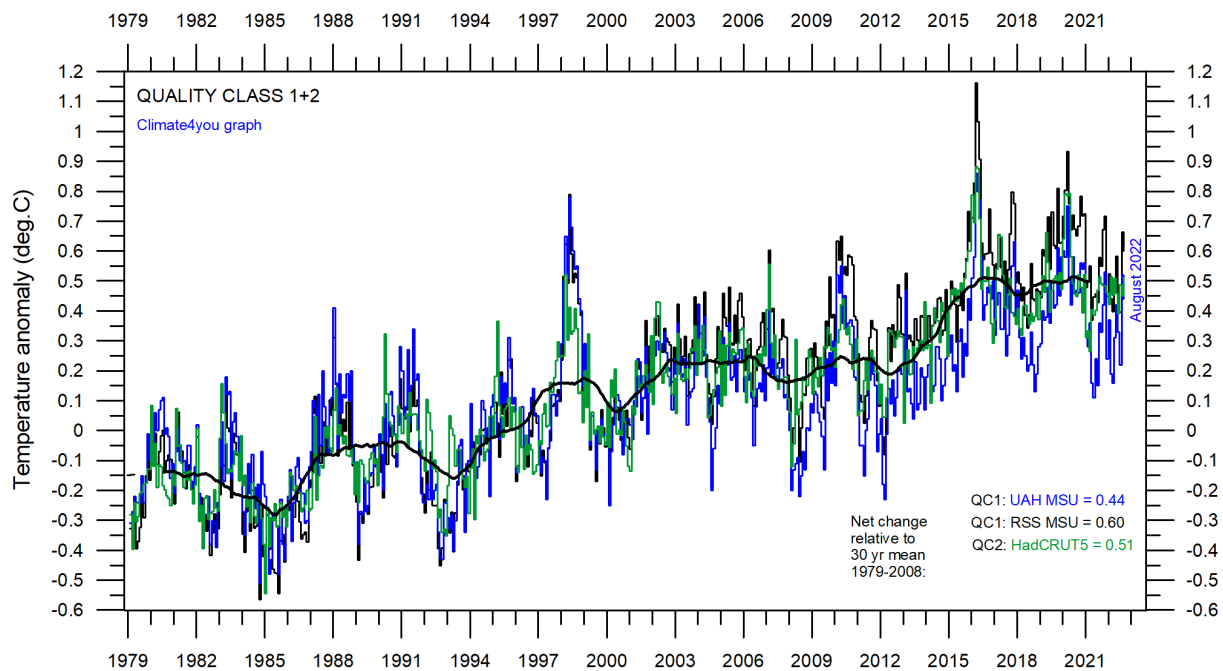
Diagram showing the latest 5, 10, 20, 30, 50, 70 and 100-year linear annual global temperature trend, calculated as the slope of the linear regression line through the data points, for three surface-based temperature estimates (GISS, NCDC and HadCRUT5).

**All in one, Quality Class 1, 2 and 3; updated to August 2022**

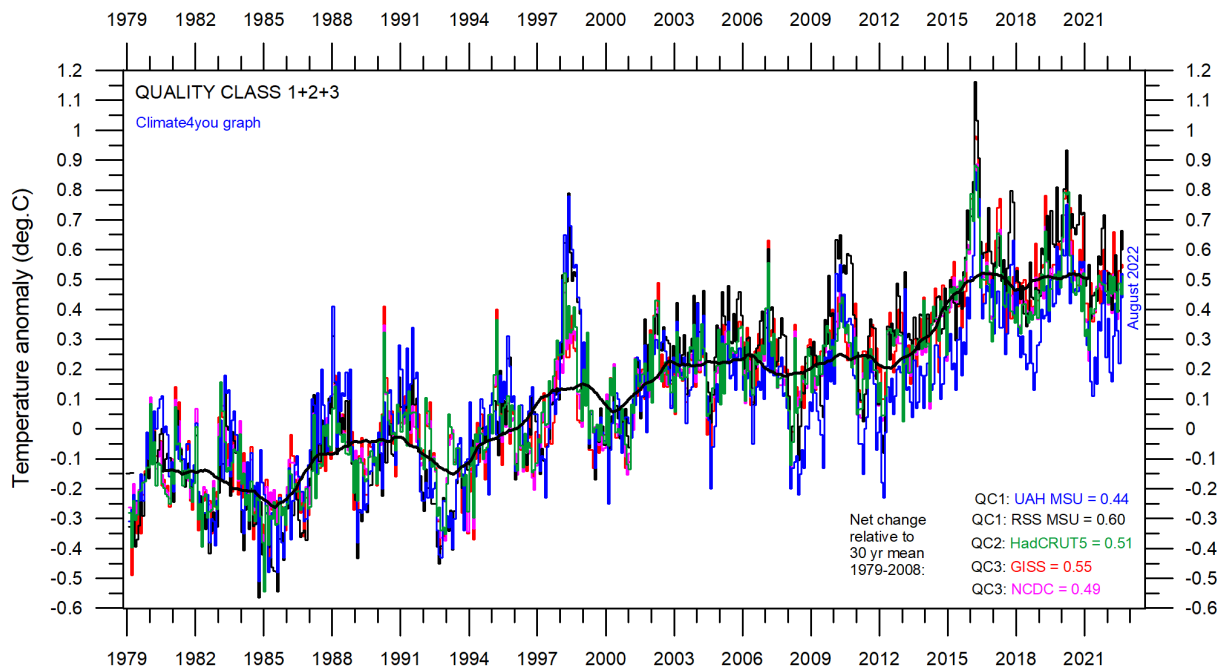


Superimposed plot of Quality Class 1 (UAH and RSS) global monthly temperature estimates. As the base period differs for the individual temperature estimates, they have all been normalised by comparing with the average value of the initial 120 months (30 years) from January 1979 to December 2008. The heavy black line represents the simple running 37 month (c. 3 year) mean of the average of both temperature records. The numbers shown in the lower right corner represent the temperature anomaly relative to the individual 1979-2008 averages.

13



Superimposed plot of Quality Class 1 and 2 (UAH, RSS and HadCRUT) global monthly temperature estimates. As the base period differs for the individual temperature estimates, they have all been normalised by comparing with the average value of the initial 120 months (30 years) from January 1979 to December 2008. The heavy black line represents the simple running 37 month (c. 3 year) mean of the average of all three temperature records. The numbers shown in the lower right corner represent the temperature anomaly relative to the individual 1979-2008 averages.



*Superimposed plot of Quality Class 1, 2 and 3 global monthly temperature estimates (UAH, RSS, HadCRUT, GISS and NCDC). As the base period differs for the individual temperature estimates, they have all been normalised by comparing with the average value of the initial 120 months (30 years) from January 1979 to December 2008. The heavy black line represents the simple running 37 month (c. 3 year) mean of the average of all five temperature records. The numbers shown in the lower right corner represent the temperature anomaly relative to the individual 1979-2008 averages.*

*Please see reflections on page 9 relating to the above three quality classes.*

Satellite- and surface-based temperature estimates are derived from different types of measurements and comparing them directly as in the above diagrams therefore may be somewhat ambiguous.

However, as both types of estimates often are discussed together in various news media, the above composite diagrams may nevertheless be of some interest.

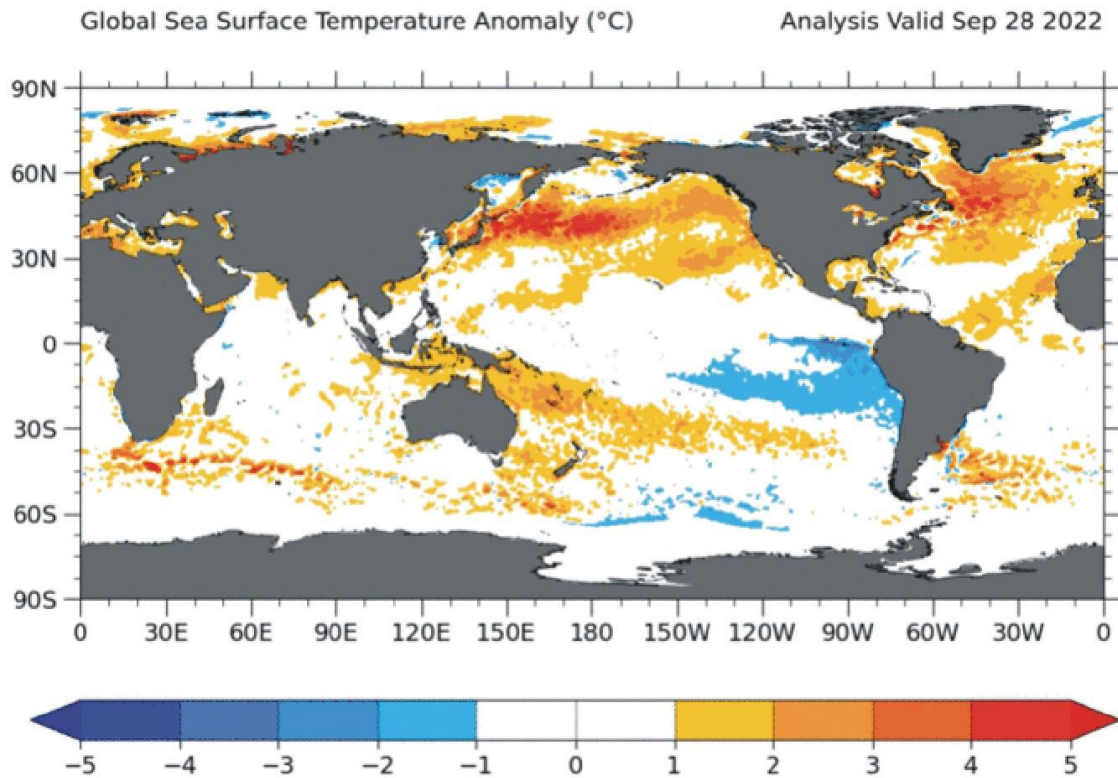
In fact, the different types of temperature estimates appear to agree as to the overall temperature variations on a 2-3-year scale, although on a shorter time scale there are often considerable differences between the individual records. However, since about 2003 the surface records used to be drifting towards higher temperatures than the combined satellite record, but this overall tendency was much removed by the major adjustment of the RSS satellite series in 2015 (see lower diagram on page 6).

The combined records (diagram above) suggest a modest global air temperature increase over the last 30 years, about 0.17°C per decade. It should be noted that the apparent temperature increases since about 2003 at least partly is the result of ongoing administrative adjustments (page 9-10). At the same time, none of the temperature records considered here indicates any general temperature decrease during the last 20 years.

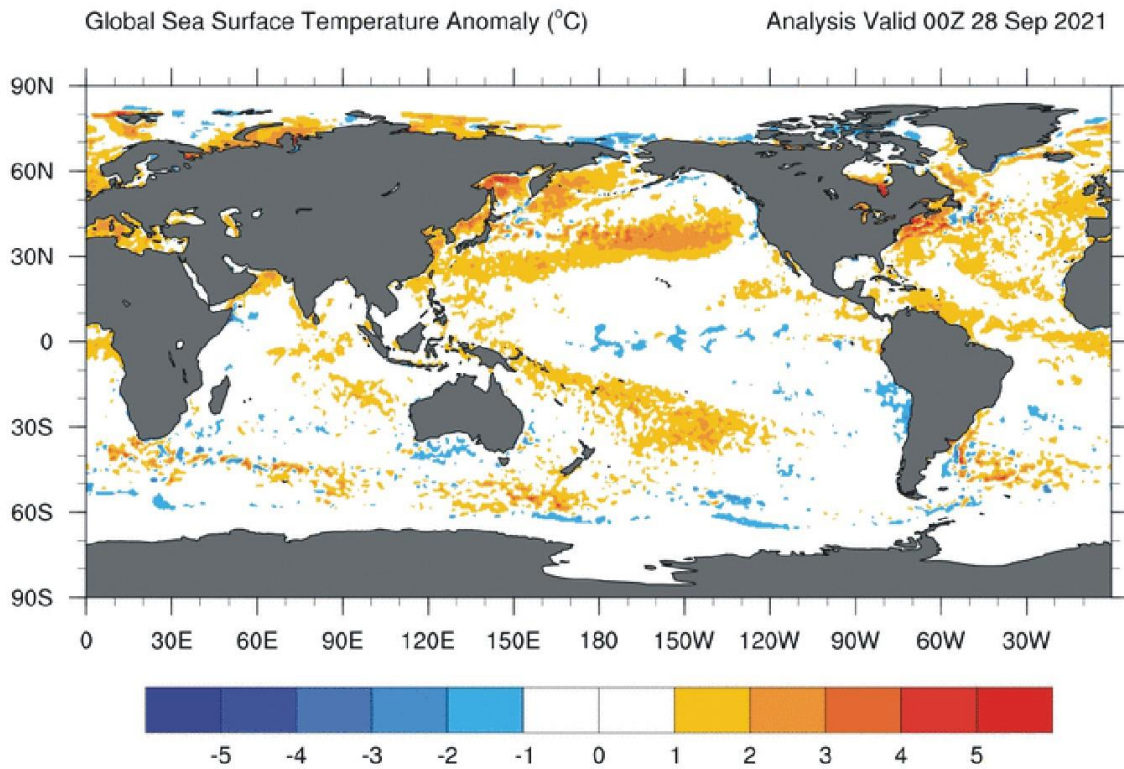
The present temperature development does not exclude the possibility that global temperatures may begin to increase significantly later. On the other hand, it also remains a possibility that Earth just now is passing an overall temperature peak, and that global temperatures may begin to decrease during the coming 5-10 years.

As always, time will show which of these possibilities is correct.

Global sea surface temperature, updated to September 2022



15



Plymouth State Weather Center

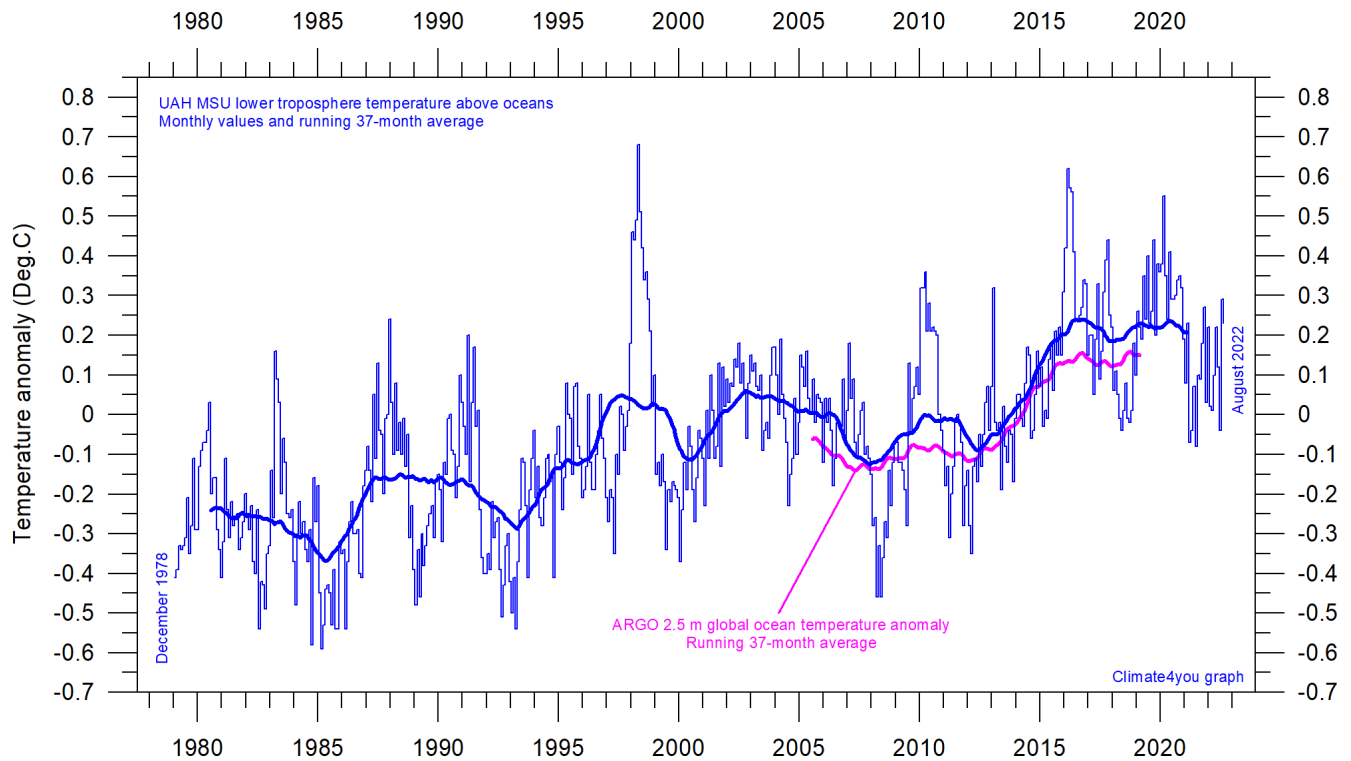
Sea surface temperature anomaly on 28 September 2022 (upper map) and 2021 (lower map). Map source: Plymouth State Weather Center. Reference period: 1977-1991.

Because of the large surface areas near Equator, the temperature of the surface water in these regions is especially important for the global atmospheric temperature (p. 6-8). In fact, no less than 50% of planet Earth's surface area is located within 30°N and 30°S.

A mixture of relatively warm and cold water presently dominates much of the global ocean surface, but with notable differences from month to month. All such ocean surface temperature changes will be influencing global air temperatures in the months to come. Just now a cold new La Niña episode is playing out in the Pacific Ocean (see p. 24). Relatively warm surface water is mainly found two bands centred around 30°N and 30°S, respectively.

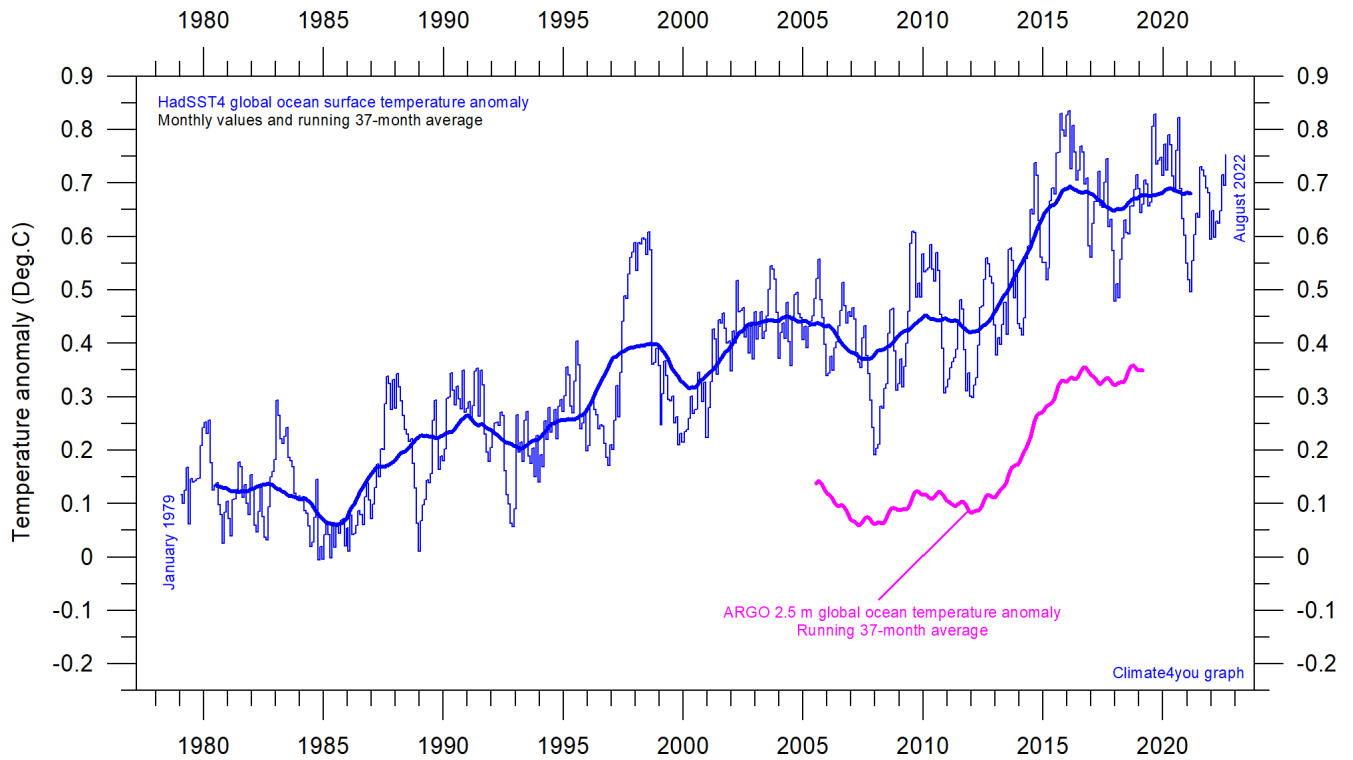
The significance of short-term cooling or warming reflected in air temperatures should never be overstated. Whenever Earth experiences cold La Niña or warm El Niño episodes major heat exchanges take place between the Pacific Ocean and the atmosphere above, sooner or later showing up in estimates of the global air temperature.

However, this does not necessarily reflect similar changes in the total heat content of the atmosphere-ocean system. In fact, global net changes can be small and such heat exchanges may mainly reflect redistribution of energy between ocean and atmosphere. What matters is the overall temperature development when seen over several years.



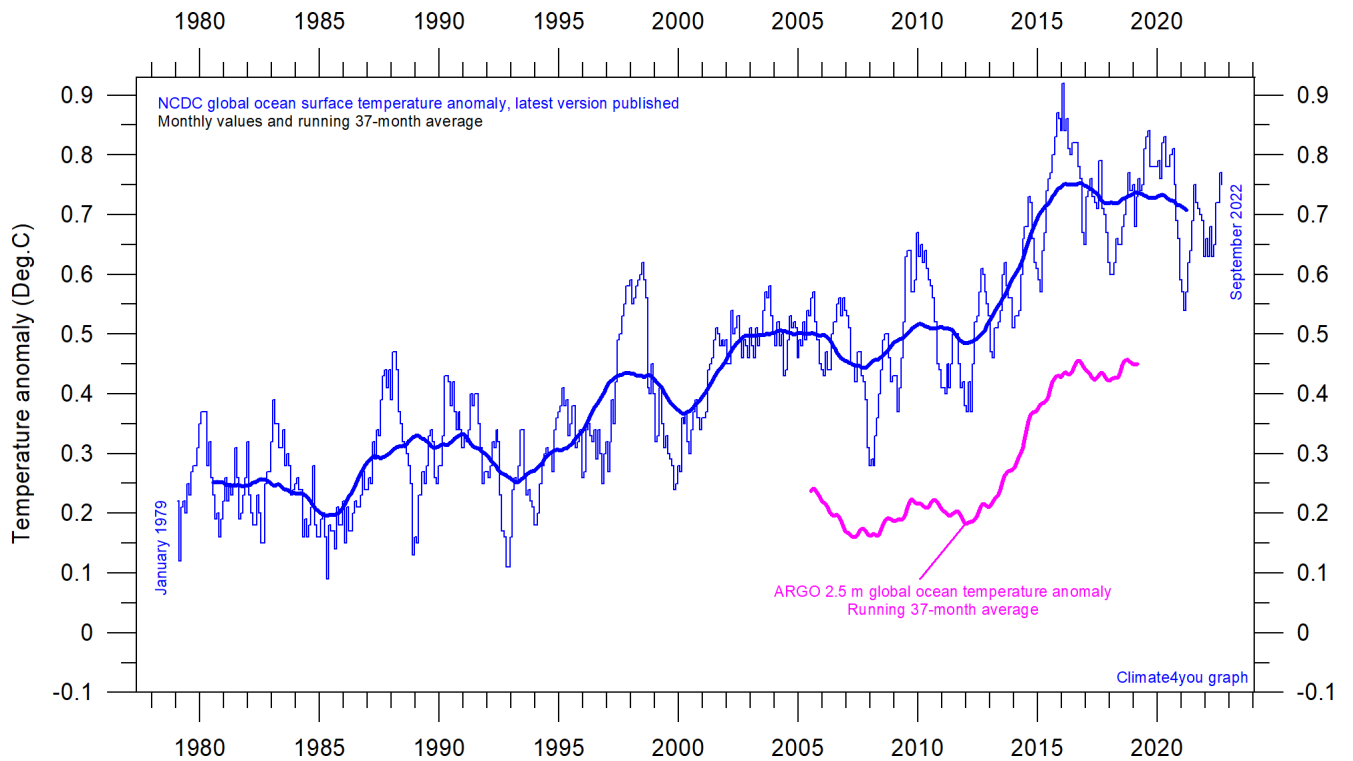
Global monthly average lower troposphere temperature over oceans (thin line) since 1979 according to [University of Alabama](#) at Huntsville, USA. The thick line is the simple running 37-month average. Insert: Argo global ocean temperature anomaly from floats, displaced vertically to make visual comparison easier. UAH reference period: 1991-2020.





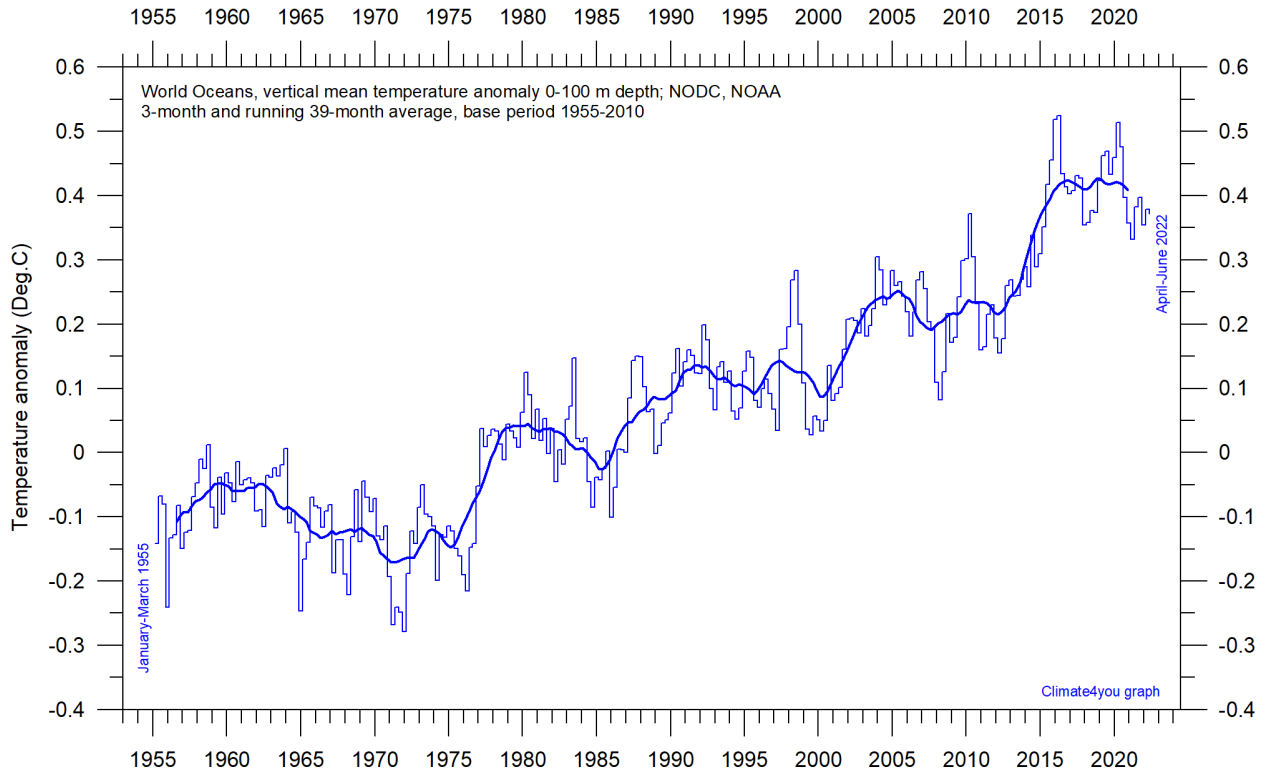
Global monthly average sea surface temperature since 1979 according to University of East Anglia's [Climatic Research Unit \(CRU\)](#), UK. Base period: 1961-1990. The thick line is the simple running 37-month average. Insert: Argo global ocean temperature anomaly from floats, displaced vertically to make visual comparison easier.

17



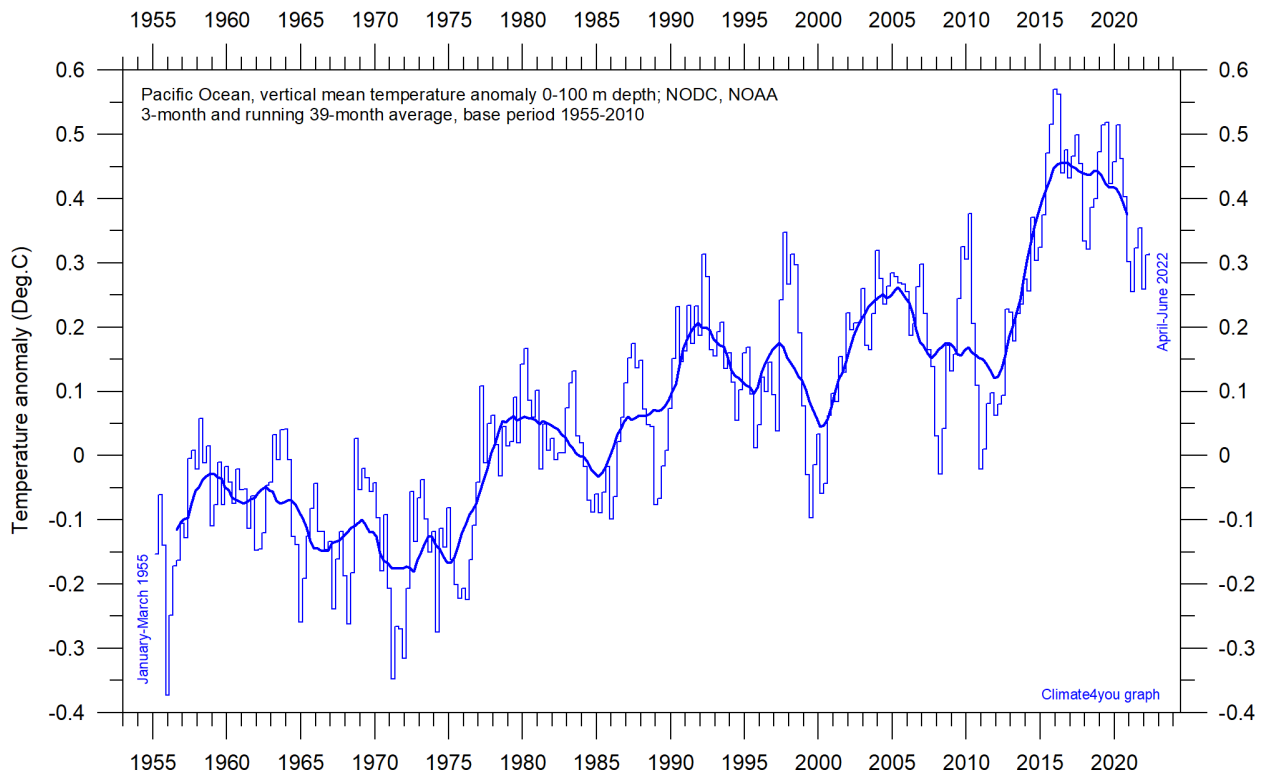
Global monthly average sea surface temperature since 1979 according to the [National Climatic Data Center \(NCDC\)](#), USA. Base period: 1901-2000. The thick line is the simple running 37-month average. Insert: Argo global ocean temperature anomaly from floats, displaced vertically to make visual comparison easier.

## Ocean temperature in uppermost 100 m, updated to June 2022

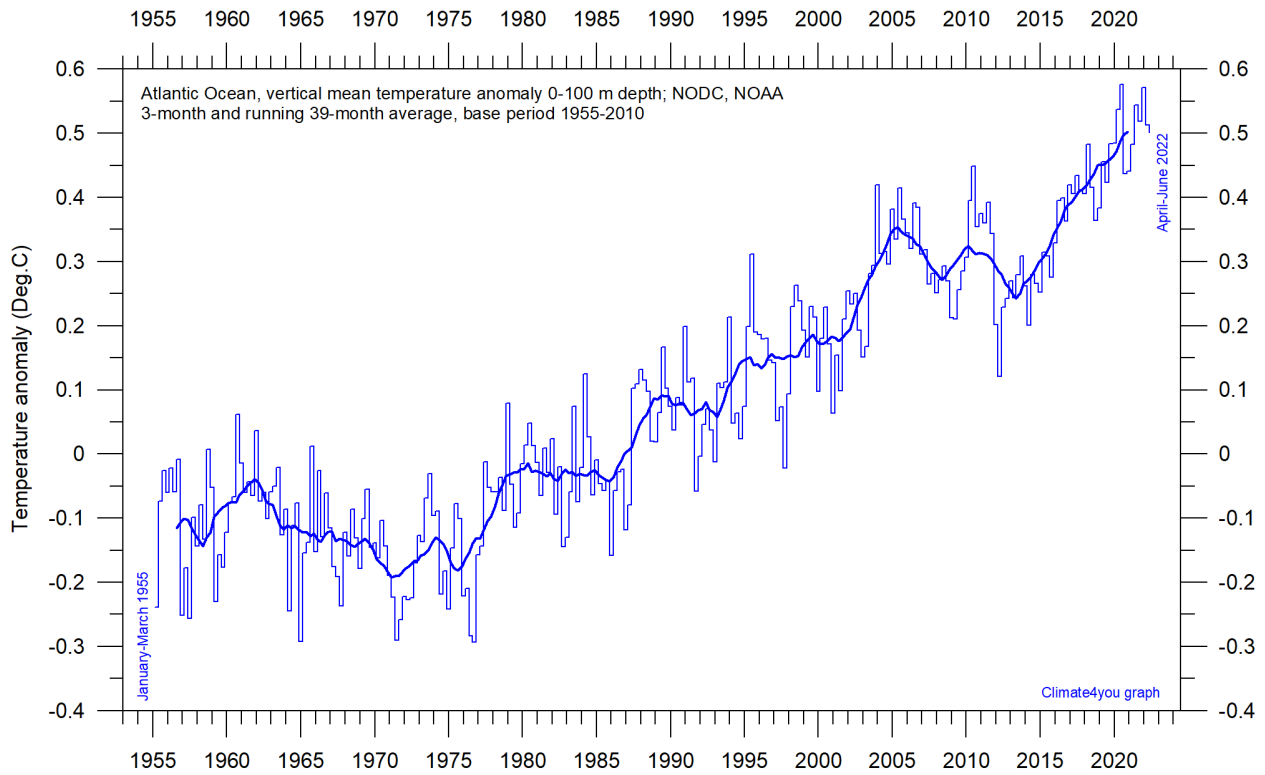


World Oceans vertical average temperature 0-100 m depth since 1955. The thin line indicates 3-month values, and the thick line represents the simple running 39-month (c. 3 year) average. Data source: [NOAA National Oceanographic Data Center](#) (NODC). Base period 1955-2010.

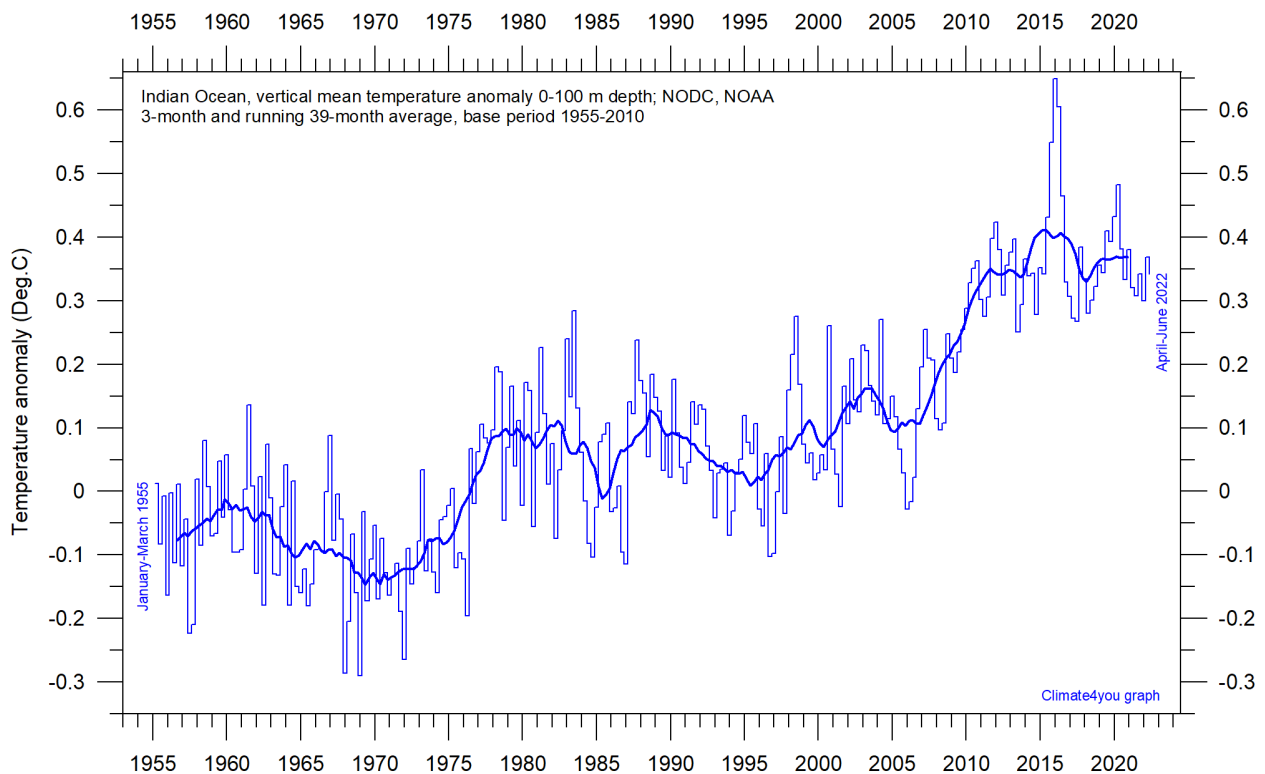
18



Pacific Ocean vertical average temperature 0-100 m depth since 1955. The thin line indicates 3-month values, and the thick line represents the simple running 39-month (c. 3 year) average. Data source: [NOAA National Oceanographic Data Center](#) (NODC). Base period 1955-2010.

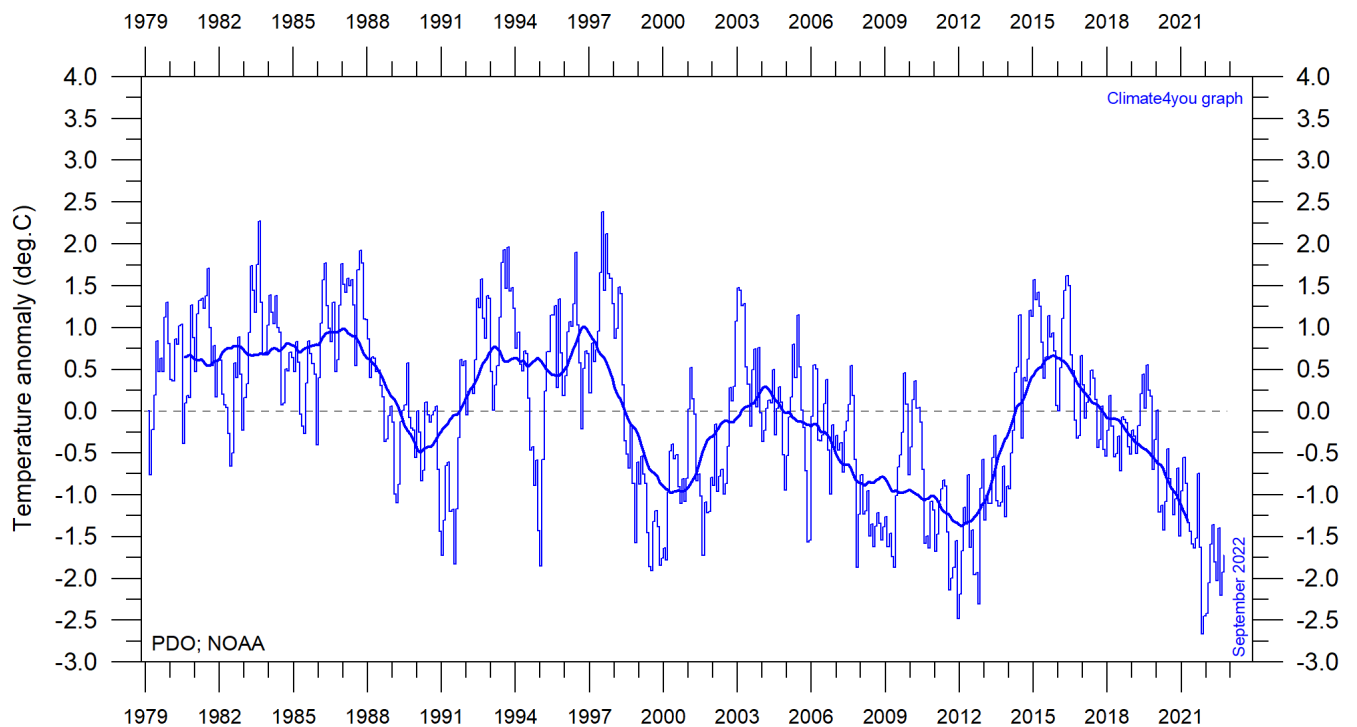


Atlantic Ocean vertical average temperature 0-100 m depth since 1955. The thin line indicates 3-month values, and the thick line represents the simple running 39-month (c. 3 year) average. Data source: [NOAA National Oceanographic Data Center](https://www.nodc.noaa.gov/) (NODC). Base period 1955-2010.



Indian Ocean vertical average temperature 0-100 m depth since 1955. The thin line indicates 3-month values, and the thick line represents the simple running 39-month (c. 3 year) average. Data source: [NOAA National Oceanographic Data Center](https://www.nodc.noaa.gov/) (NODC). Base period 1955-2010.

## Pacific Decadal Oscillation (PDO), updated to September 2022



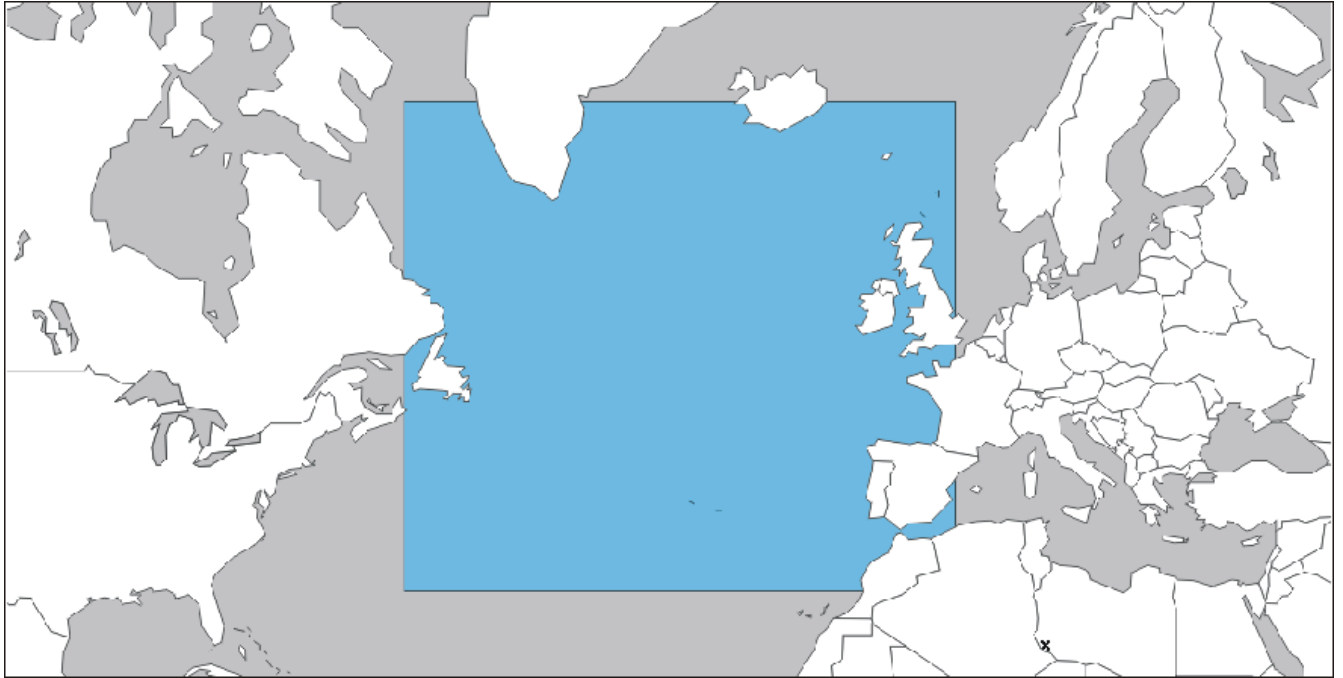
Monthly values of the Pacific Decadal Oscillation (PDO) since January 1979. The PDO is a long-lived El Niño-like pattern of Pacific climate variability, and the data series goes back to January 1854. Base period: 1982-2002. The thin line indicates monthly PDO values, and the thick line is the simple running 37-month average. Data source: [NOAA Physical Science Laboratory](#) (version PDO ERSST V5 plotted above).

The PDO is a long-lived El Niño-like pattern of Pacific climate variability, with data extending back to January 1854. Causes for PDO are not currently known, but even in the absence of a theoretical understanding, PDO climate information improves season-to-season and year-to-year climate forecasts for North America because of its strong tendency for multi-season and multi-year persistence. The PDO also appears to be roughly in phase with global temperature changes. Thus, from a societal impact's perspective, recognition of PDO is important because it shows that "normal" climate conditions can vary over time periods comparable to the length of a human's lifetime.

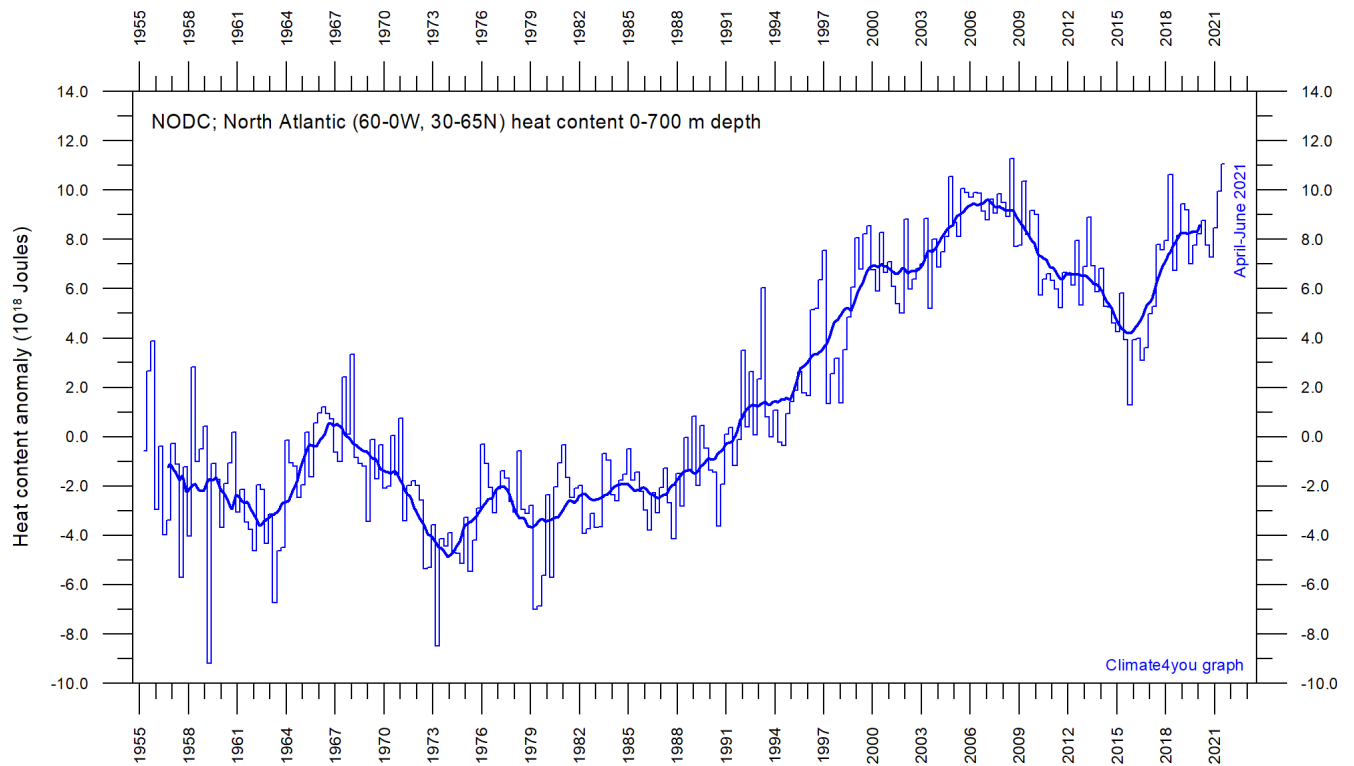
The PDO illustrates how global temperatures are tied to sea surface temperatures in the Pacific Ocean, the largest ocean on Earth. When sea surface temperatures are relatively low (negative phase PDO), as it was from 1945 to 1977, global air temperature decreases. When Pacific Ocean surface temperatures are high (positive phase PDO), as from 1977 to 1998, global surface air temperature increases.

A Fourier frequency analysis (not shown here) shows the entire PDO record since 1854 to be influenced by a 5.7-year cycle, and possibly also by a longer about 53-year long cycle.

## North Atlantic heat content uppermost 700 m, updated to June 2021

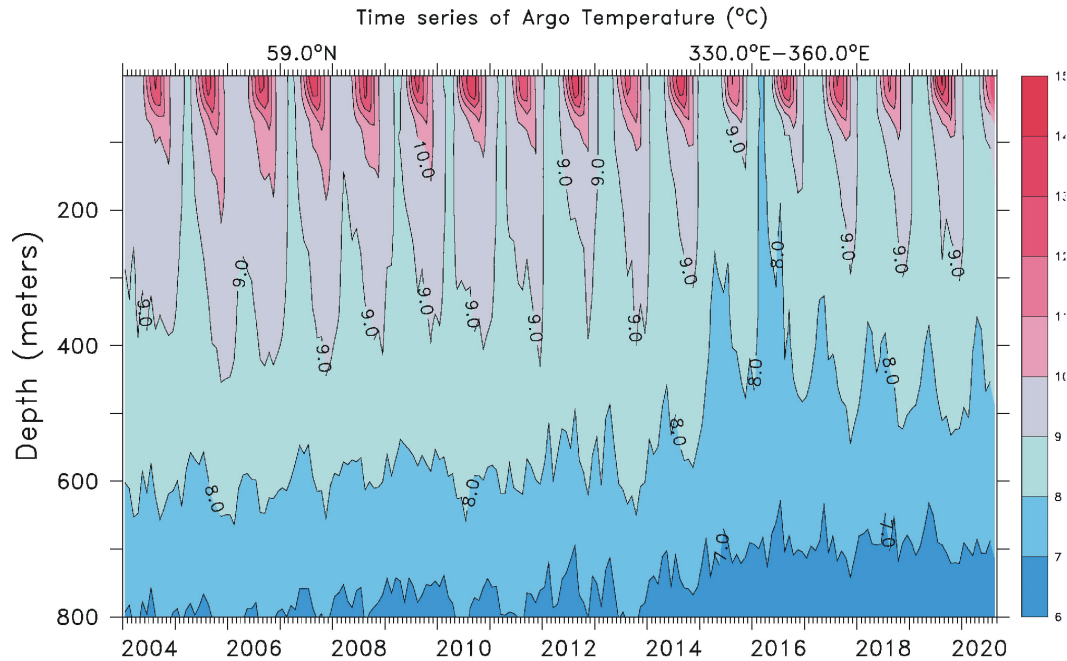


21



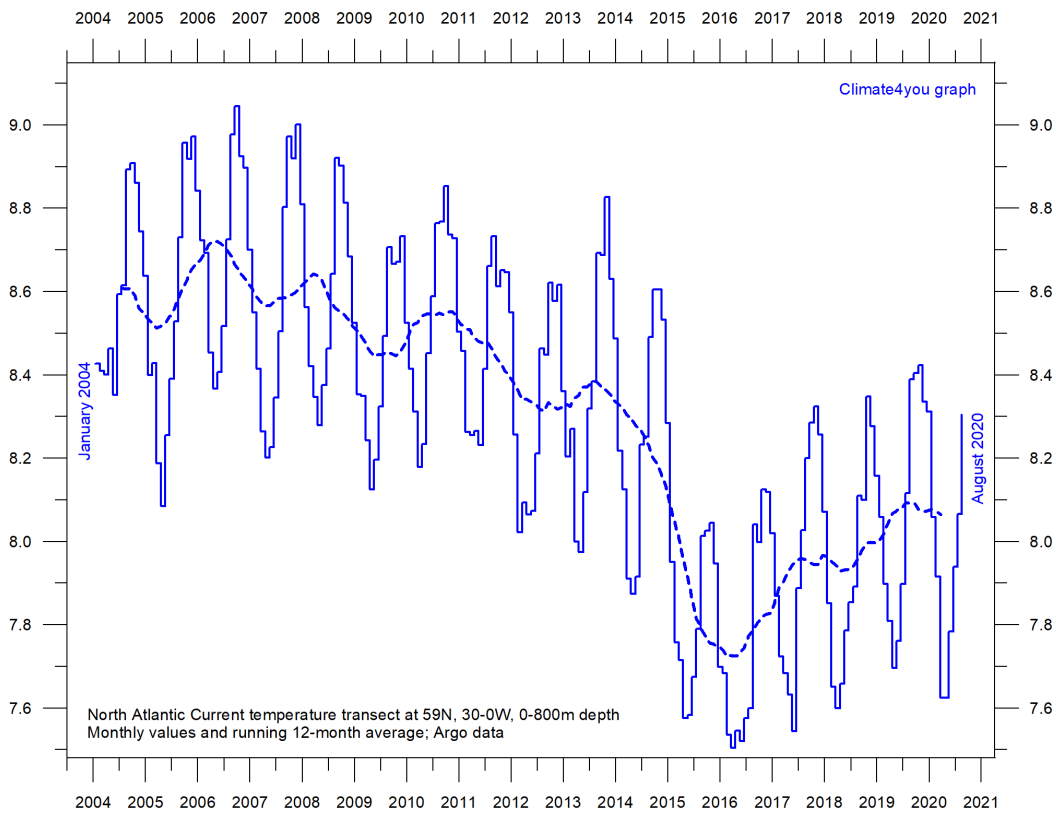
Global monthly heat content anomaly ( $10^{18}$  Joules) in the uppermost 700 m of the North Atlantic (60-0W, 30-65N; see map above) ocean since January 1955. The thin line indicates monthly values, and the thick line represents the simple running 37-month (c. 3 year) average. Data source: [National Oceanographic Data Center](#) (NODC).

## North Atlantic temperatures 0-800 m depth along 59°N, 30-0W, updated to August 2020



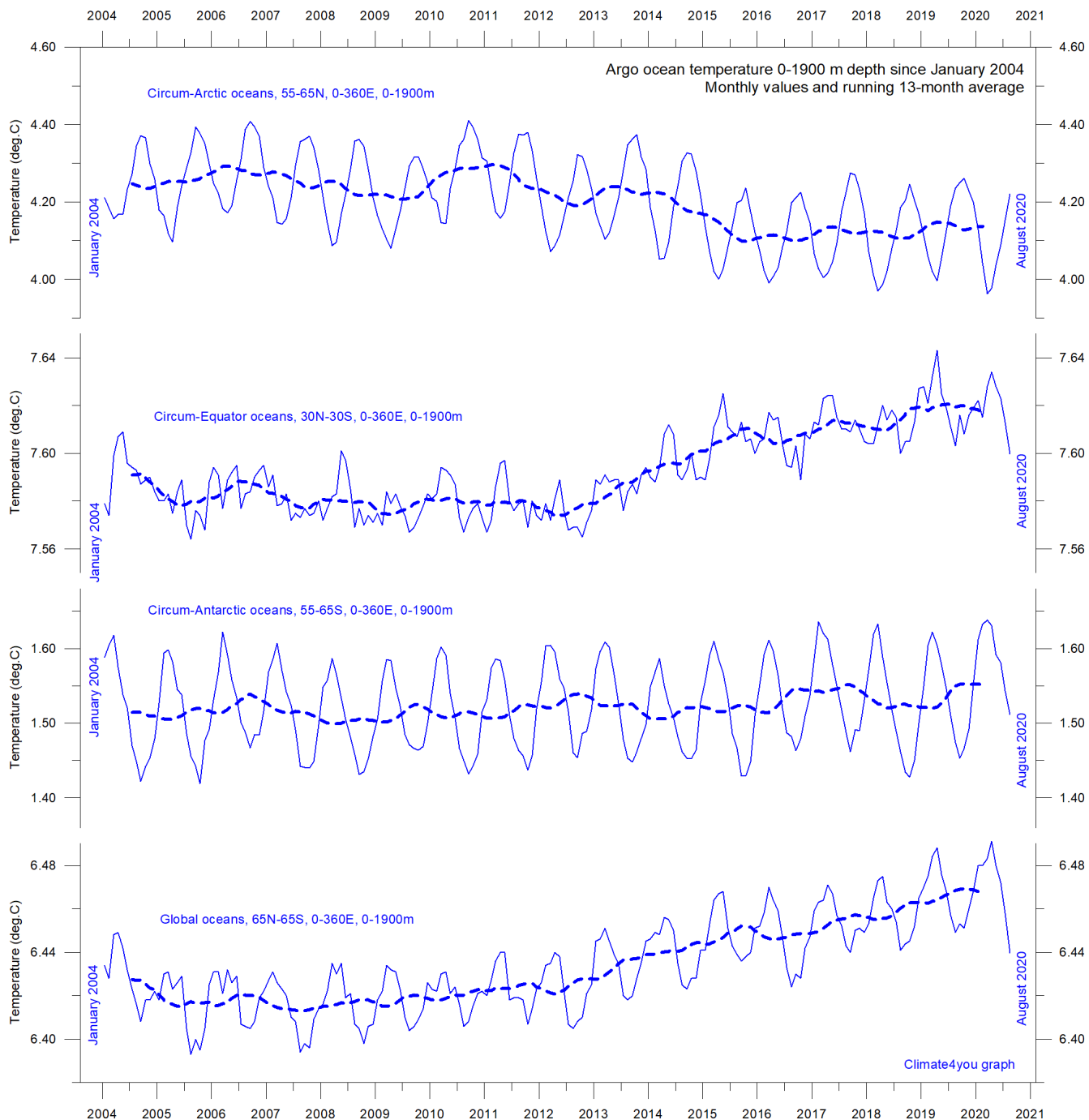
Time series depth-temperature diagram along 59 N across the North Atlantic Current from 30°W to 0°W, from surface to 800 m depth. Source: [Global Marine Argo Atlas](#). See also the diagram below.

22



Average temperature along 59 N, 30-0W, 0-800m depth, corresponding to the main part of the North Atlantic Current, using Argo-data. Source: [Global Marine Argo Atlas](#). Additional information can be found in: Roemmich, D. and J. Gilson, 2009. The 2004-2008 mean and annual cycle of temperature, salinity, and steric height in the global ocean from the Argo Program. [Progress in Oceanography](#), 82, 81-100.

## Global ocean temperature 0-1900 m depth summary, updated to August 2020

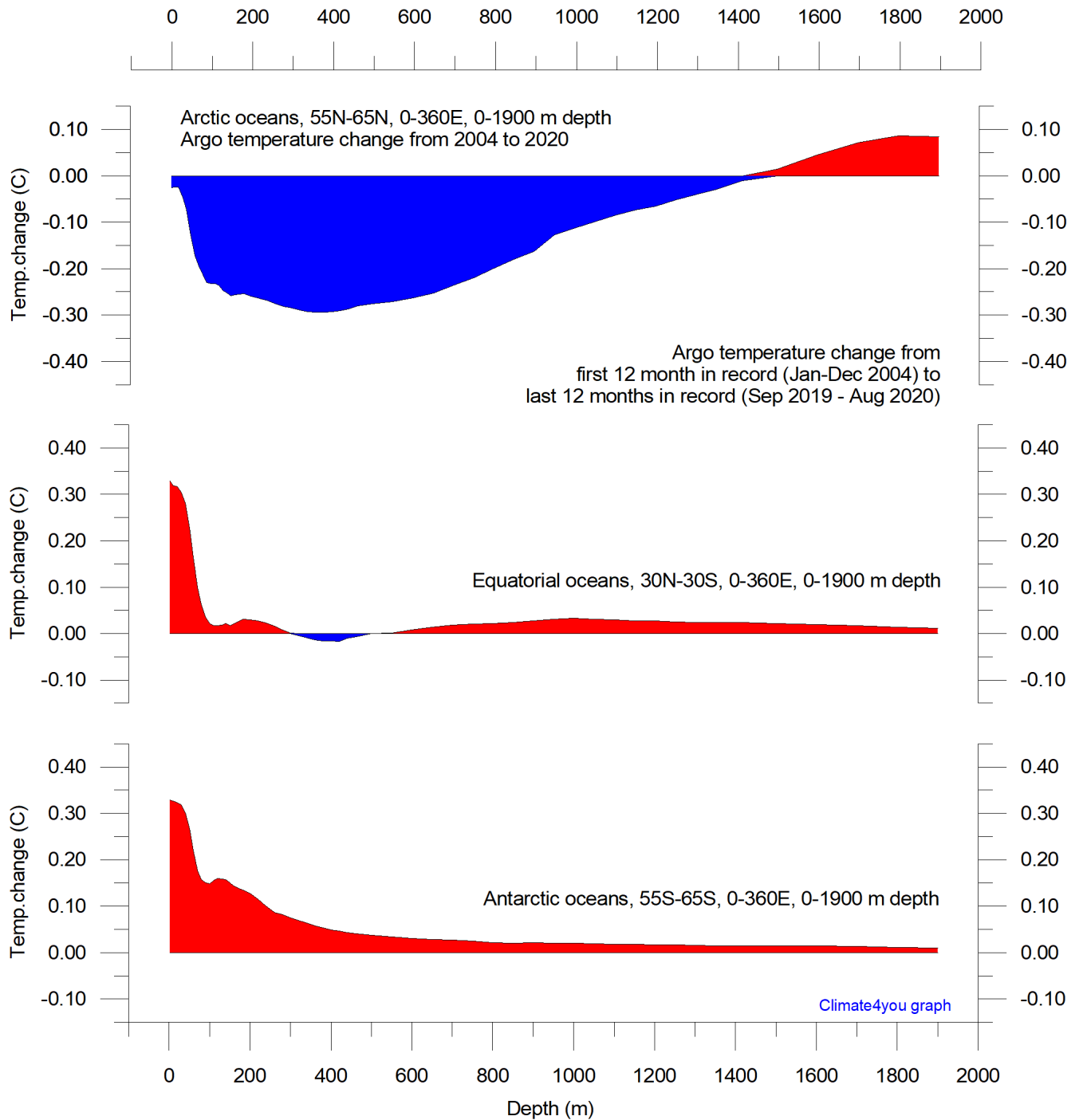


Summary of average temperature in uppermost 1900 m in different parts of the global oceans, using [Argo](#)-data. Source: [Global Marine Argo Atlas](#). Additional information can be found in: Roemmich, D. and J. Gilson, 2009. The 2004-2008 mean and annual cycle of temperature, salinity, and steric height in the global ocean from the Argo Program. [Progress in Oceanography](#), 82, 81-100.

The global summary diagram above shows that, on average, the temperature of the global oceans down to 1900 m depth has been increasing since about 2011. It is also seen that this increase since 2013 dominantly is due to oceanic changes occurring near the Equator, between

30°N and 30°S. In contrast, for the circum-Arctic oceans north of 55°N, depth-integrated ocean temperatures have been decreasing since 2011. Near the Antarctic, south of 55°S, temperatures have essentially been stable. At most latitudes, a clear annual rhythm is evident.

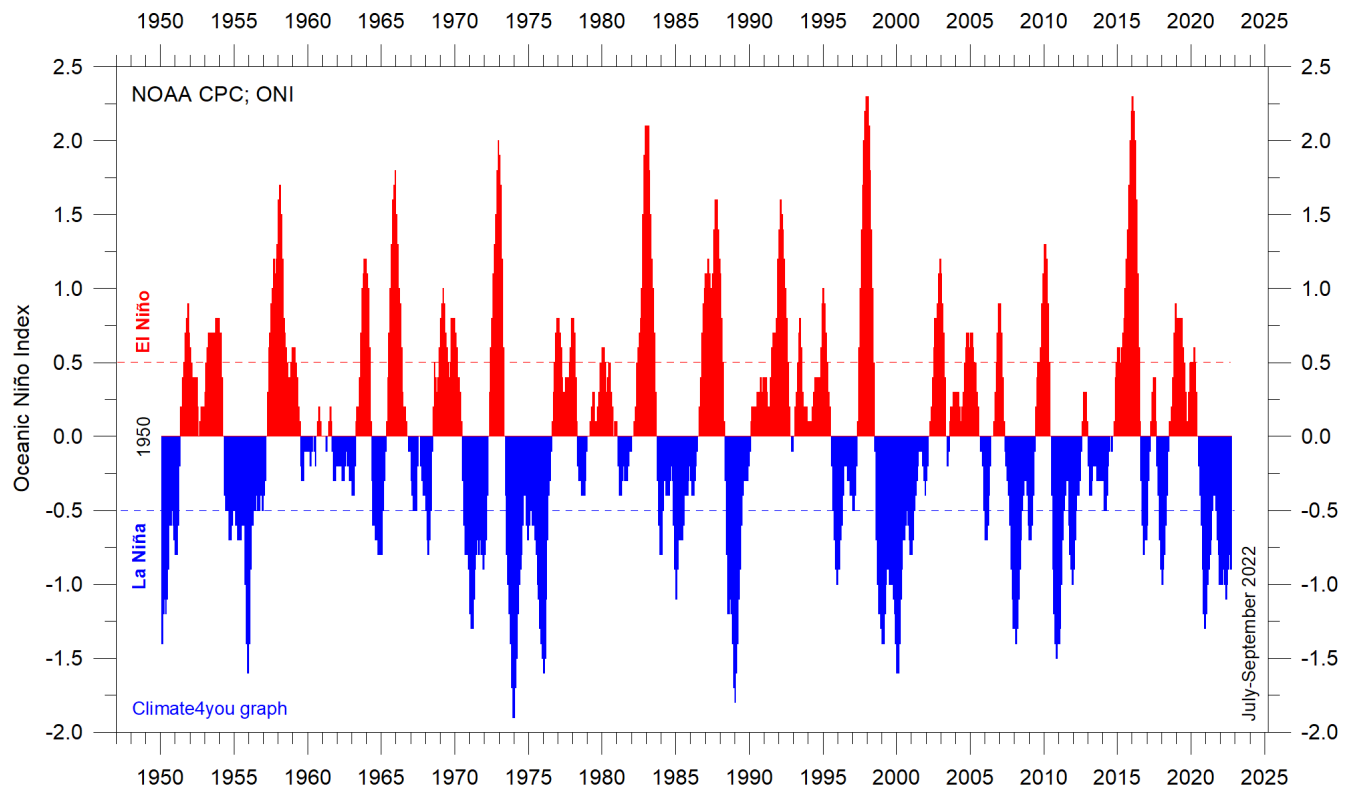
Global ocean net temperature change since 2004 at different depths, updated to August 2020



Net temperature change since 2004 from surface to 1900 m depth in different parts of the global oceans, using [Argo](#)-data. Source: [Global Marine Argo Atlas](#). Additional information can be found in: Roemmich, D. and J. Gilson, 2009. The 2004-2008 mean and annual cycle of temperature, salinity, and steric height in the global ocean from the Argo Program. [Progress in Oceanography](#), 82, 81-100. Please note that due to the spherical form of Earth, northern and southern latitudes represent only small ocean volumes, compared to latitudes near the Equator.



## La Niña and El Niño episodes, Oceanic Niño Index (ONI), updated to September 2022



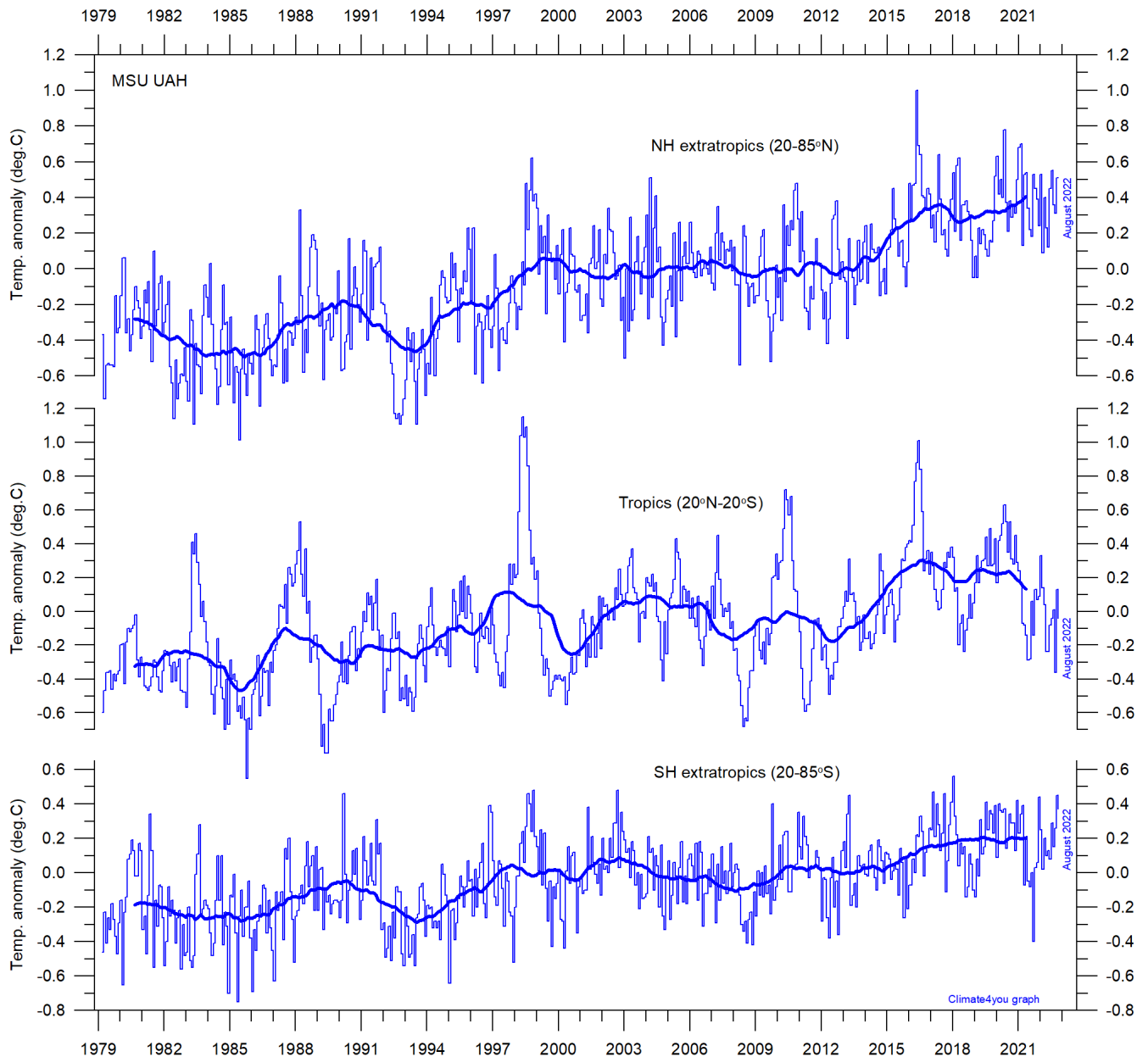
25

Warm ( $>+0.5^{\circ}\text{C}$ ) and cold ( $<0.5^{\circ}\text{C}$ ) episodes for the [Oceanic Niño Index \(ONI\)](#), defined as 3 month running mean of ERSSTv4 SST anomalies in the Niño 3.4 region ( $5^{\circ}\text{N}$ - $5^{\circ}\text{S}$ ,  $120^{\circ}$ - $170^{\circ}\text{W}$ ). For historical purposes cold and warm episodes are defined when the threshold is met for a minimum of 5 consecutive over-lapping seasons. Anomalies are centred on 30-yr base periods updated every 5 years.

The 2015-16 El Niño episode is among the strongest since the beginning of the record in 1950. Considering the entire record, however, recent

variations between El Niño and La Niña episodes do not appear abnormal in any way. See also diagrams on pages 44 and 53.

## Zonal lower troposphere temperatures from satellites, updated to August 2022

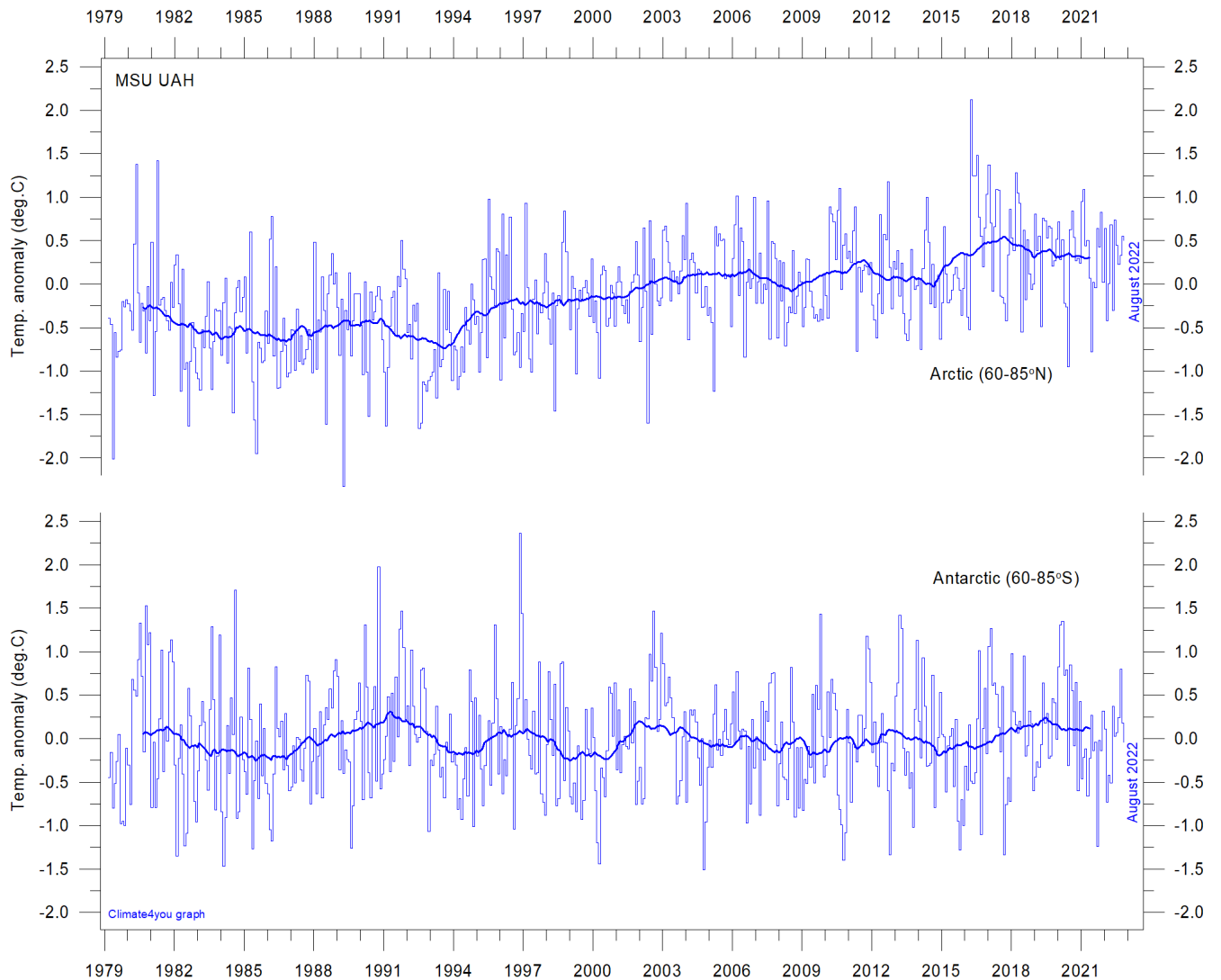


Global monthly average lower troposphere temperature since 1979 for the tropics and the northern and southern extratropics, according to University of Alabama at Huntsville, USA. Thin lines show the monthly temperature. Thick lines represent the simple running 37-month average, nearly corresponding to a running 3-year average. Reference period 1981-2010.

The overall warming since 1980 has dominantly been a northern hemisphere phenomenon, and mainly played out as a marked step change between 1994 and 1999. However, this rather rapid temperature change is influenced by the Mt. Pinatubo eruption 1992-93 and the

subsequent 1997 El Niño episode. The diagram also shows the temperature effects of the strong Equatorial El Niño's in 1997 and 2015-16, as well as the moderate El Niño in 2019. Apparently, these effects were spreading to higher latitudes in both hemispheres with some delay.

## Arctic and Antarctic lower troposphere temperature, updated to August 2022



Global monthly average lower troposphere temperature since 1979 for the North Pole and South Pole regions, based on satellite observations ([University of Alabama](#) at Huntsville, USA). Thin lines show the monthly temperature. The thick line is the simple running 37-month average, nearly corresponding to a running 3-year average. Reference period 1991-2020.

In the Arctic region, warming mainly took place 1994-96, and less so subsequently. In 2016, however, temperatures peaked for several months, presumably because of oceanic heat given off to the atmosphere during the 2015-15 El Niño (see also figure on page 25) and subsequently advected to higher latitudes.

This underscores how Arctic air temperatures may be affected not only by variations in local conditions but also by variations playing out in geographically remote

regions. A slight, but persistent, temperature decrease has characterised the Arctic since the 2016 peak (see also diagrams on page 28-30).

In the Antarctic region, temperatures have basically remained stable since the onset of the satellite record in 1979. In 2016-17 a small temperature peak visible in the monthly record may be interpreted as the subdued effect of the recent El Niño episode.

## Arctic and Antarctic surface air temperature, updated to December 2021

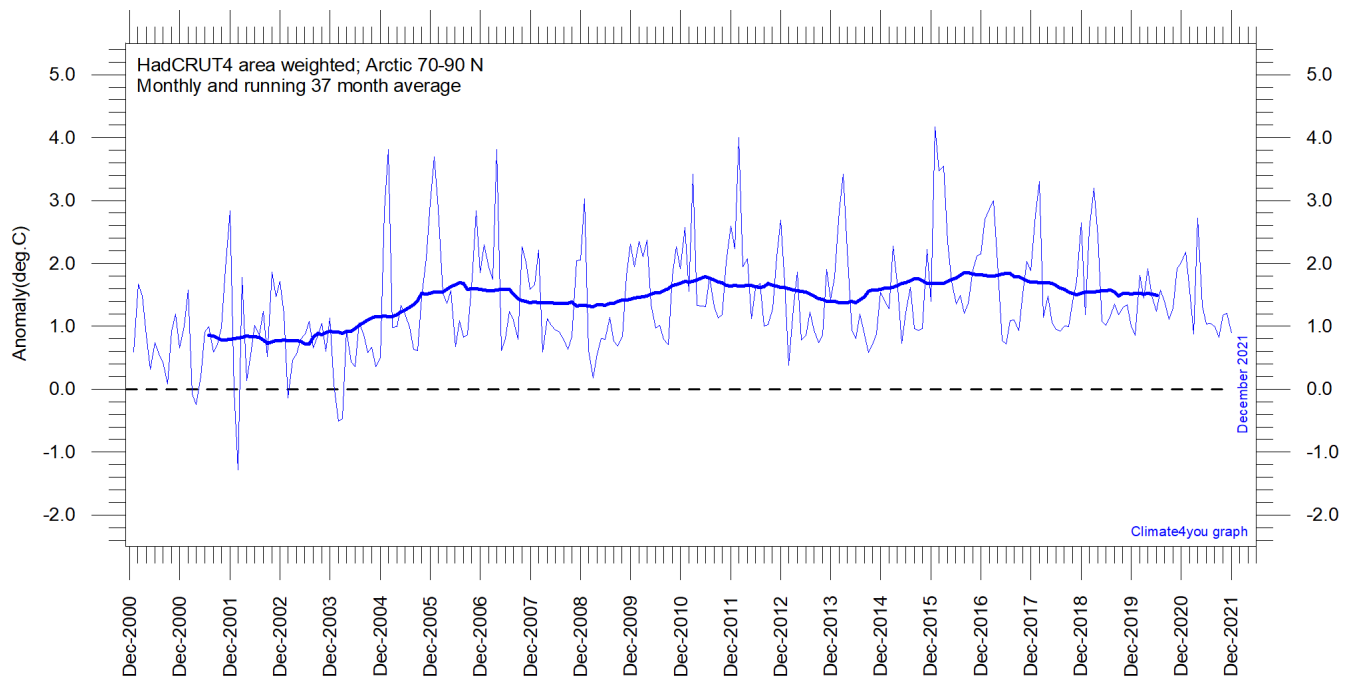


Diagram showing area weighted Arctic (70-90°N) monthly surface air temperature anomalies ([HadCRUT4](#)) since January 2000, in relation to the WMO [normal period](#) 1961-1990. The thin line shows the monthly temperature anomaly, while the thicker line shows the running 37-month (c. 3 year) average.

28

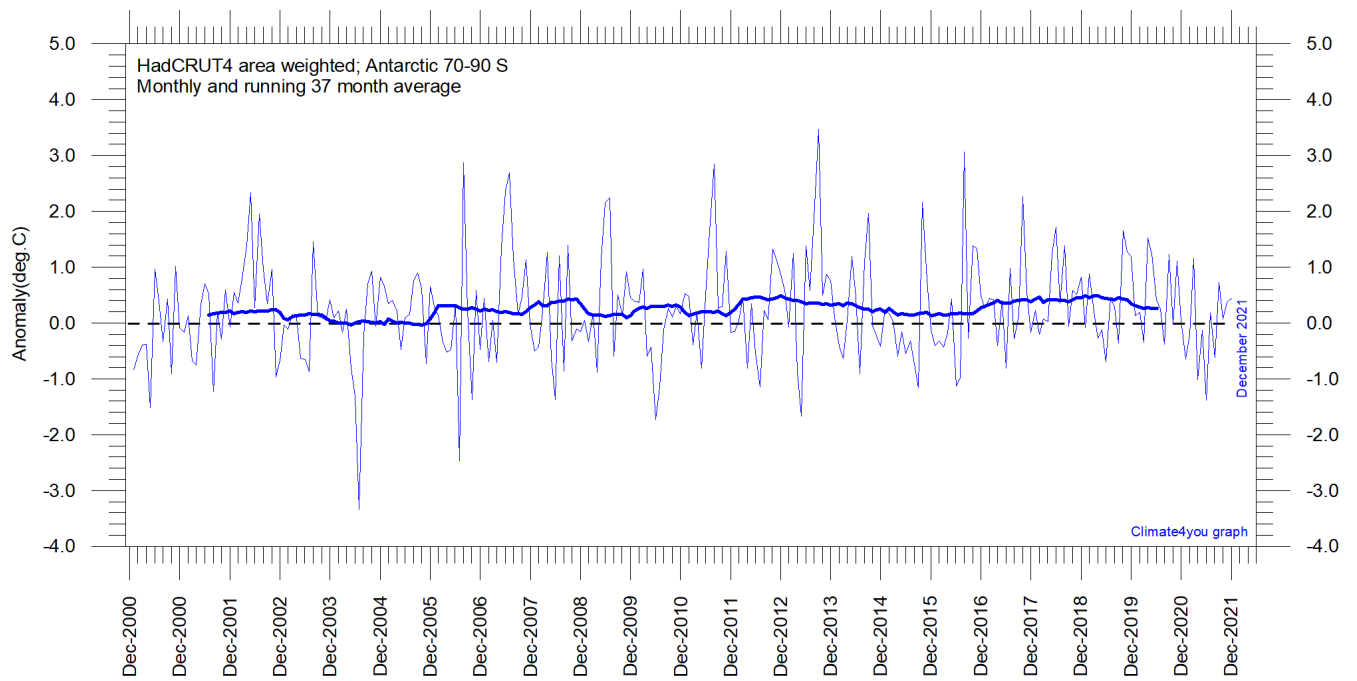


Diagram showing area weighted Antarctic (70-90°S) monthly surface air temperature anomalies ([HadCRUT4](#)) since January 2000, in relation to the WMO [normal period](#) 1961-1990. The thin line shows the monthly temperature anomaly, while the thicker line shows the running 37-month (c. 3 year) average.

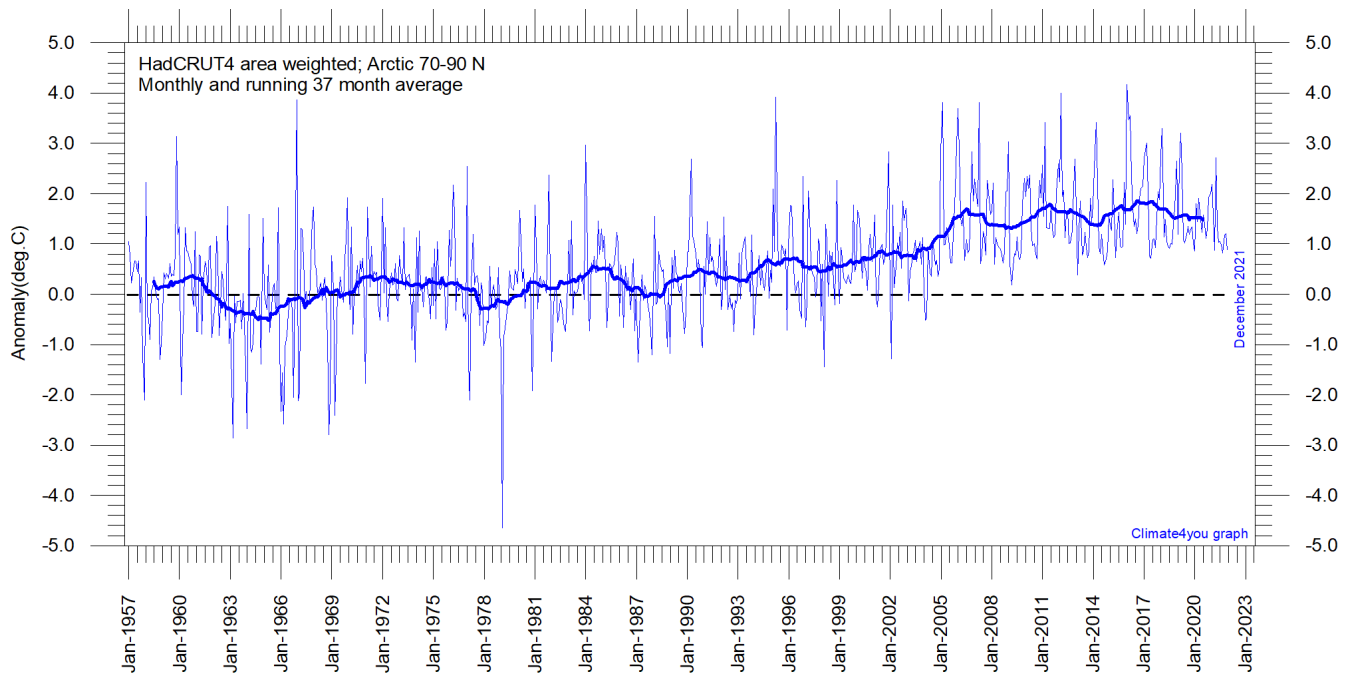


Diagram showing area weighted Arctic (70-90°N) monthly surface air temperature anomalies ([HadCRUT4](#)) since January 1957, in relation to the WMO [normal period](#) 1961-1990. The thin line shows the monthly temperature anomaly, while the thicker line shows the running 37-month (c. 3 year) average.

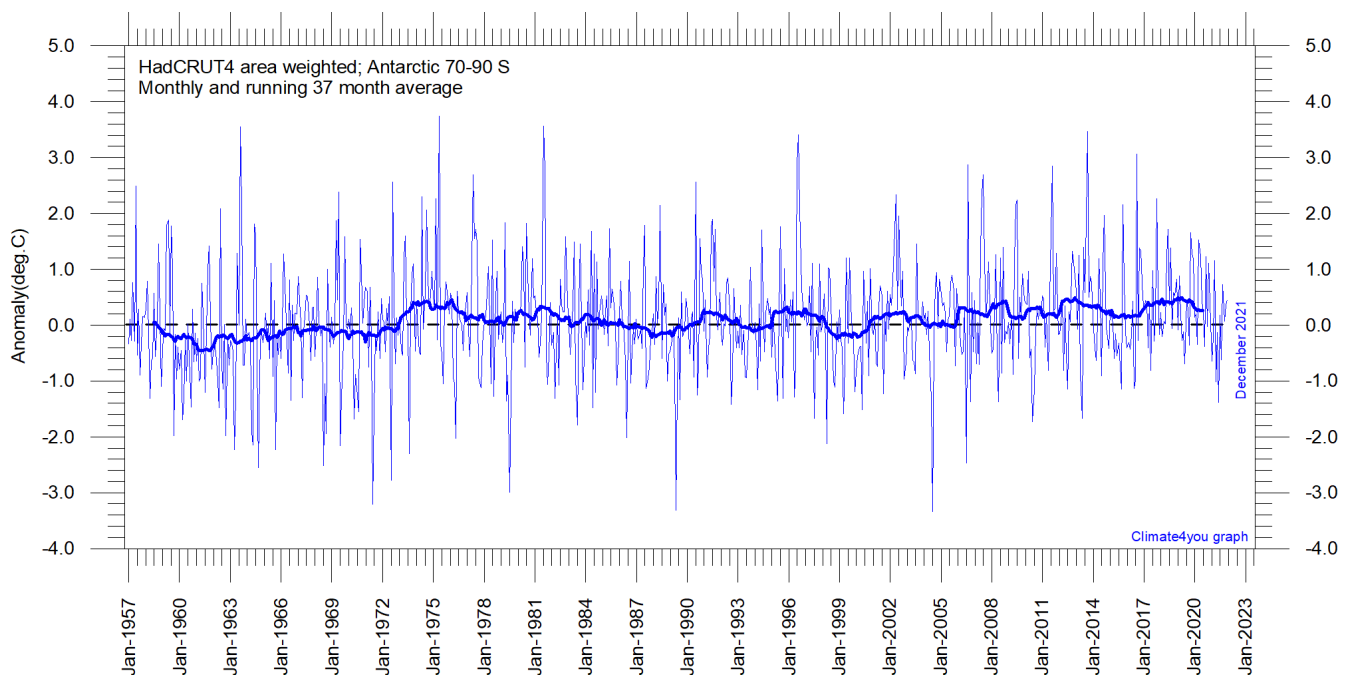


Diagram showing area weighted Antarctic (70-90°S) monthly surface air temperature anomalies ([HadCRUT4](#)) since January 1957, in relation to the WMO [normal period](#) 1961-1990. The thin line shows the monthly temperature anomaly, while the thicker line shows the running 37-month (c. 3 year) average.

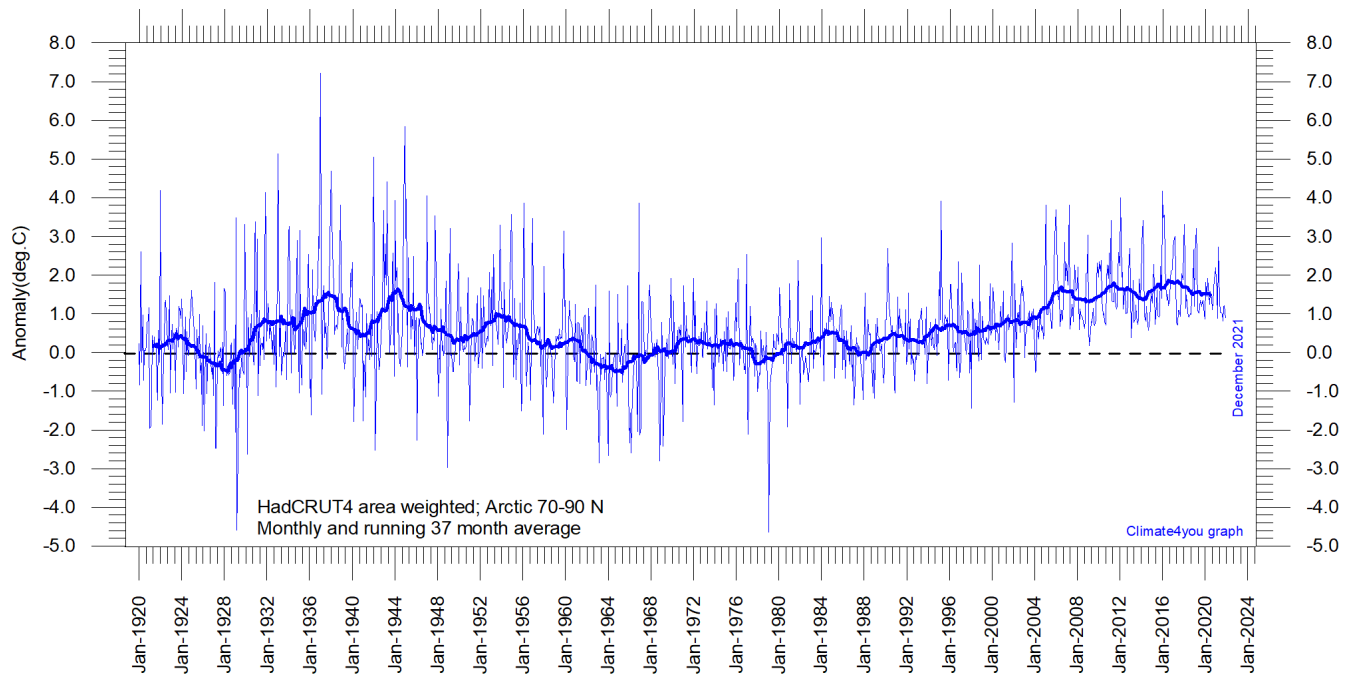


Diagram showing area-weighted Arctic (70-90°N) monthly surface air temperature anomalies ([HadCRUT4](#)) since January 1920, in relation to the WMO [normal period](#) 1961-1990. The thin line shows the monthly temperature anomaly, while the thicker line shows the running 37-month (c. 3 year) average.

Because of the relatively small number of Arctic stations before 1930, month-to-month variations in the early part of the Arctic temperature record 1920-2018 are higher than later (diagram above).

The period from about 1930 saw the establishment of many new Arctic meteorological stations, first in Russia and Siberia, and following the 2<sup>nd</sup> World War, also in North America, explaining the above difference.

The period since 2005 is warm, about as warm as the period 1930-1940.

As the HadCRUT4 data series has improved high latitude coverage data coverage (compared to the HadCRUT3 series), the individual 5°x5° grid cells have been weighted according to their surface area. This area correction is especially important for polar

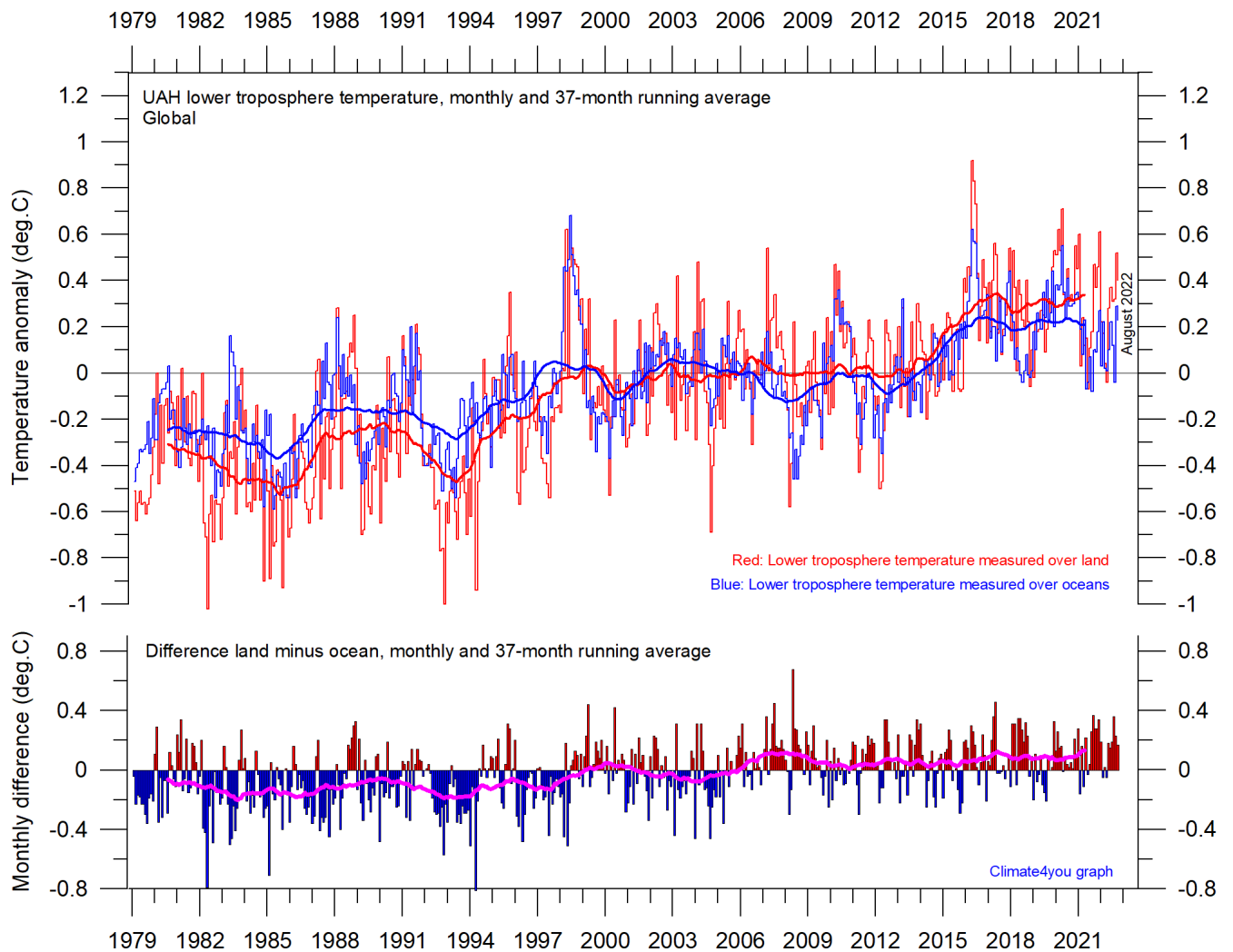
regions, where longitudes converge rapidly. This approach differs from the approach used by Gillett et al. 2008, which calculated a simple average, with no correction for the substantial latitudinal surface area effect in polar regions.

The area weighted Arctic HadCRUT4 surface air temperature anomalies (p.28-30) correspond rather well to the lower troposphere temperature anomalies recorded by satellites (p.27).

Literature:

Gillett, N.P., Stone, D.A., Stott, P.A., Nozawa, T., Karpechko, A.Y.U., Hegerl, G.C., Wehner, M.F. and Jones, P.D. 2008. Attribution of polar warming to human influence. *Nature Geoscience* 1, 750-754.

## Temperature over land versus over oceans, updated to August 2022

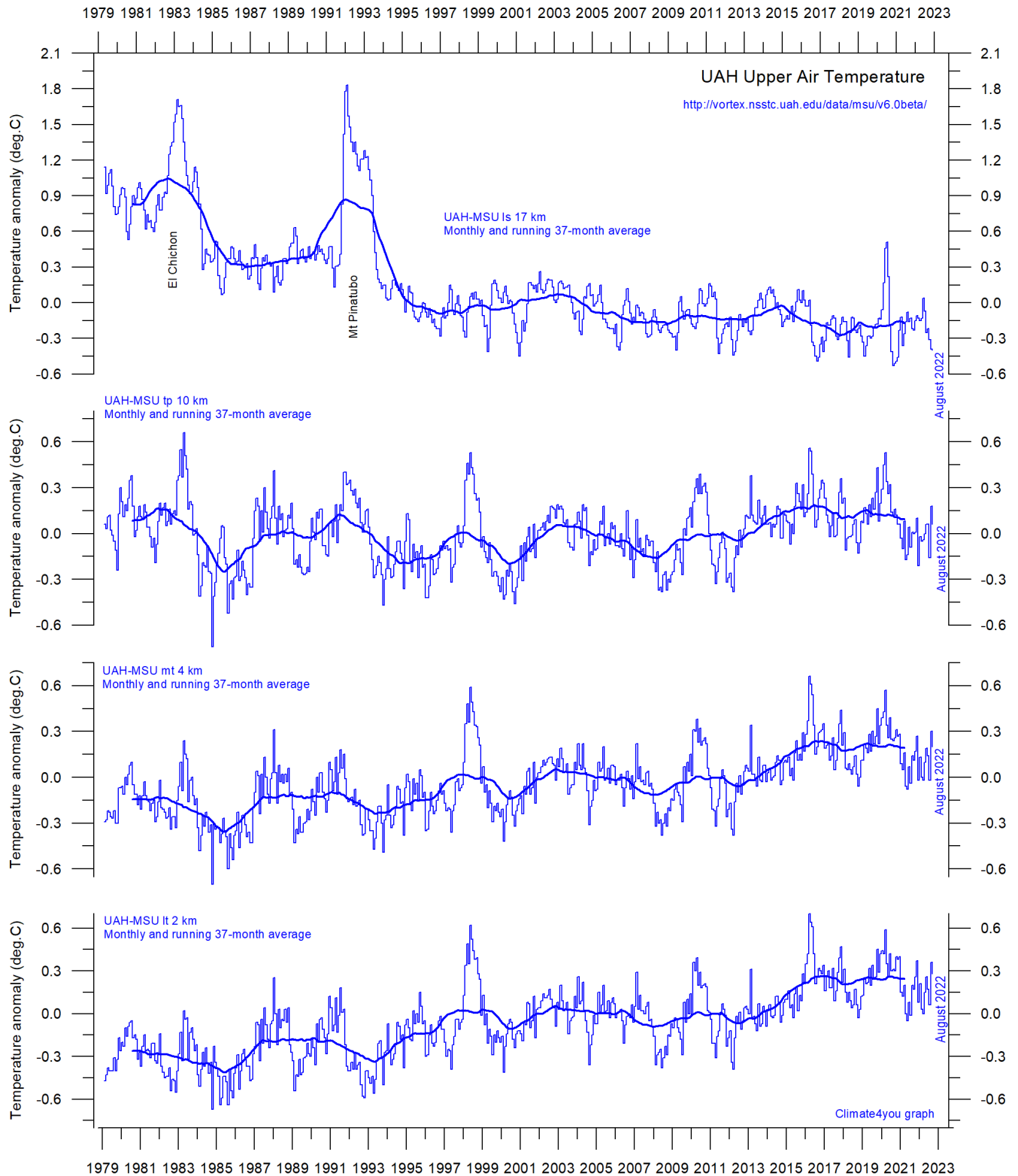


Global monthly average lower troposphere temperature since 1979 measured over land and oceans, respectively, according to [University of Alabama](#) at Huntsville, USA. Thick lines are the simple running 37-month average, nearly corresponding to a running 3-year average. Reference period 1991-2020.

Since 1979, the lower troposphere over land has warmed much more than over oceans, suggesting that the overall warming is derived mainly from incoming solar radiation. In addition, there may be

supplementary reasons for this divergence, such as, e.g., variations in cloud cover and changes in land use.

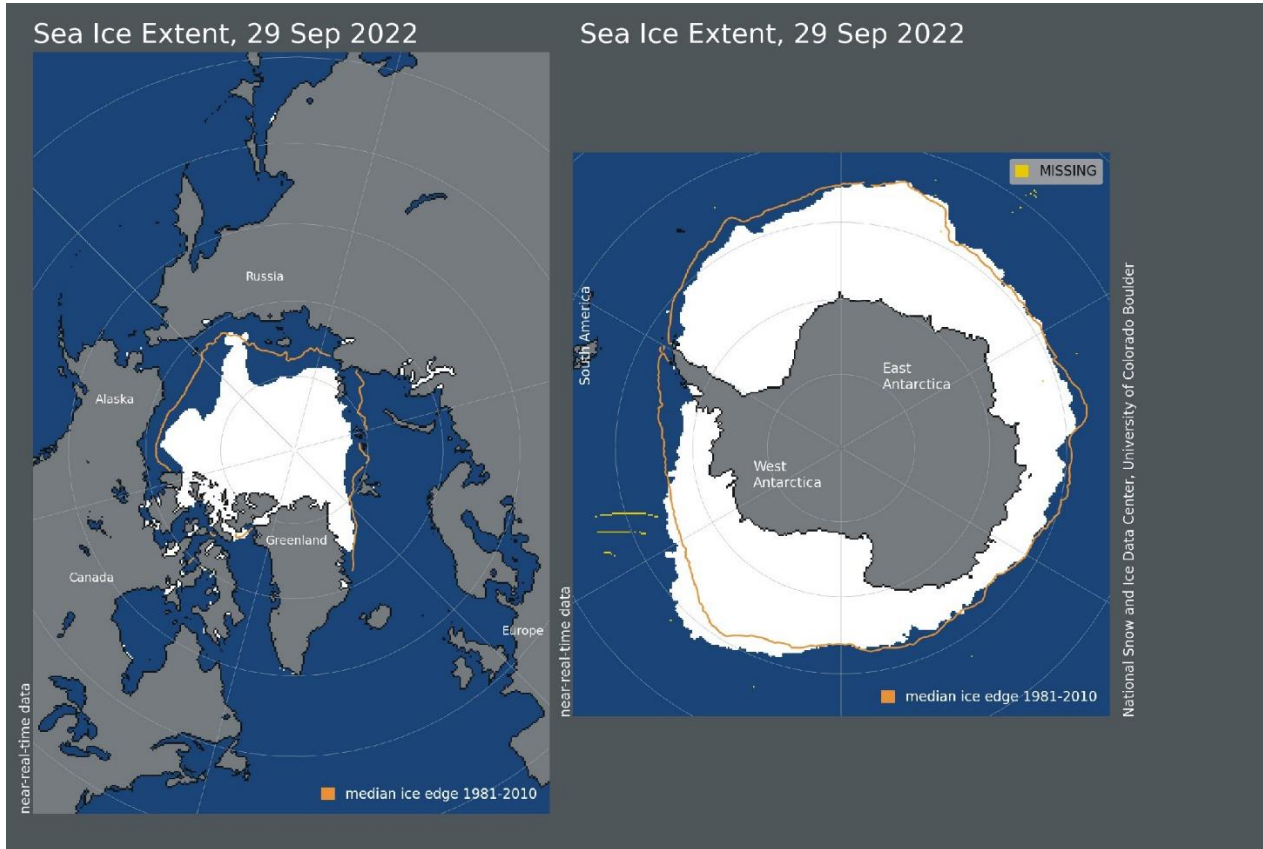
# Troposphere and stratosphere temperatures from satellites, updated to August 2022



Global monthly average temperature in different according to University of Alabama at Huntsville, USA. The thin lines represent the monthly average, and the thick line the simple running 37-month average, nearly corresponding to a running 3-year average. Reference period 1991-2020.

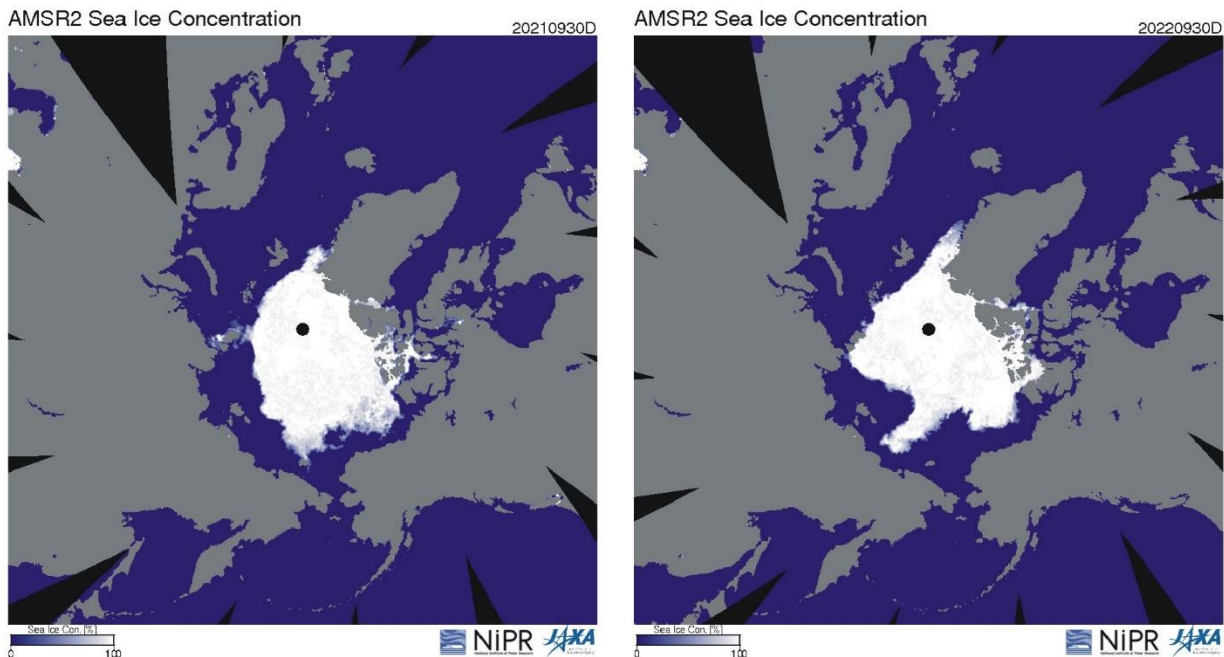


Arctic and Antarctic sea ice, updated to September 2022

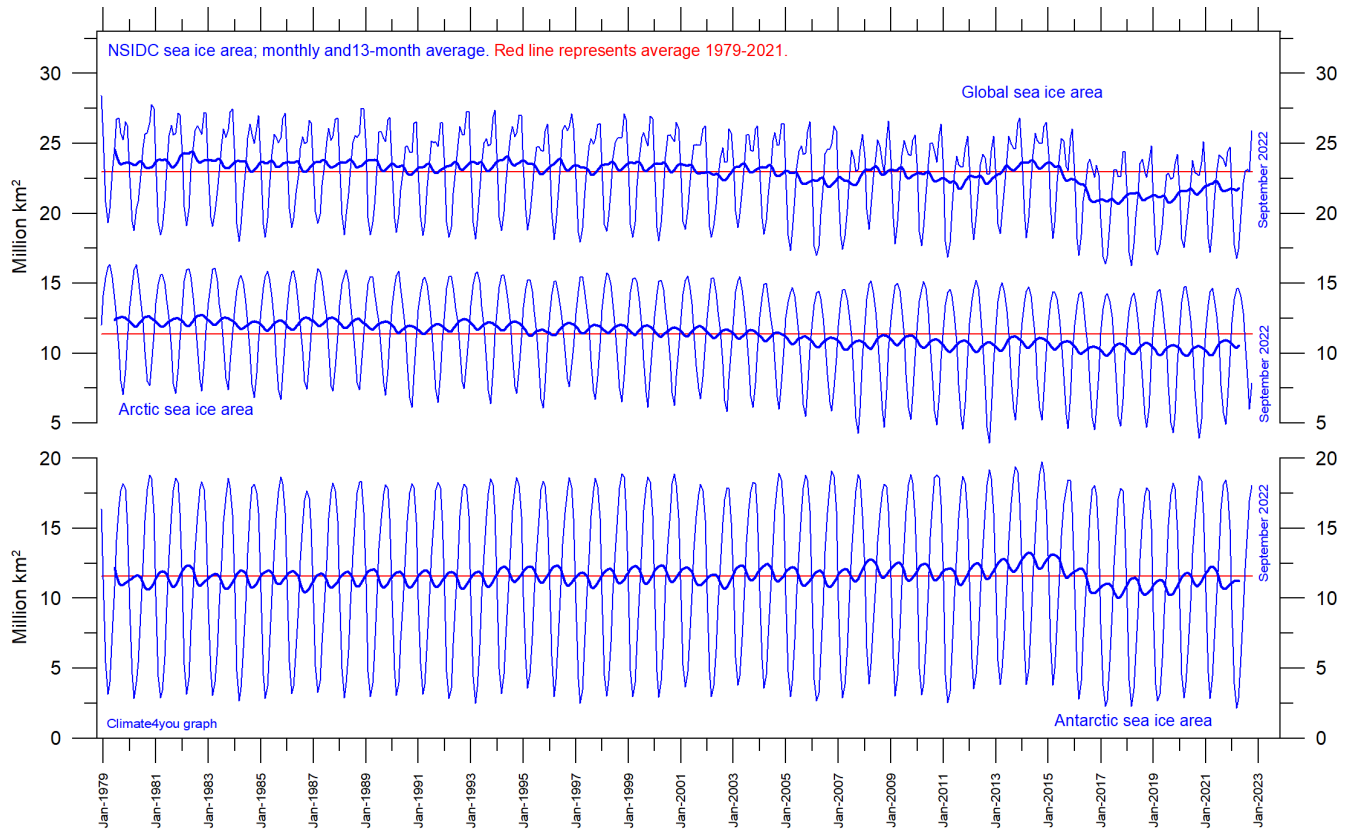


33

Sea ice extent 29 September 2022. The median limit of sea ice (orange line) is defined as 15% sea ice cover, according to the average of satellite observations 1981-2010 (both years included). Sea ice may therefore well be encountered outside and open water areas inside the limit shown in the diagrams above. Map source: National Snow and Ice Data Center (NSIDC).



Diagrams showing Arctic sea ice extent and concentration 30 September 2021 (left) and 2022 (right), according to the Japan Aerospace Exploration Agency (JAXA).



Graphs showing monthly Antarctic, Arctic, and global sea ice extent since November 1978, according to the [National Snow and Ice data Center \(NSIDC\)](#).

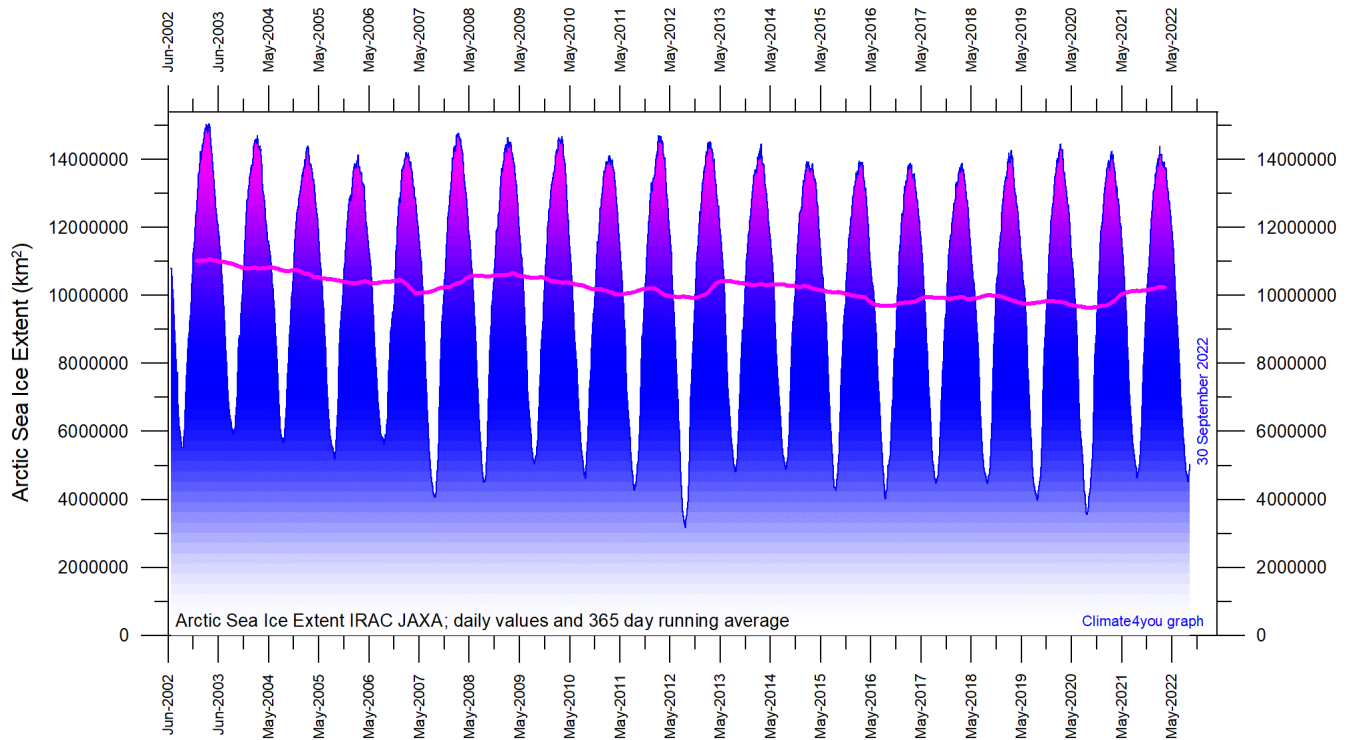
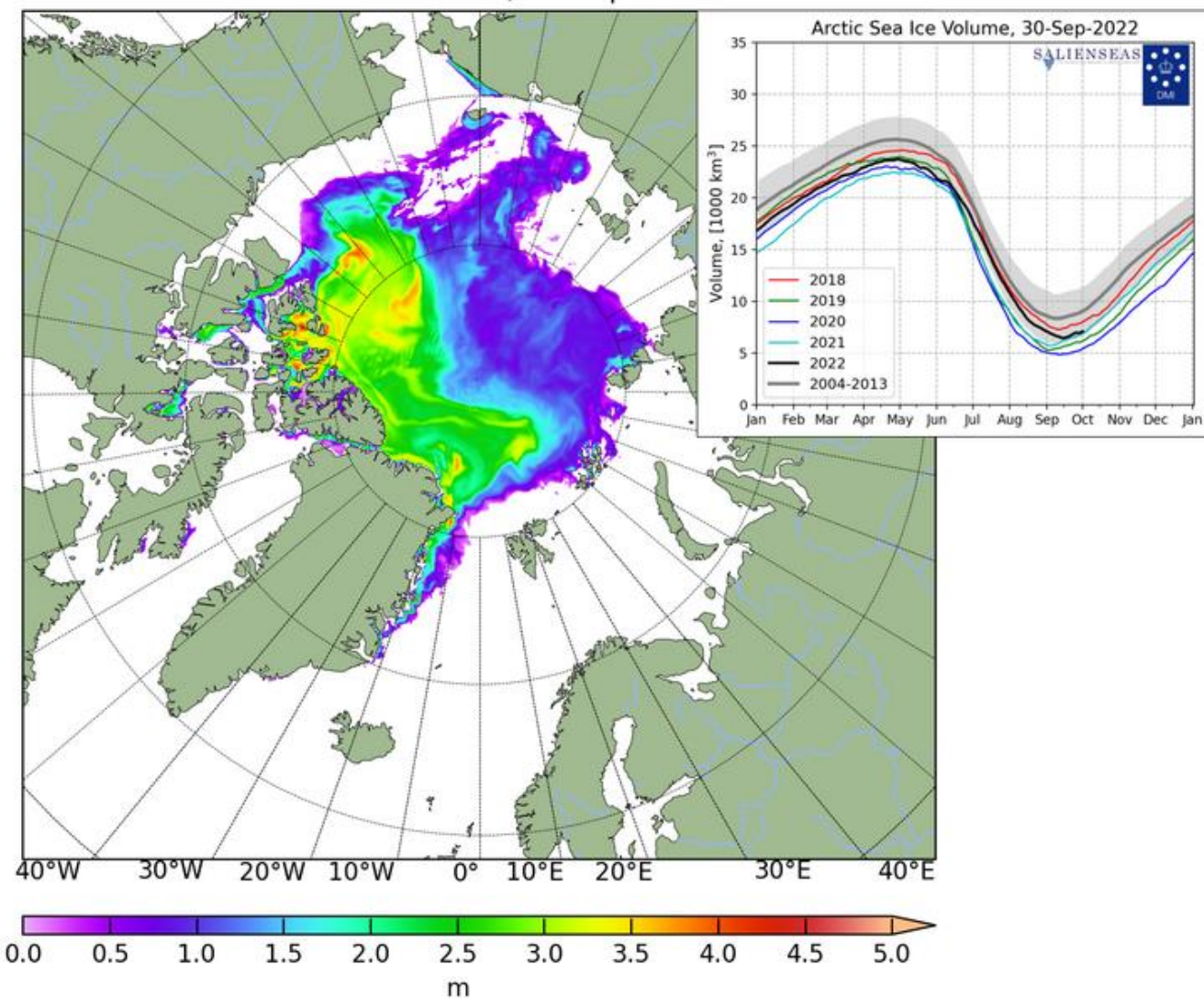
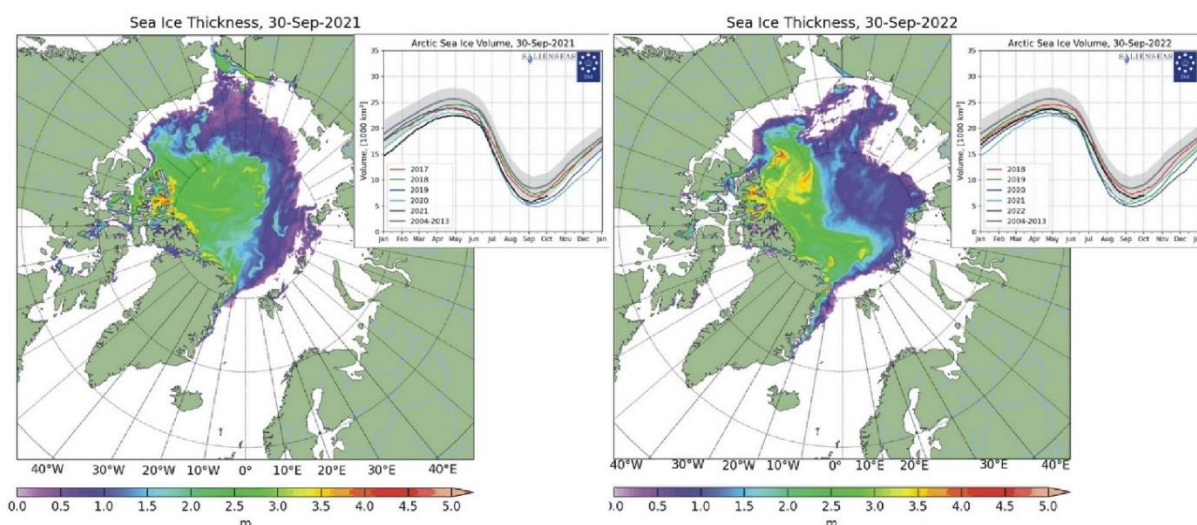


Diagram showing daily Arctic sea ice extent since June 2002, to 30 September 2022, by courtesy of [Japan Aerospace Exploration Agency \(JAXA\)](#).

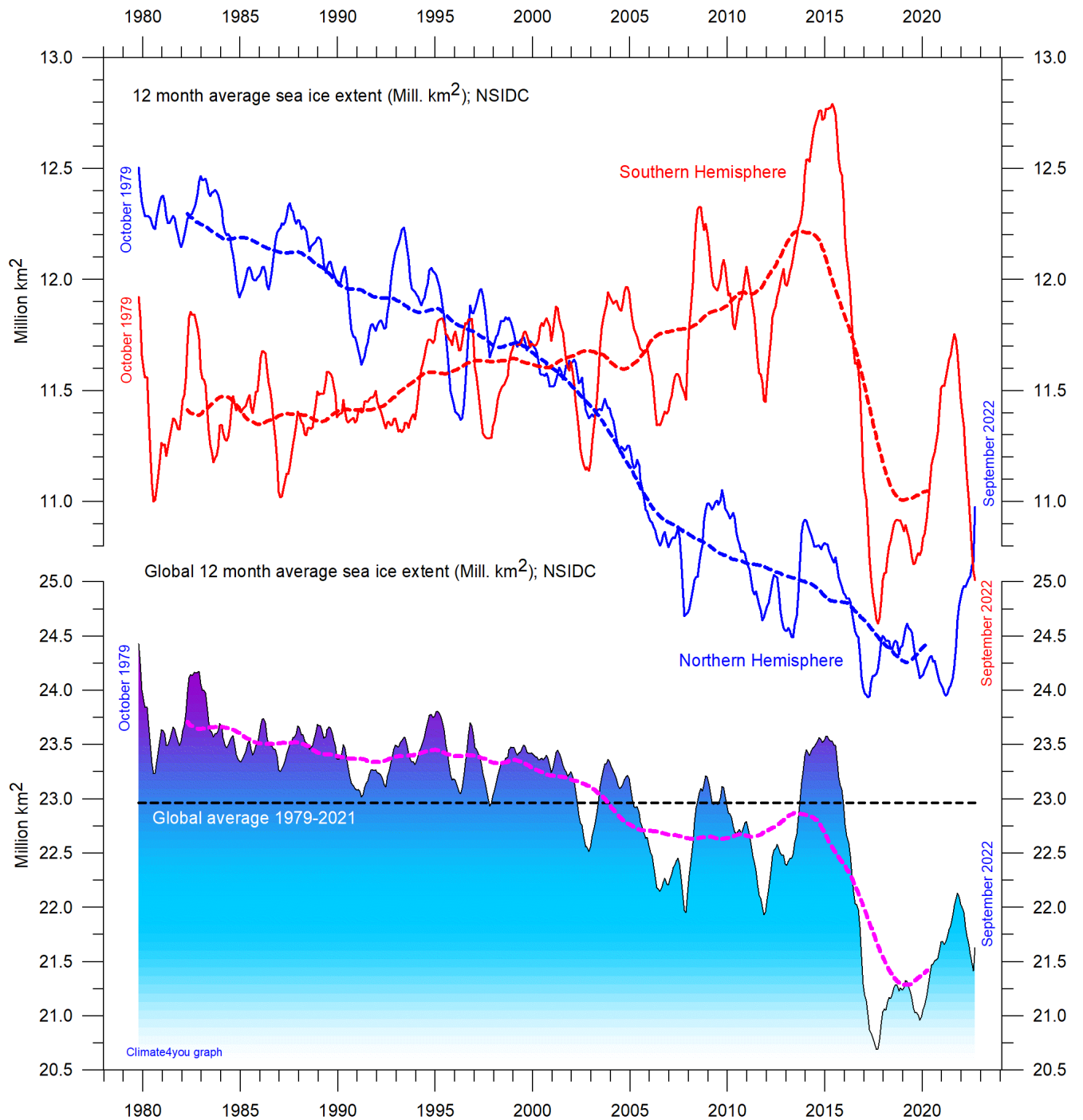
## Sea Ice Thickness, 30-Sep-2022



35



Diagrams showing Arctic sea ice extent and thickness 30 September 2021 (left) and 2022 (right and above) and the seasonal cycles of the calculated total arctic sea ice volume, according to [The Danish Meteorological Institute \(DMI\)](http://www.dmi.dk/). The mean sea ice volume and standard deviation for the period 2004-2013 are shown by grey shading. Please note that DMI on 7 December 2021 changed their sea ice calculation model. DMI's description of the model version change can be read here: <http://polarportal.dk/en/sea-ice-and-icebergs/sea-ice-thickness-and-volume/>



12 month running average sea ice extension, global and in both hemispheres since 1979, the satellite-era. The October 1979 value represents the monthly 12-month average of November 1978 - October 1979, the November 1979 value represents the average of December 1978 - November 1979, etc. The stippled lines represent a 61-month (ca. 5 years) average. Data source: National Snow and Ice Data Center (NSIDC).

## Sea level in general

Global (or eustatic) sea-level change is measured relative to an idealised reference level, the geoid, which is a mathematical model of planet Earth's surface (Carter et al. 2014). Global sea-level is a function of the volume of the ocean basins and the volume of water they contain. Changes in global sea-level are caused by – but not limited to - four main mechanisms:

1. Changes in local and regional air pressure and wind, and tidal changes introduced by the Moon.
2. Changes in ocean basin volume by tectonic (geological) forces.
3. Changes in ocean water density caused by variations in currents, water temperature and salinity.
4. Changes in the volume of water caused by changes in the mass balance of terrestrial glaciers.

In addition to these there are other mechanisms influencing sea-level, such as storage of ground water, storage in lakes and rivers, evaporation, etc.

Mechanism 1 is controlling sea-level at many sites on a time scale from months to several years. As an example, many coastal stations show a pronounced annual variation reflecting seasonal changes in air pressures and wind speed. Longer-term climatic changes playing out over decades or centuries will also affect measurements of sea-level changes. Hansen et al. (2011, 2015) provide excellent analyses of sea-level changes caused by recurrent changes of the orbit of the Moon and other phenomena.

Mechanism 2 – with the important exception of earthquakes and tsunamis - typically operates over long (geological) time scales and is not significant on human time scales. It may relate to variations in the seafloor spreading rate, causing volume changes in mid-ocean mountain ridges, and to the slowly changing configuration of land and oceans. Another effect may be the slow rise of basins due to isostatic offloading by deglaciation after an ice age. The floor of the Baltic Sea and the Hudson Bay are presently rising, causing a slow net transfer of

water from these basins into the adjoining oceans. Slow changes of excessively big glaciers (ice sheets) and movements in the mantle will affect the gravity field and thereby the vertical position of the ocean surface. Any increase of the total water mass as well as sediment deposition into oceans increase the load on their bottom, generating sinking by viscoelastic flow in the mantle below. The mantle flow is directed towards the surrounding land areas, which will rise, thereby partly compensating for the initial sea level increase induced by the increased water mass in the ocean.

Mechanism 3 (temperature-driven expansion) only affects the uppermost part of the oceans on human time scales. Usually, temperature-driven changes in density are more important than salinity-driven changes. Seawater is characterised by a relatively small coefficient of expansion, but the effect should however not be overlooked, especially when interpreting satellite altimetry data. Temperature-driven expansion of a column of seawater will not affect the total mass of water within the column considered and will therefore not affect the potential at the top of the water column. Temperature-driven ocean water expansion will therefore not in itself lead to any lateral displacement of water, but only locally lift the ocean surface. Near the coast, where people are living, the depth of water approaches zero, so no measurable temperature-driven expansion will take place here (Mörner 2015). Mechanism 3 is for that reason not important for coastal regions.

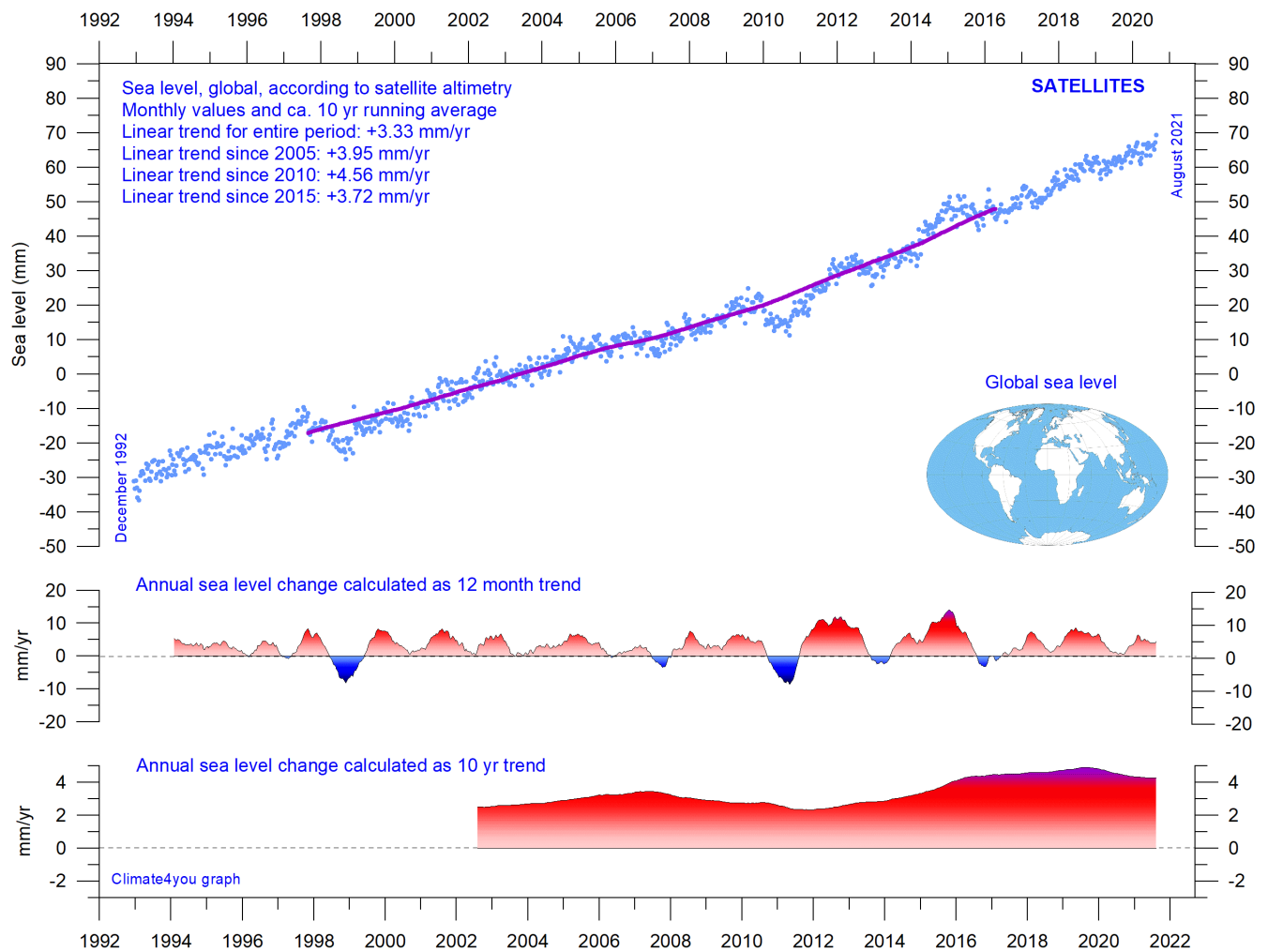
Mechanism 4 (changes in glacier mass balance) is an important driver for global sea-level changes along coasts, for human time scales. Volume changes of floating glaciers – ice shelves – has no influence on the global sea-level, just like volume changes of floating sea ice has no influence. Only the mass-balance of grounded or land-based glaciers is important for the global sea-level along coasts.

Summing up: Presumably, mechanism 1 and 4 are the most important for understanding sea-level changes along coasts.

### References:

- Carter R.M., de Lange W., Hansen, J.M., Humlum O., Idso C., Kear, D., Legates, D., Mörner, N.A., Ollier C., Singer F. & Soon W. 2014. Commentary and Analysis on the Whitehead& Associates 2014 NSW Sea-Level Report. Policy Brief, NIPCC, 24. September 2014, 44 pp. <http://climatechangereconsidered.org/wp-content/uploads/2014/09/NIPCC-Report-on-NSW-Coastal-SL-9z-corrected.pdf>
- Hansen, J.-M., Aagaard, T. and Binderup, M. 2011. Absolute sea levels and isostatic changes of the eastern North Sea to central Baltic region during the last 900 years. *Boreas*, 10.1111/j.1502-3885.2011.00229.x. ISSN 0300-9483.
- Hansen, J.-M., Aagaard, T. and Huijpers, A. 2015. Sea-Level Forcing by Synchronization of 56- and 74-Year Oscillations with the Moon's Nodal Tide on the Northwest European Shelf (Eastern North Sea to Central Baltic Sea). *Journ. Coastal Research*, 16 pp.
- Mörner, Nils-Axel 2015. Sea Level Changes as recorded in nature itself. *Journal of Engineering Research and Applications*, Vol.5, 1, 124-129.

## Global sea level from satellite altimetry, updated to August 2021



Global sea level since December 1992 according to the Colorado Center for Astrodynamics Research at University of Colorado at Boulder. The blue dots are the individual observations, and the purple line represents the running 121-month (ca. 10 year) average. The two lower panels show the annual sea level change, calculated for 1 and 10-year time windows, respectively. These values are plotted at the end of the interval considered.

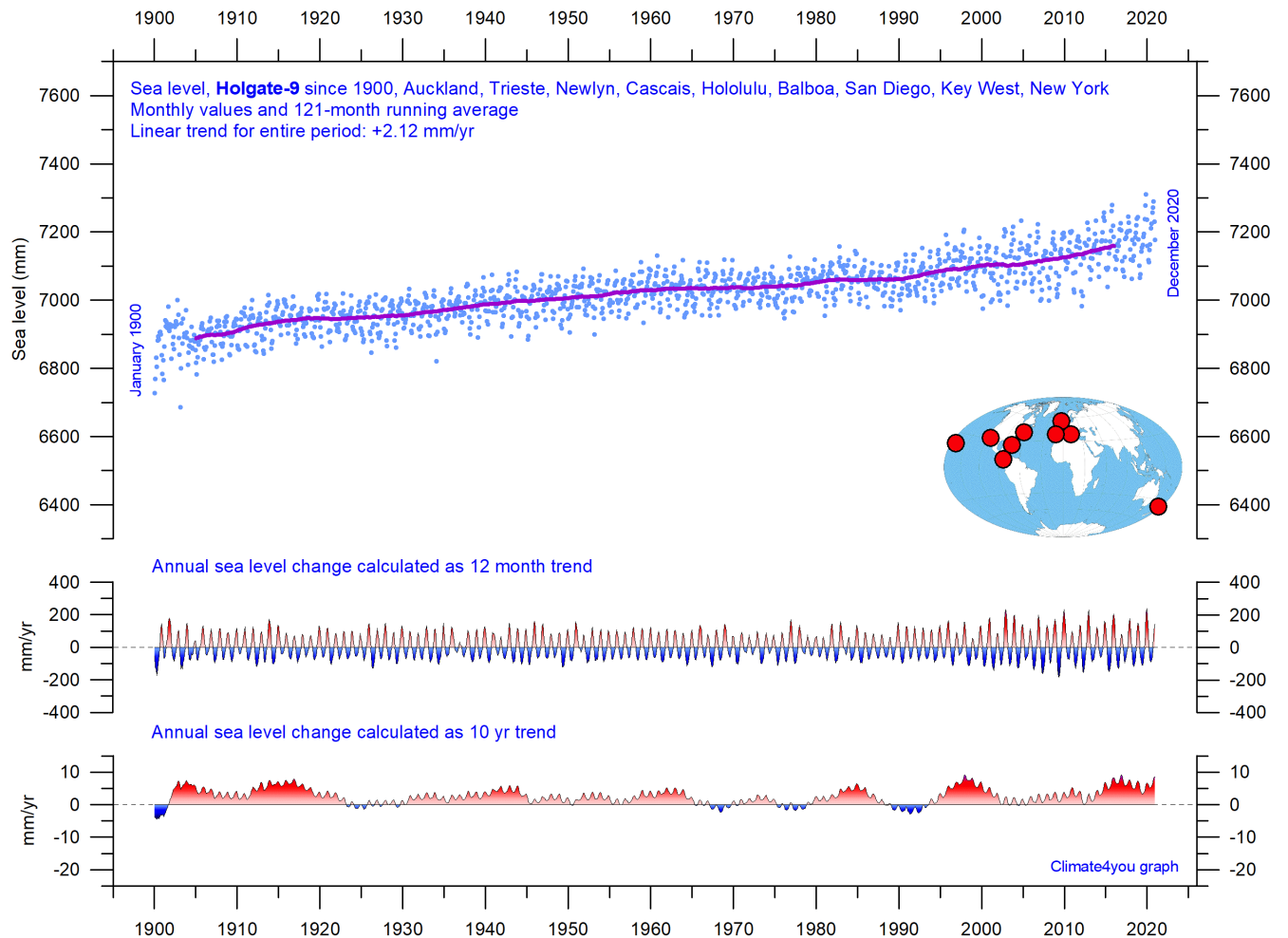
**Ground truth** is a term used in various fields to refer to information provided by direct observation as opposed to information provided by inference, such as, e.g., by satellite observations.

In remote sensing using satellite observations, ground truth data refers to information collected on location. Ground truth allows the satellite data to be related to real features observed on the planet surface. The collection of ground truth data enables calibration of remote-sensing

data, and aids in the interpretation and analysis of what is being sensed or recorded by satellites. Ground truth sites allow the remote sensor operator to correct and improve the interpretation of satellite data.

For satellite observations on sea level ground true data are provided by the classical tide gauges (example diagram on next page), that directly measures the local sea level many places distributed along the coastlines on the surface of the planet.

## Global sea level from tide-gauges, updated to December 2020



*Holgate-9* monthly tide gauge data from PSMSL Data Explorer. *Holgate (2007)* suggested the nine stations listed in the diagram to capture the variability found in a larger number of stations over the last half century studied previously. For that reason, average values of the *Holgate-9* group of tide gauge stations are interesting to follow, even though Auckland (New Zealand) has not reported data since 2000, and Cascais (Portugal) not since 1993. Unfortunately, by this data loss the *Holgate-9* series since 2000 is underrepresented with respect to the southern hemisphere and should therefore not be overinterpreted. The blue dots are the individual average monthly observations, and the purple line represents the running 121-month (ca. 10 year) average. The two lower panels show the annual sea level change, calculated for 1 and 10-year windows, respectively. These values are plotted at the end of the interval considered.

Data from tide-gauges all over the world suggest an average global sea-level rise of 1-2 mm/year, while the satellite-derived record (page 37) suggest a rise of about 3.3 mm/year, or more. The noticeable difference (about 1:2) between the two data sets is remarkable but has no

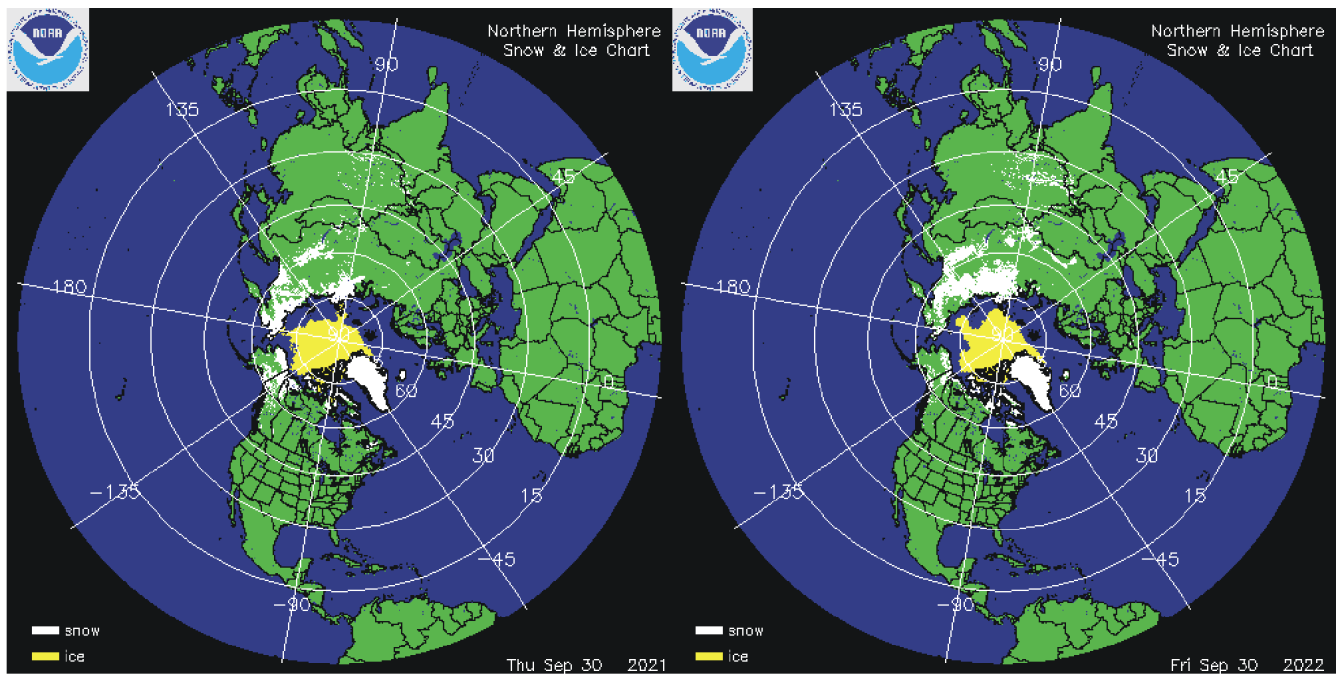
generally accepted explanation. It is however known that satellite observations are facing several complications in areas near the coast. Vignudelli et al. (2019) provide an updated overview of the current limitations of classical satellite altimetry in coastal regions.

### References:

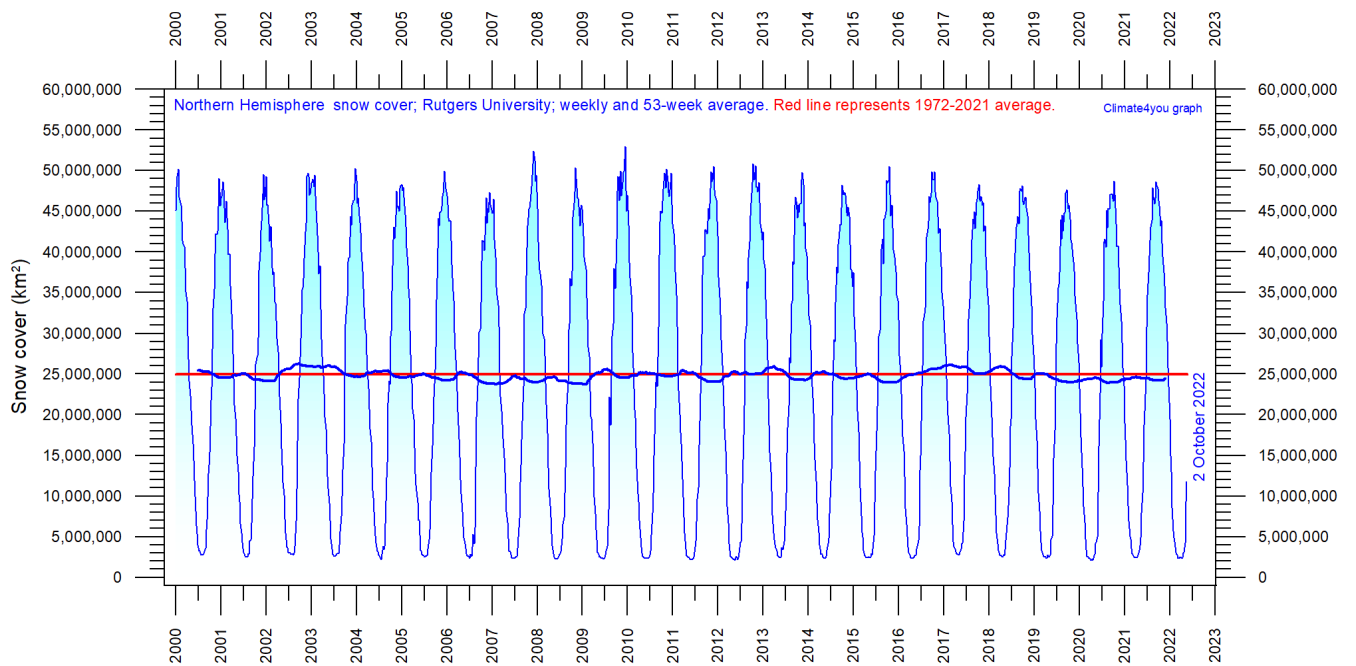
Holgate, S.J. 2007. On the decadal rates of sea level change during the twentieth century. *Geophys. Res. Letters*, 34, L01602, doi:10.1029/2006GL028492

Vignudelli et al. 2019. Satellite Altimetry Measurements of Sea Level in the Coastal Zone. *Surveys in Geophysics*, Vol. 40, p. 1319–1349. <https://link.springer.com/article/10.1007/s10712-019-09569-1>

**Northern Hemisphere weekly and seasonal snow cover, updated to September 2022**

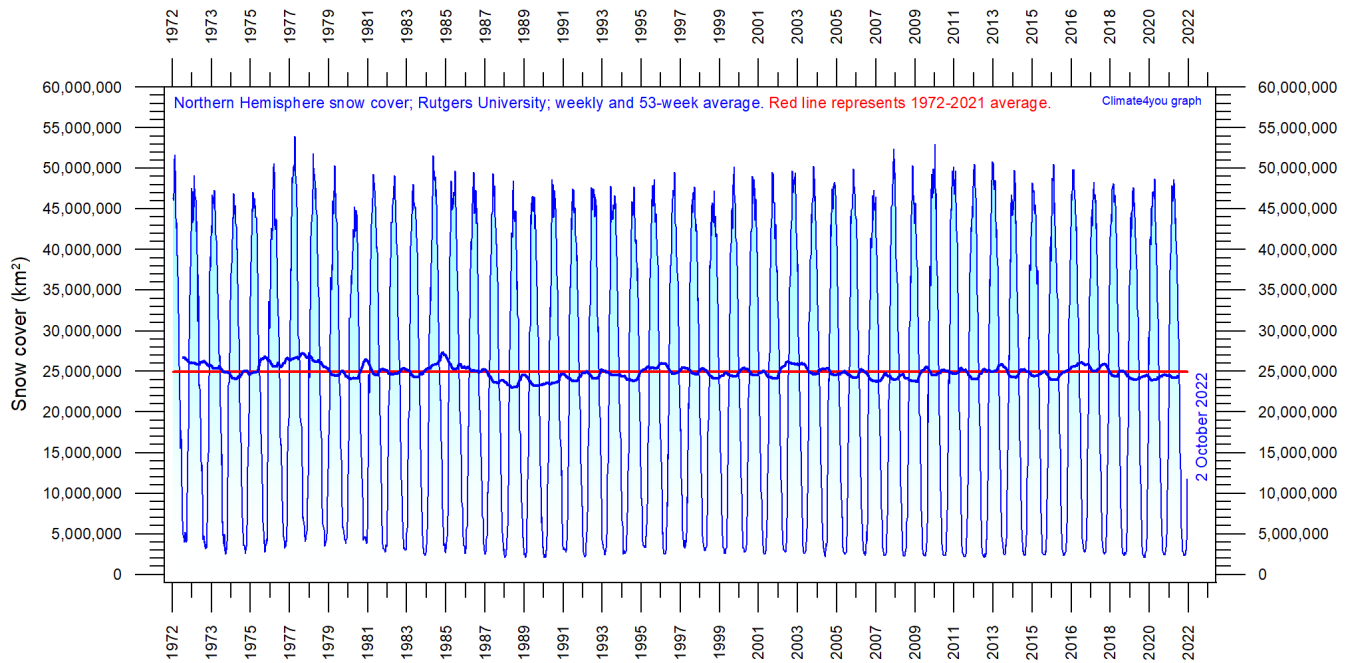


Northern hemisphere snow cover (white) and sea ice (yellow) 30 September 2021 (left) and 2022 (right). Map source: [National Ice Center \(NIC\)](#).

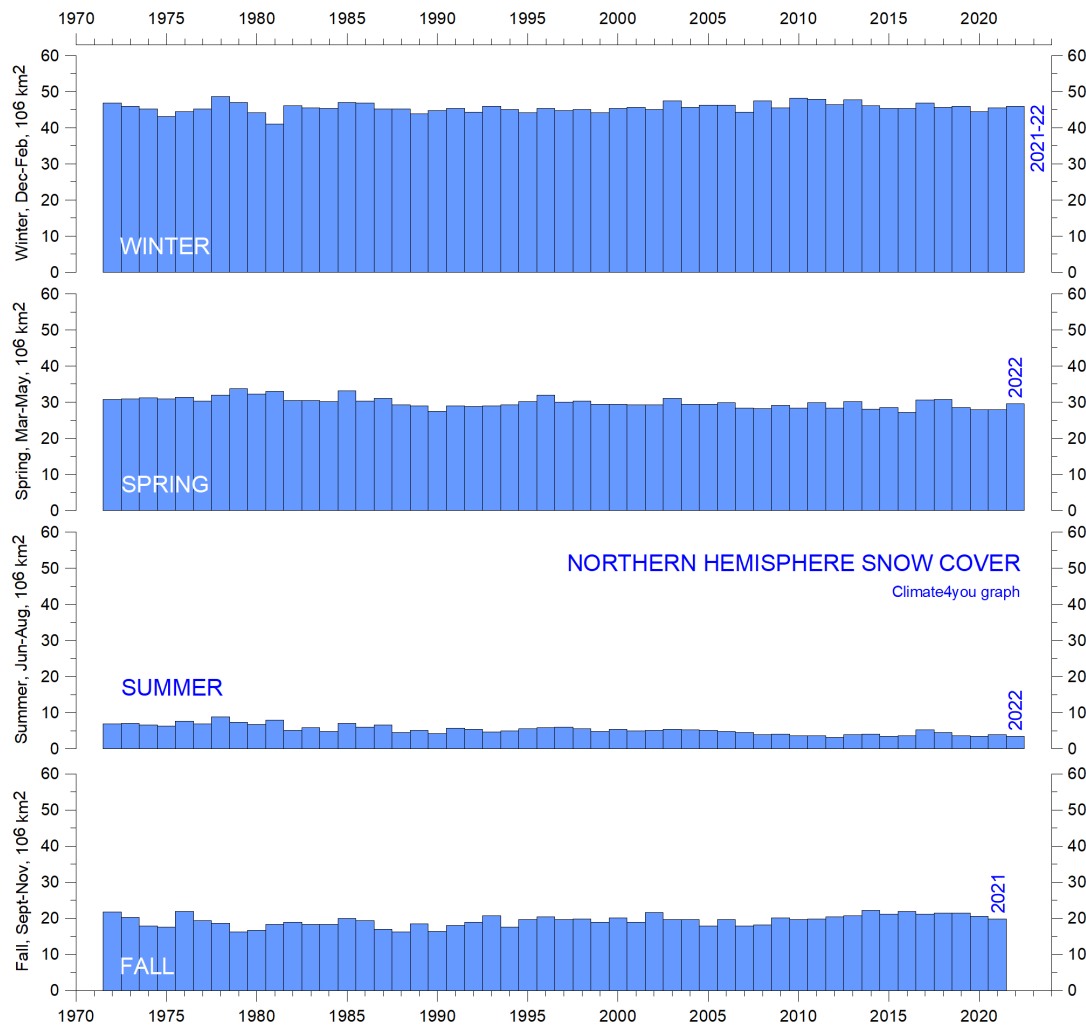


Northern hemisphere weekly snow cover since January 2000 according to Rutgers University Global Snow Laboratory. The thin blue line is the weekly data, and the thick blue line is the running 53-week average (approximately 1 year). The horizontal red line is the 1972-2021 average.





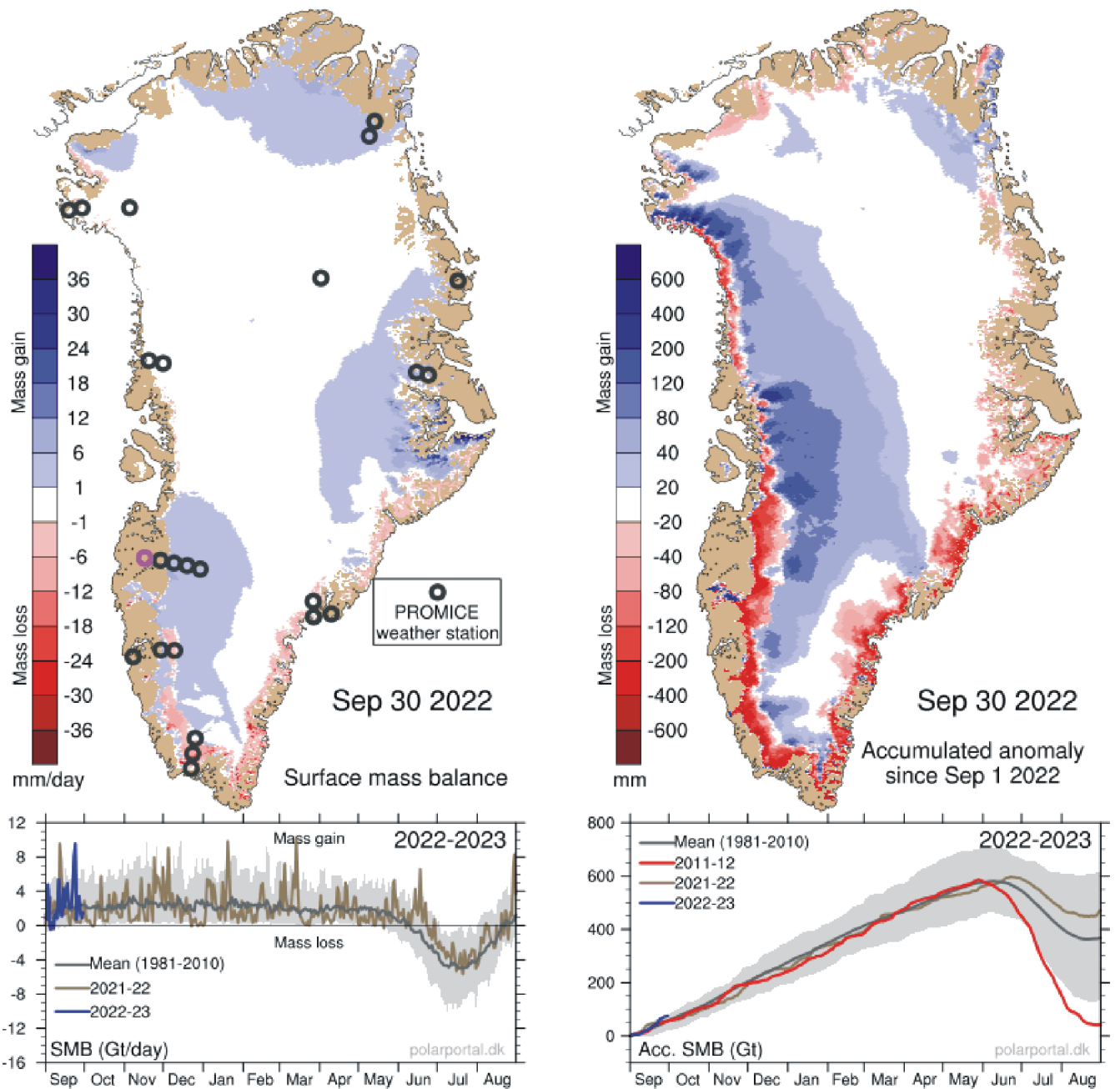
Northern hemisphere weekly snow cover since January 1972 according to Rutgers University Global Snow Laboratory. The thin blue line is the weekly data, and the thick blue line is the running 53-week average (approximately 1 year). The horizontal red line is the 1972-2021 average.



Northern hemisphere seasonal snow cover since January 1972 according to Rutgers University Global Snow Laboratory.

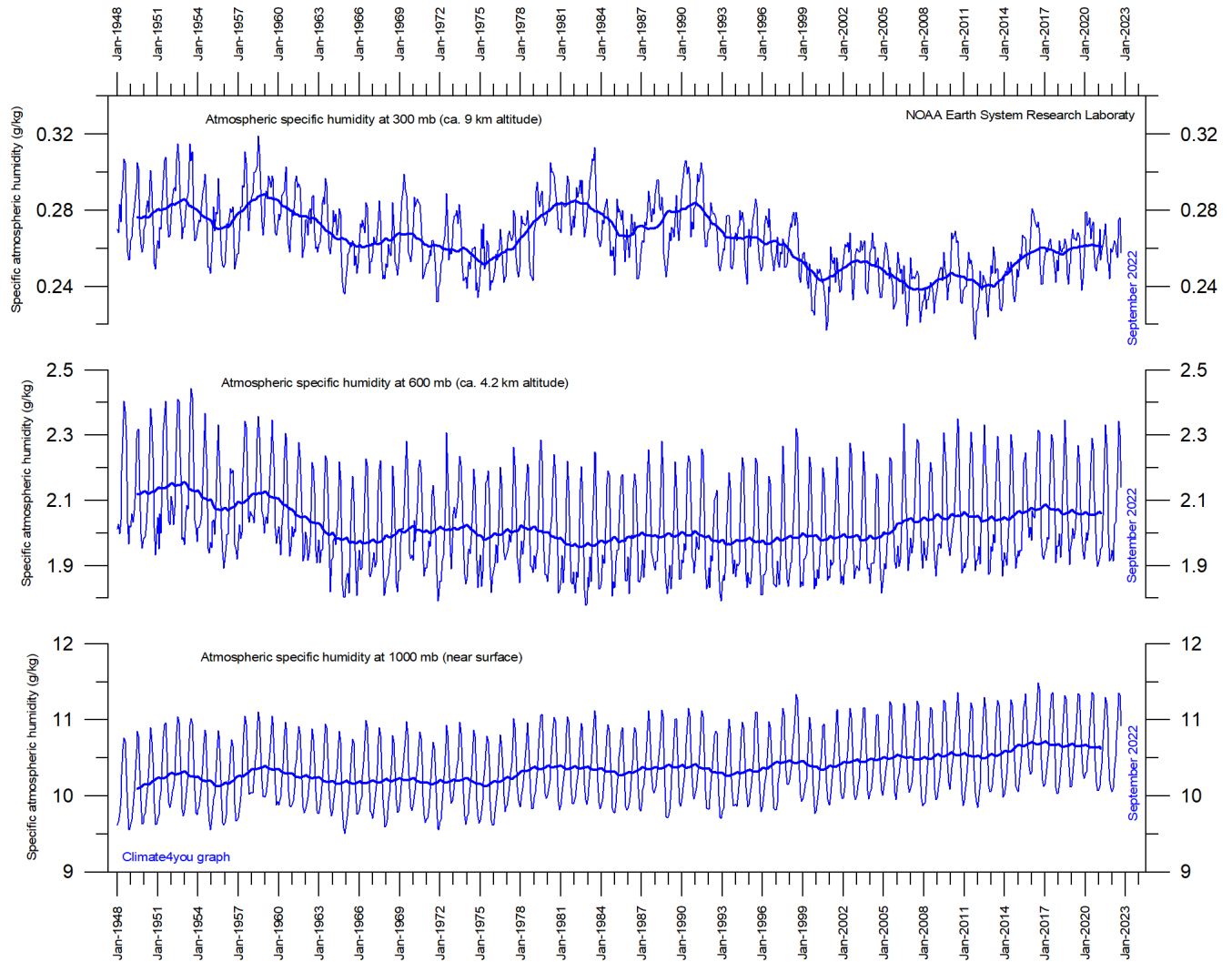
Greenland Ice Sheet net surface mass balance, updated to September 2022

42



Left: Surface mass balance 30 September 2022. Right: Net surface mass balance anomaly since September 1, 2022. Courtesy of Danish Meteorological Institute (DMI).

## Atmospheric specific humidity, updated to September 2022



[Specific atmospheric humidity](#) (g/kg) at three different altitudes in the lower part of the atmosphere ([the Troposphere](#)) since January 1948 ([Kalnay et al. 1996](#)). The thin blue lines show monthly values, while the thick blue lines show the running 37-month average (about 3 years). Data source: [Earth System Research Laboratory \(NOAA\)](#).

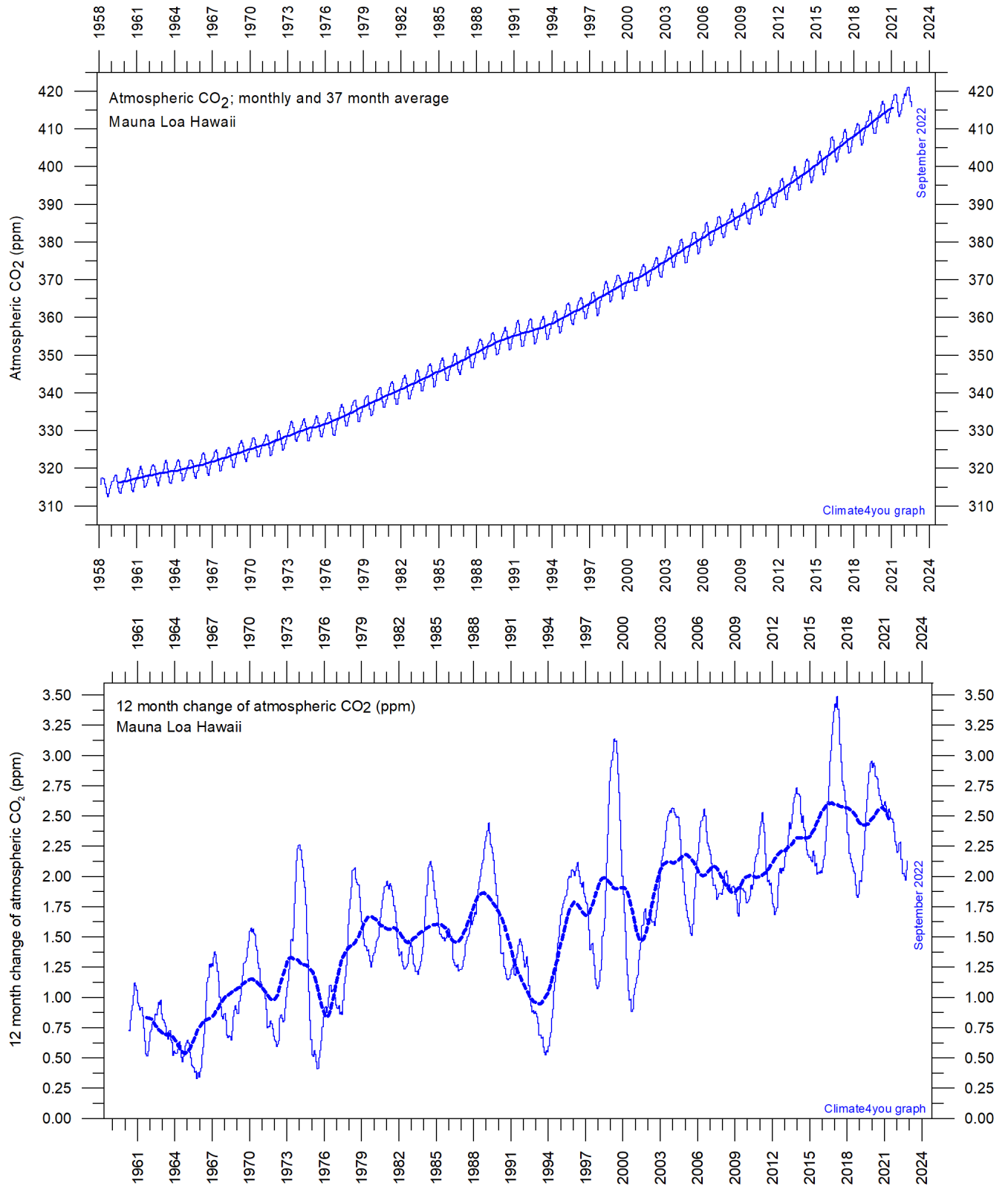
Water vapor is the most important greenhouse gas in the Troposphere. The highest concentration is found within a latitudinal range from 50°N to 60°S. The two polar regions of the Troposphere are comparatively dry.

The diagram above shows the specific atmospheric humidity to be stable or slightly increasing up to about 4-5 km altitude. At higher levels in the Troposphere (about 9 km), the specific humidity has been decreasing for the duration of the record (since 1948), but with shorter

variations superimposed on the falling trend. A Fourier frequency analysis (not shown here) shows these variations to be influenced especially by a periodic variation of about 3.7-year duration.

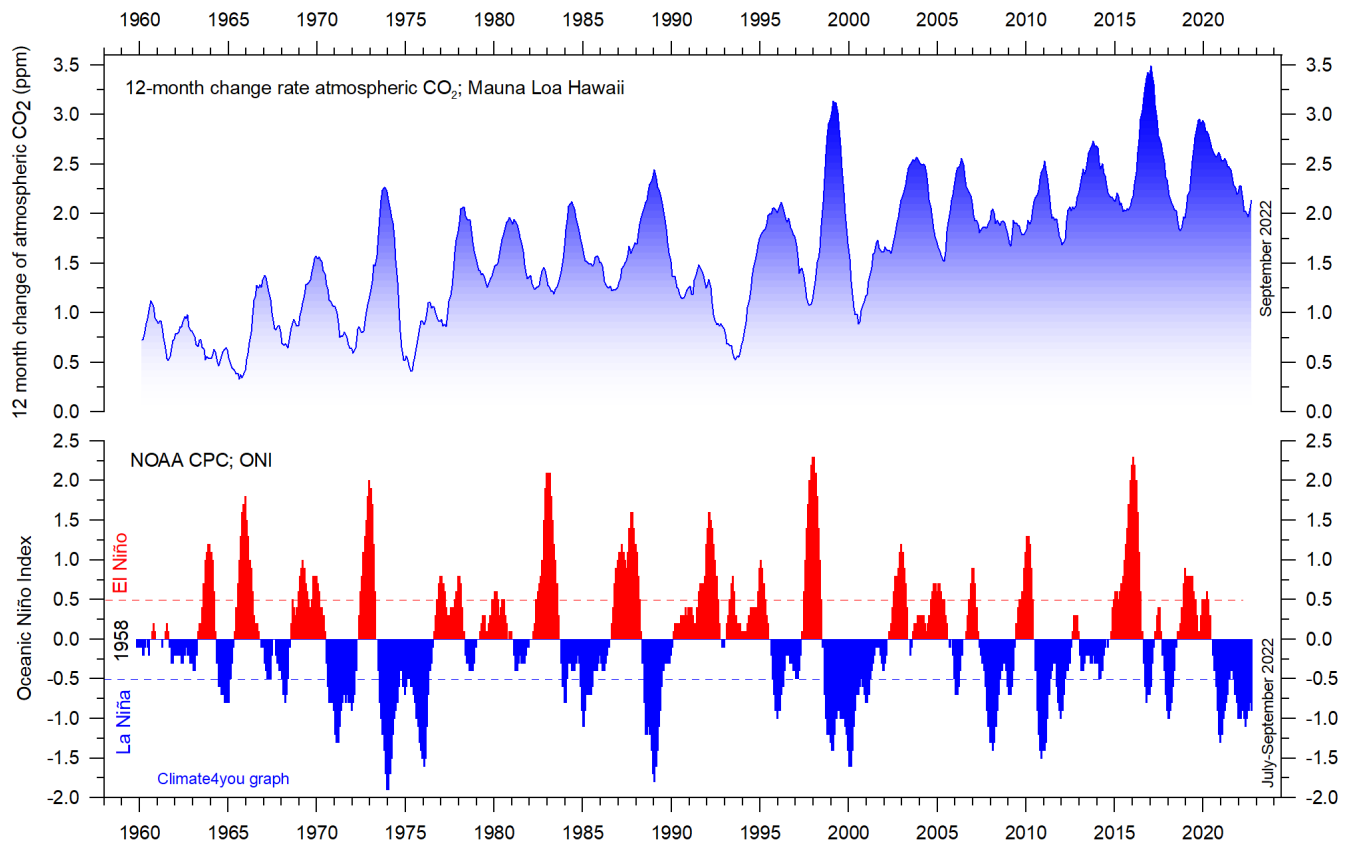
The persistent decrease in specific humidity at about 9 km altitude is particularly noteworthy, as this altitude roughly corresponds to the level where the theoretical temperature effect of increased atmospheric CO<sub>2</sub> is expected initially to play out.

## Atmospheric CO<sub>2</sub>, updated to September 2022



Monthly amount of atmospheric CO<sub>2</sub> (upper diagram) and annual growth rate (lower diagram); average last 12 months minus average preceding 12 months, thin line) of atmospheric CO<sub>2</sub> since 1959, according to data provided by the [Mauna Loa Observatory](#), Hawaii, USA. The thick, stippled line is the simple running 37-observation average, nearly corresponding to a running 3-year average. A Fourier frequency analysis (not shown here) shows the 12-month change of Tropospheric CO<sub>2</sub> to be influenced especially by periodic variations of 2.5- and 3.8-years' duration.

## The relation between annual change of atmospheric CO<sub>2</sub> and La Niña and El Niño episodes, updated to September 2022



45

*Visual association between annual growth rate of atmospheric CO<sub>2</sub> (upper panel) and Oceanic Niño Index (lower panel). See also diagrams on page 40 and 22, respectively.*

Changes in the global atmospheric CO<sub>2</sub> is seen to vary roughly in concert with changes in the Oceanic Niño Index. The typical sequence of events is that changes in the global atmospheric CO<sub>2</sub> to a certain degree follows changes in the Oceanic Niño Index, but clearly not in all details. Many processes, natural as well as anthropogenic, controls the amount of atmospheric CO<sub>2</sub>, but oceanographic processes are clearly particularly important (see also diagram on next page).

### Atmospheric CO<sub>2</sub> and the present coronavirus pandemic

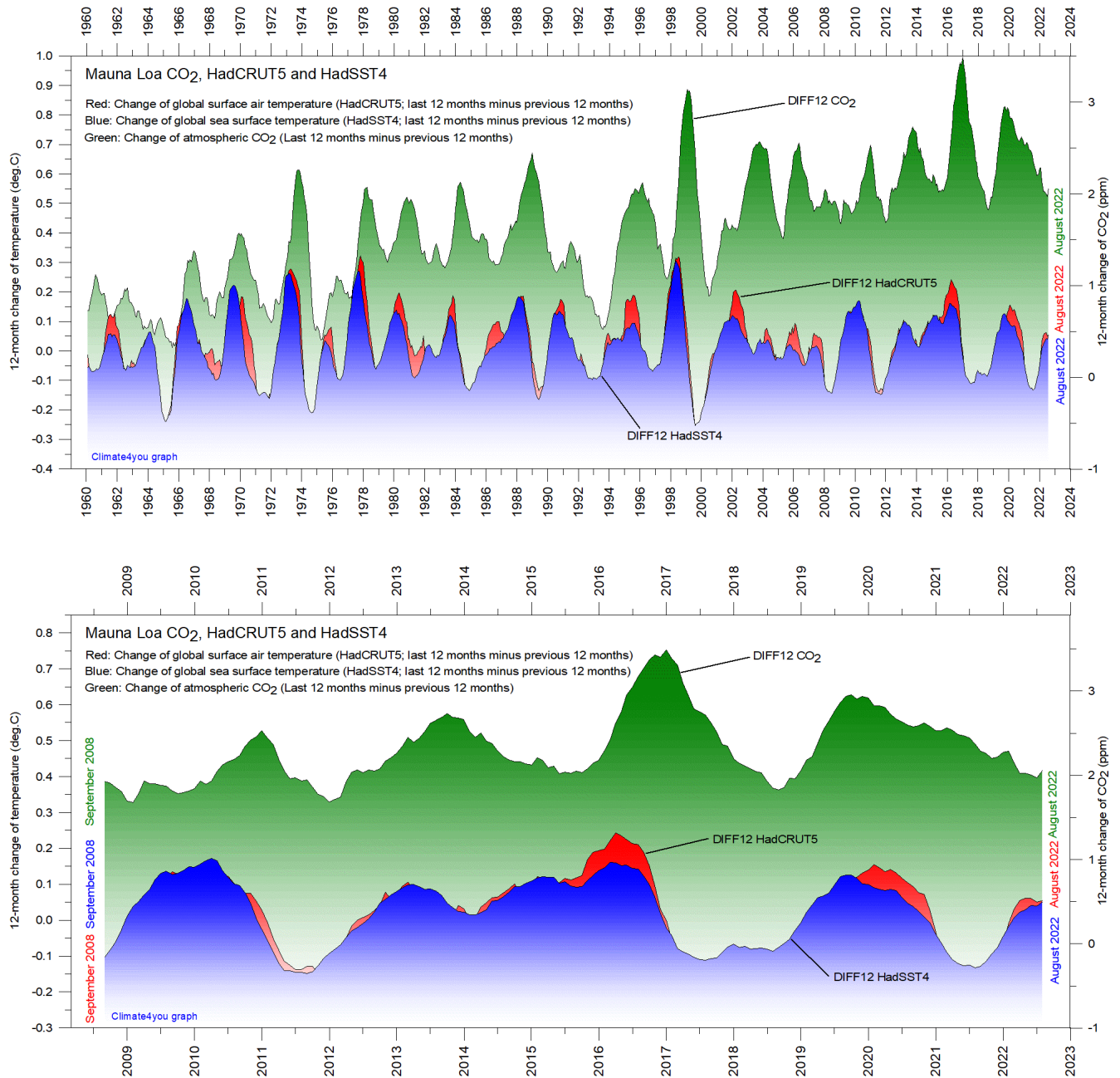
Modern political initiatives usually assume the human influence (mainly the burning of fossil fuels) to represent

the core reason for the observed increase in atmospheric CO<sub>2</sub> since 1958 (diagrams on page 43).

The coronavirus pandemic since January 2020 resulted in a marked reduction in the global consumption of fossil fuels. It is therefore enlightening to follow the effect of this reduction on the amount of atmospheric CO<sub>2</sub>.

However, there is still no clear effect to be seen of the above reduction in release of CO<sub>2</sub> from fossil fuels. Presumably, the main explanation for this is that the human contribution is too small compared to the numerous natural sources and sinks for atmospheric CO<sub>2</sub> to appear in diagrams showing the amount of atmospheric CO<sub>2</sub> (see, e.g., diagrams on p. 43-45).

## The phase relation between atmospheric CO<sub>2</sub> and global temperature, updated to August 2022



12-month change of global atmospheric CO<sub>2</sub> concentration ([Mauna Loa](#); green), global sea surface temperature ([HadSST4](#); blue) and global surface air temperature ([HadCRUT5](#); red dotted). Entire data series since 1958 in upper figure, and last 15 years in lower figure, to enhance modern dynamics. All graphs are showing monthly values of DIFF12, the difference between the average of the last 12 month and the average for the previous 12 months for each data series.

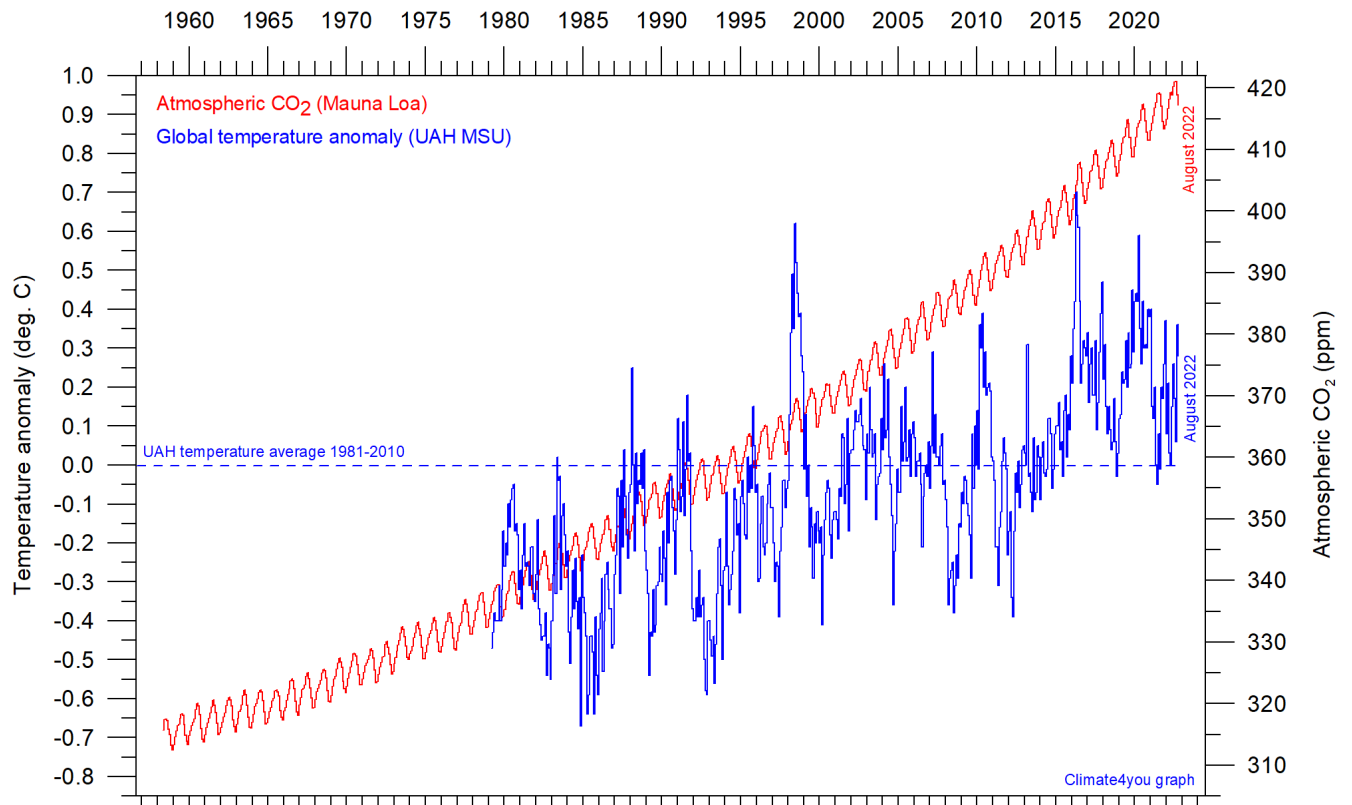
The typical sequence of events is seen to be that changes in the global atmospheric CO<sub>2</sub> follow changes in global surface air temperature, which again follow changes in global ocean surface temperatures. Thus, changes in

global atmospheric CO<sub>2</sub> usually are lagging 9.5–10 months behind changes in global air surface temperature, and 11–12 months behind changes in global sea surface temperature.

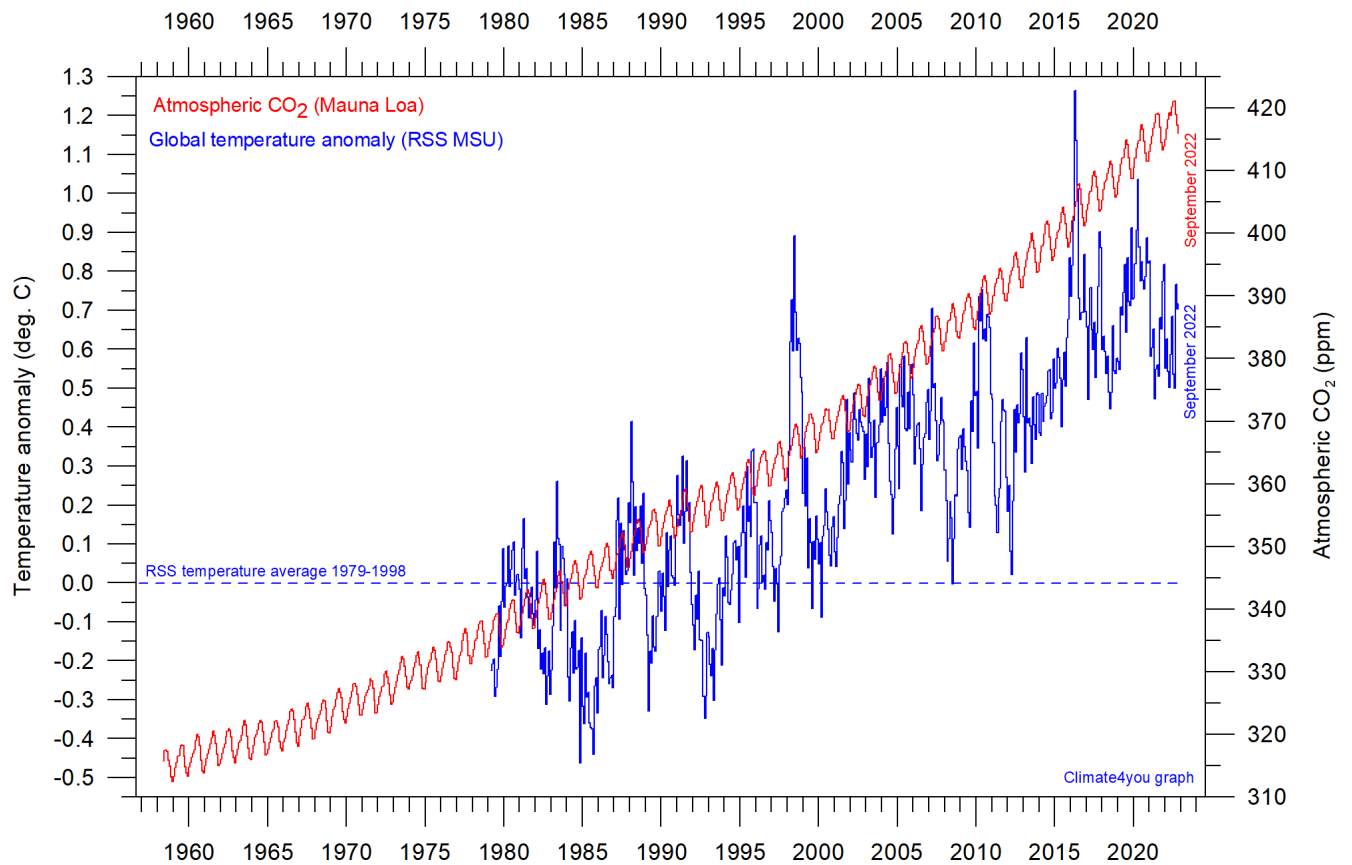
**Reference:** Humlum, O., Stordahl, K. and Solheim, J-E. 2012. The phase relation between atmospheric carbon dioxide and global temperature. *Global and Planetary Change*, August 30, 2012.

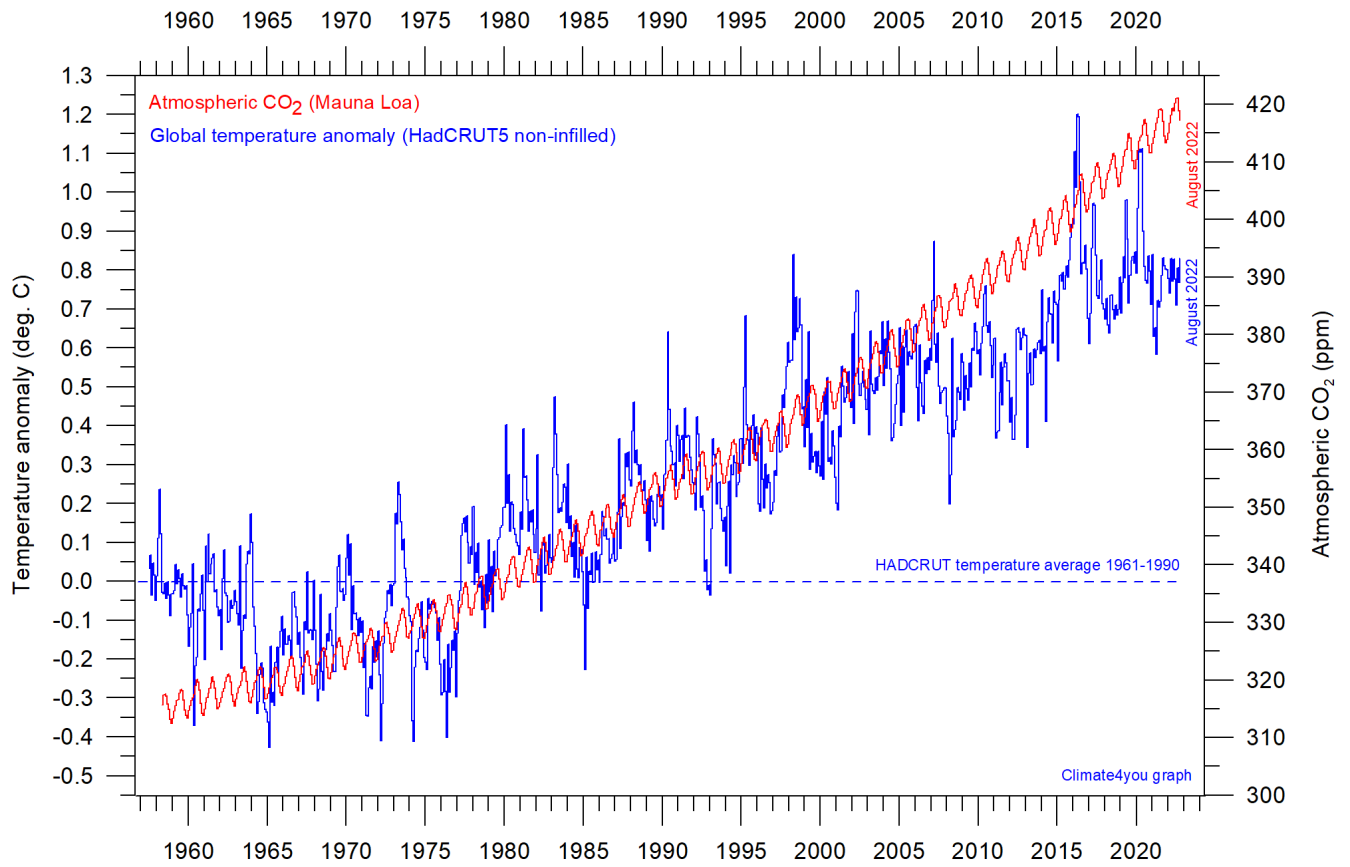
<http://www.sciencedirect.com/science/article/pii/S0921818112001658?v=s5>

## Global air temperature and atmospheric CO<sub>2</sub>, updated to September 2022

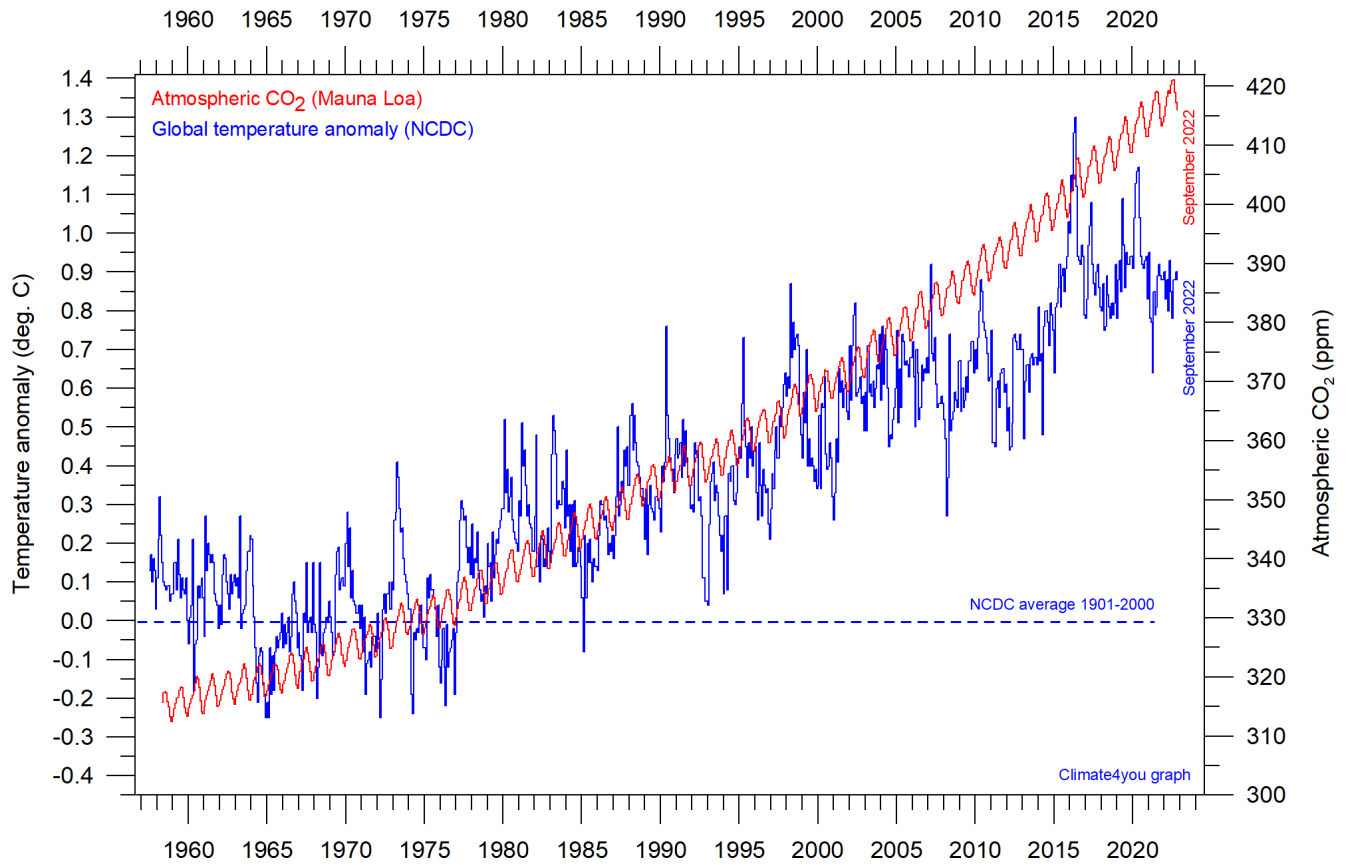


47

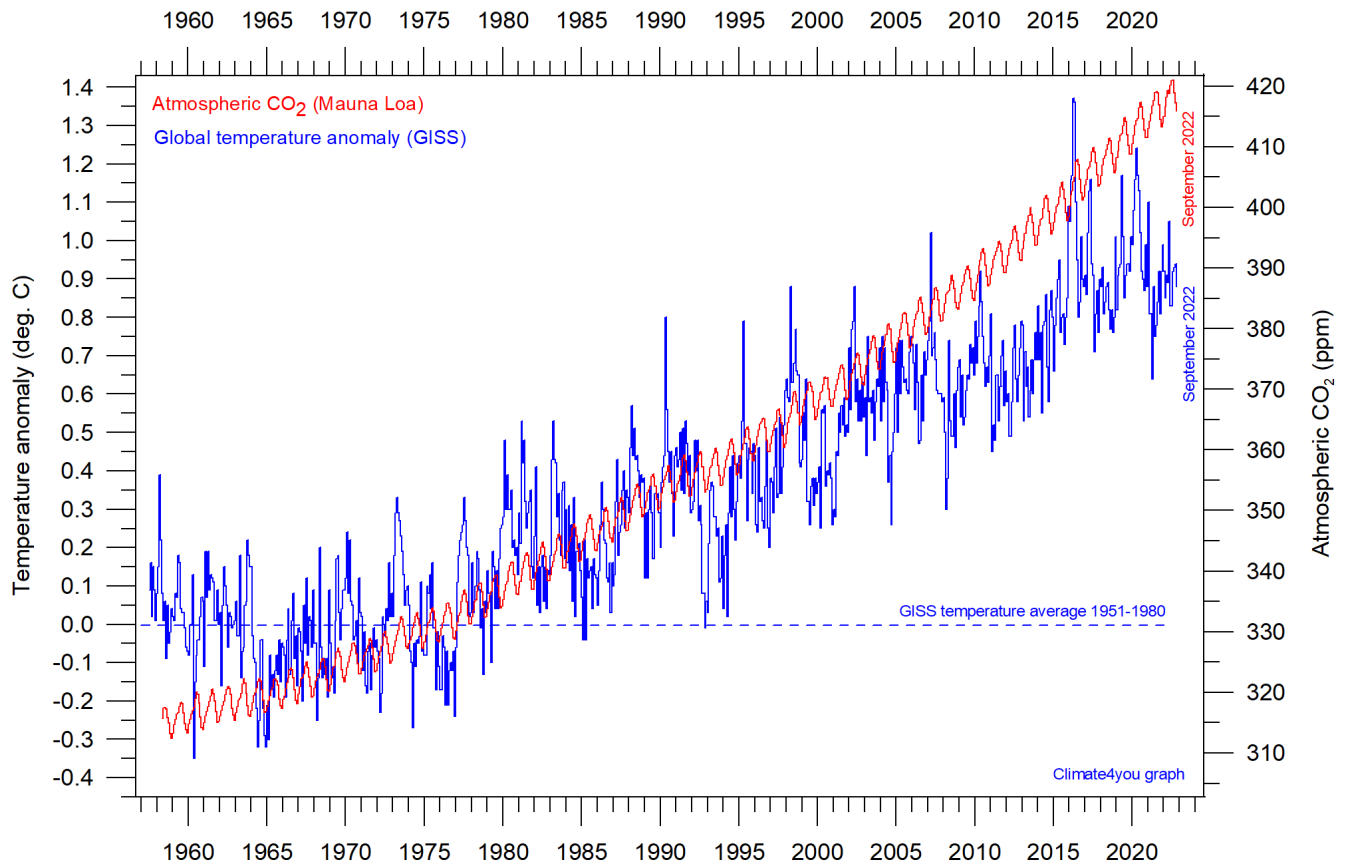




48







Diagrams showing UAH, RSS, HadCRUT5, NCDC and GISS monthly global air temperature estimates (blue) and the monthly atmospheric CO<sub>2</sub> content (red) according to the [Mauna Loa Observatory](#), Hawaii. The Mauna Loa data series begins in March 1958, and 1958 was therefore chosen as starting year for all diagrams above. Reconstructions of past atmospheric CO<sub>2</sub> concentrations (before 1958) are not incorporated in this diagram, as such past CO<sub>2</sub> values are derived by other means (ice cores, stomata, or older measurements using different methodology), and therefore are not directly comparable with direct atmospheric measurements.

Most climate models are programmed to give the greenhouse gas carbon dioxide CO<sub>2</sub> significant influence on the calculated global air temperature. It is therefore relevant to compare different air temperature records with measurements of atmospheric CO<sub>2</sub>, as shown in the diagrams above.

Any comparison, however, should not be made on a monthly or annual basis, but for a longer time, as other effects (oceanographic, cloud cover, etc.) may override the potential influence of CO<sub>2</sub> on short time scales such as just a few years.

It is of cause equally inappropriate to present new meteorological record values, whether daily, monthly, or annual, as demonstrating the legitimacy of the hypothesis ascribing high importance of atmospheric CO<sub>2</sub> for global air temperatures. Any such meteorological record value

may well be the result of other phenomena. Unfortunately, many media repeatedly fall into this trap.

What exactly defines the critical length of a relevant period length to consider for evaluating the alleged importance of CO<sub>2</sub> remains elusive and still represents a theme for discussions.

Nonetheless, the length of the critical period must be inversely proportional to the temperature sensitivity of CO<sub>2</sub>, including feedback effects. Thus, if the net temperature effect of atmospheric CO<sub>2</sub> is strong, the critical period will be short, and vice versa.

However, past climate research history provides some clues as to what has traditionally been considered the relevant length of period over which to compare temperature and atmospheric CO<sub>2</sub>.

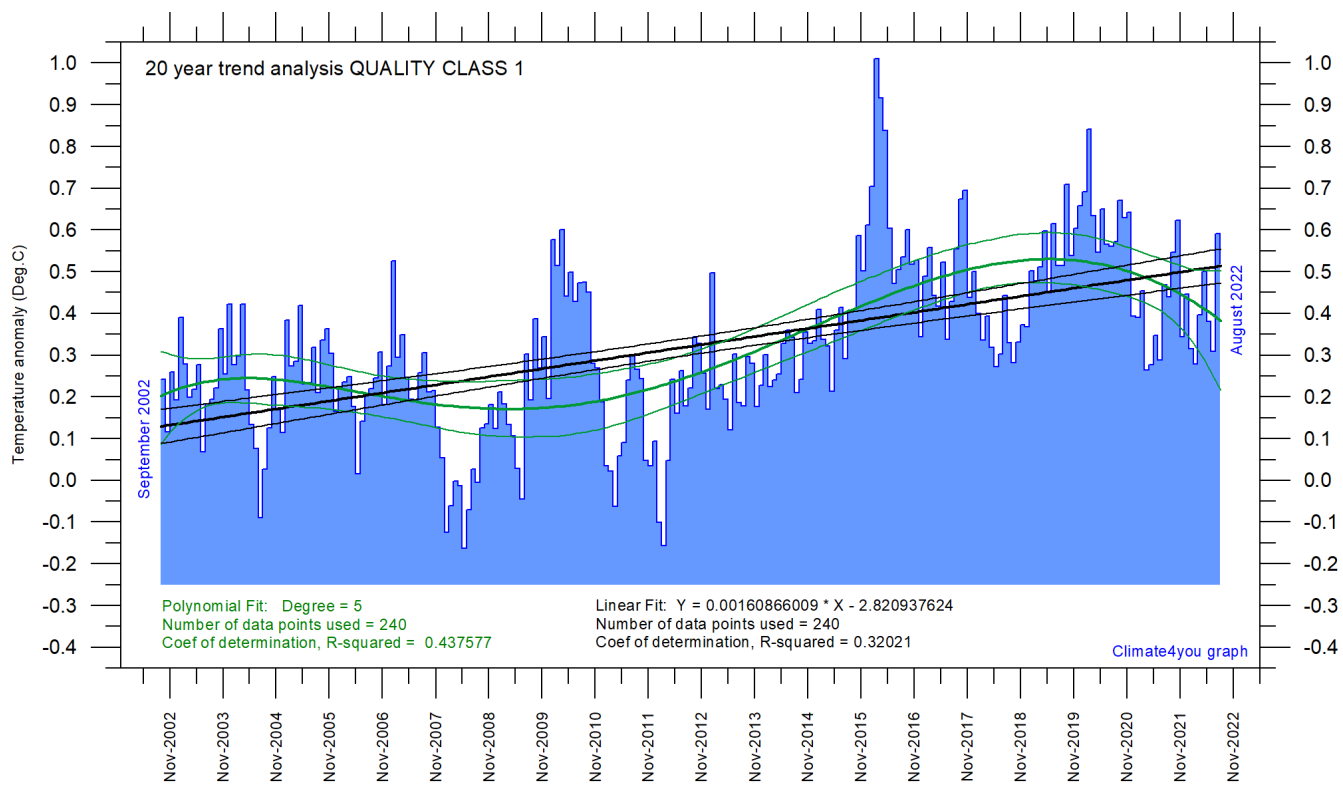
After about 10 years of concurrent global temperature- and CO<sub>2</sub>-increase, IPCC was established in 1988. For obtaining public and political support for the CO<sub>2</sub>-hypothesis the 10-year warming period leading up to 1988 most likely was considered important. Had the global temperature instead been decreasing at that time, political support for the hypothesis probably would have been difficult to obtain in 1988.

Based on the previous 10 years of concurrent temperature- and CO<sub>2</sub>-increase, many climate

scientists in 1988 presumably felt that their understanding of climate dynamics was enough to conclude about the importance of CO<sub>2</sub> for affecting observed global temperatures.

Thus, it may with confidence be concluded that 10 years in 1988 was considered a period long enough to demonstrate the effect of increasing atmospheric CO<sub>2</sub> on global temperatures. The 10-year period is also basis for the temperature anomaly diagrams shown on page 4.

## Latest 20-year QC1 global monthly air temperature changes, updated to August 2022



51

Last 20 years' global monthly average air temperature according to Quality Class 1 (UAH and RSS; see p.6 and 9) global monthly temperature estimates. The thin blue line represents the monthly values. The thick black line is the linear fit, with 95% confidence intervals indicated by the two thin black lines. The thick green line represents a 5-degree polynomial fit, with 95% confidence intervals indicated by the two thin green lines. A few key statistics are given in the lower part of the diagram (please note that the linear trend is the monthly trend).

In the enduring scientific climate debate, the following question is often put forward: Is the surface air temperature still increasing or has it basically remained without significant changes during the last 15-16 years?

The diagram above may be useful in this context and demonstrates the differences between two often used statistical approaches to determine recent temperature trends. Please also note that such fits only attempt to describe the past, and usually have small, if any, predictive power.

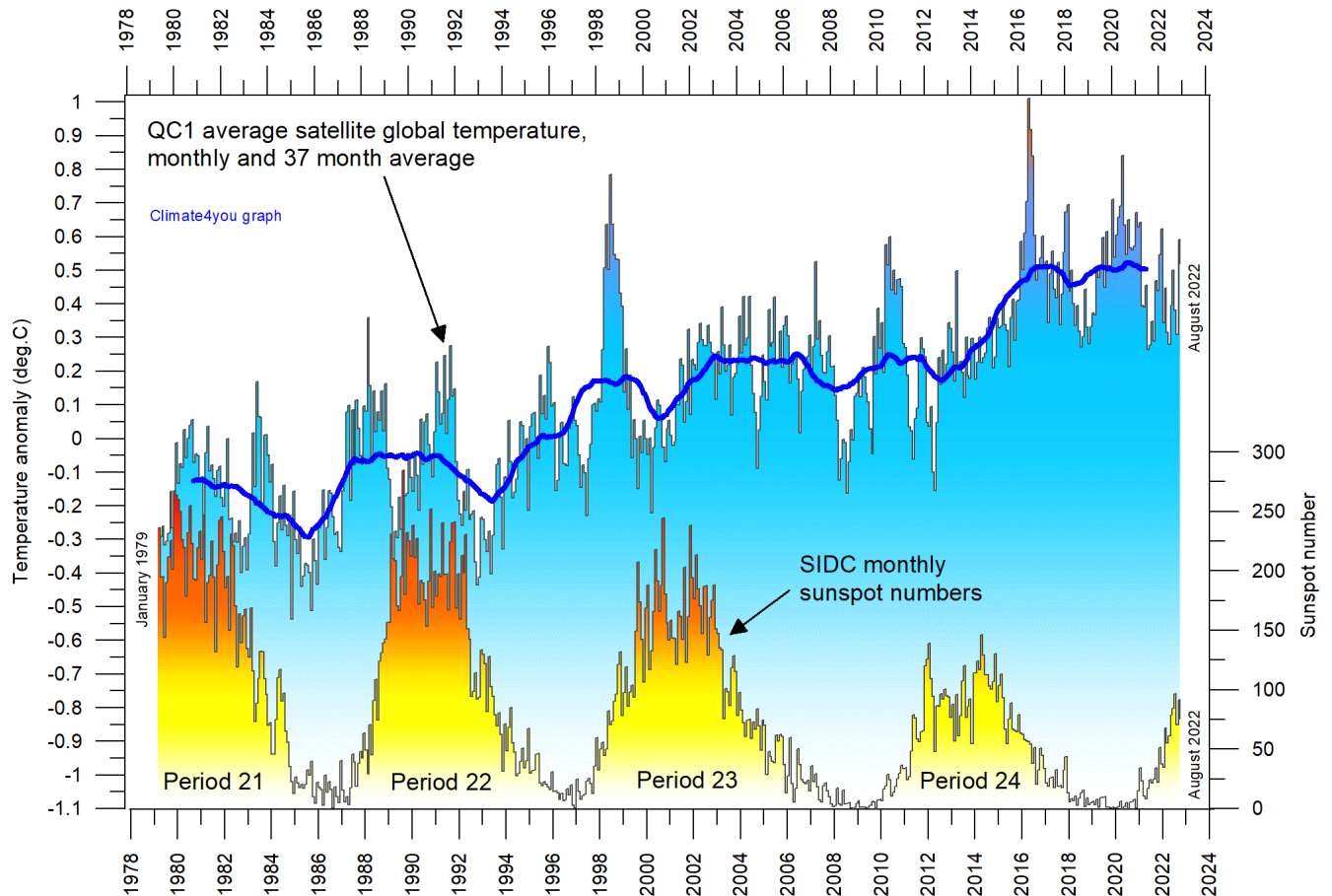
In addition, before using any linear trend (or other) analysis of time series a proper statistical model should be chosen, based on statistical justification.

For global temperature time series, there is no *a priori* physical reason why the long-term trend should be linear in time. In fact, climatic time series often have trends for which a straight line is not a good approximation, as is clearly demonstrated by several of the diagrams shown in the present report.

For an commendable description of problems often encountered by analyses of temperature time series analyses, please see [Keenan, D.J. 2014: Statistical Analyses of Surface Temperatures in the IPCC Fifth Assessment Report.](#)

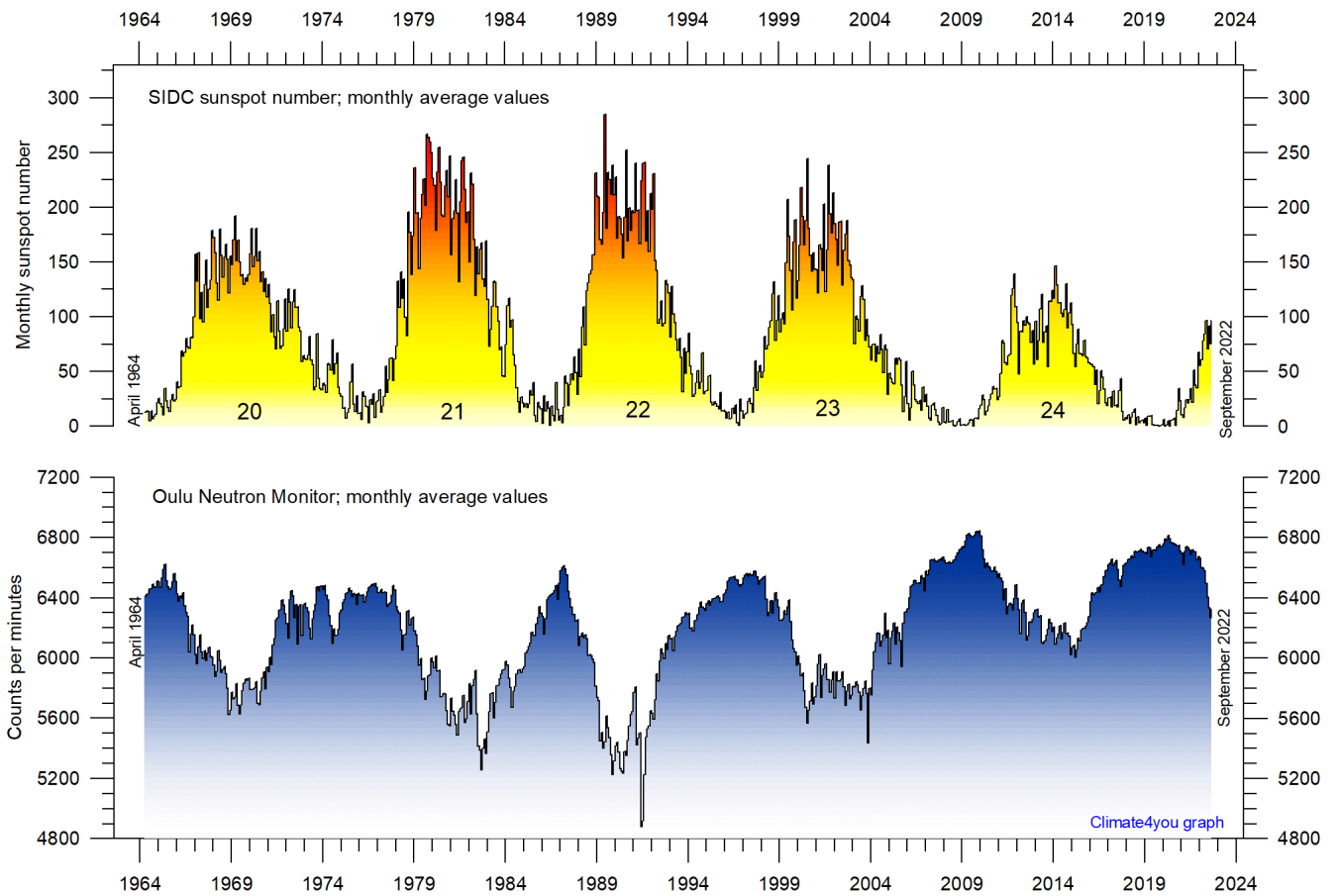
See also diagrams on page 12.

**Sunspot activity (SIDC) and QC1 average satellite global air temperature, updated to August 2022**



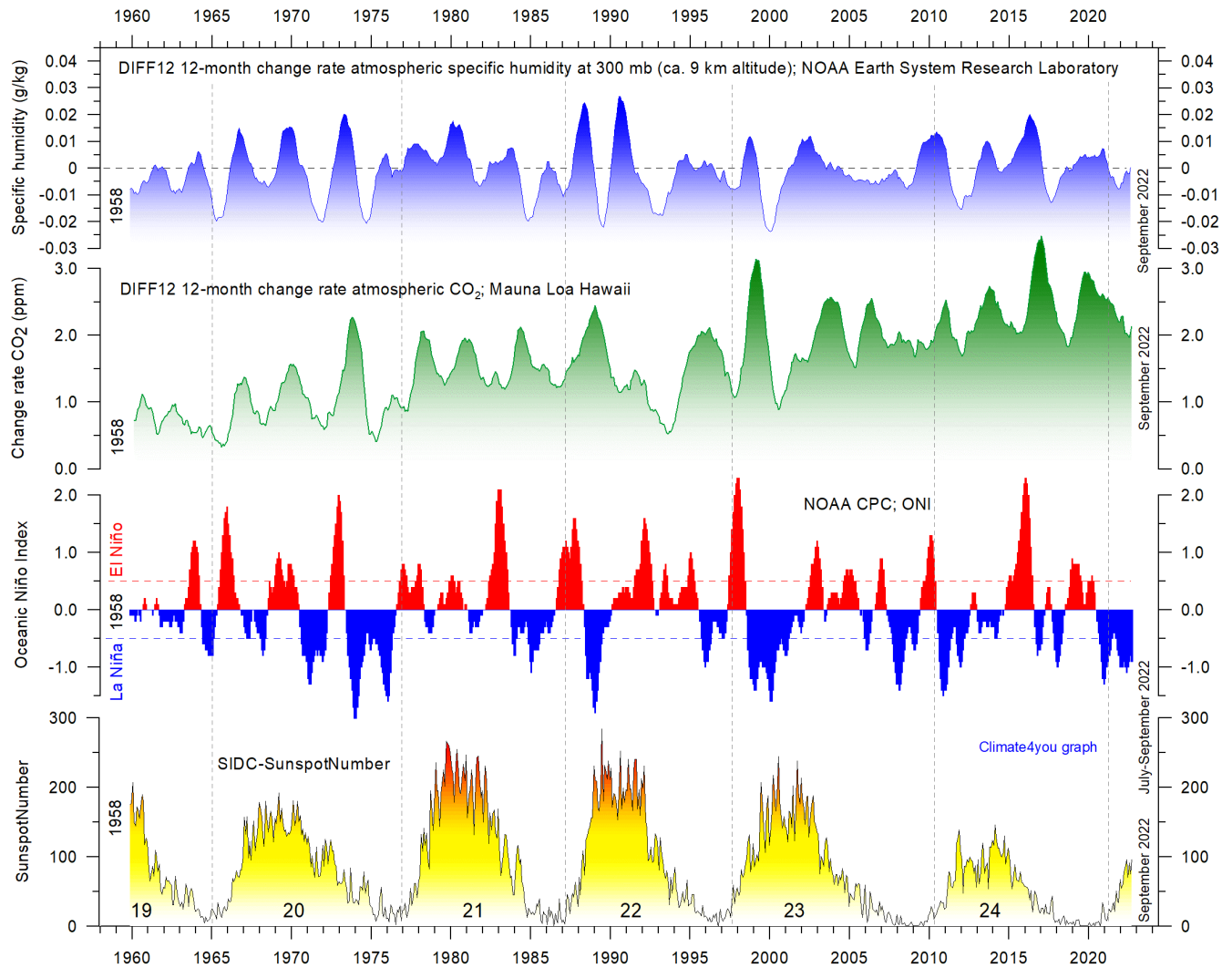
*Variation of global monthly air temperature according to Quality Class 1 (UAH and RSS; see p.4) and observed sunspot number as provided by the Solar Influences Data Analysis Center (SIDC), since 1979. The thin lines represent the monthly values, while the thick line is the simple running 37-month average, nearly corresponding to a running 3-year average. The asymmetrical temperature 'bump' around 1998 is influenced by the oceanographic El Niño phenomenon in 1998, as is the case also for 2015-16. Temperatures in year 2019-20 was influenced by a moderate El Niño.*

## Monthly sunspot activity (SIDC) and average neutron counts (Oulu, Finland), updated to September 2022



Observed monthly sunspot number (Solar Influences Data Analysis Center (SIDC) since April 1964, and (lower panel) monthly average counts of the Oulu (Finland) neutron monitor, adjusted for barometric pressure and efficiency.

**Monthly sunspot activity (SIDC), Oceanic Niño Index (ONI), and change rates of atmospheric CO<sub>2</sub> and specific humidity, updated to September 2022**

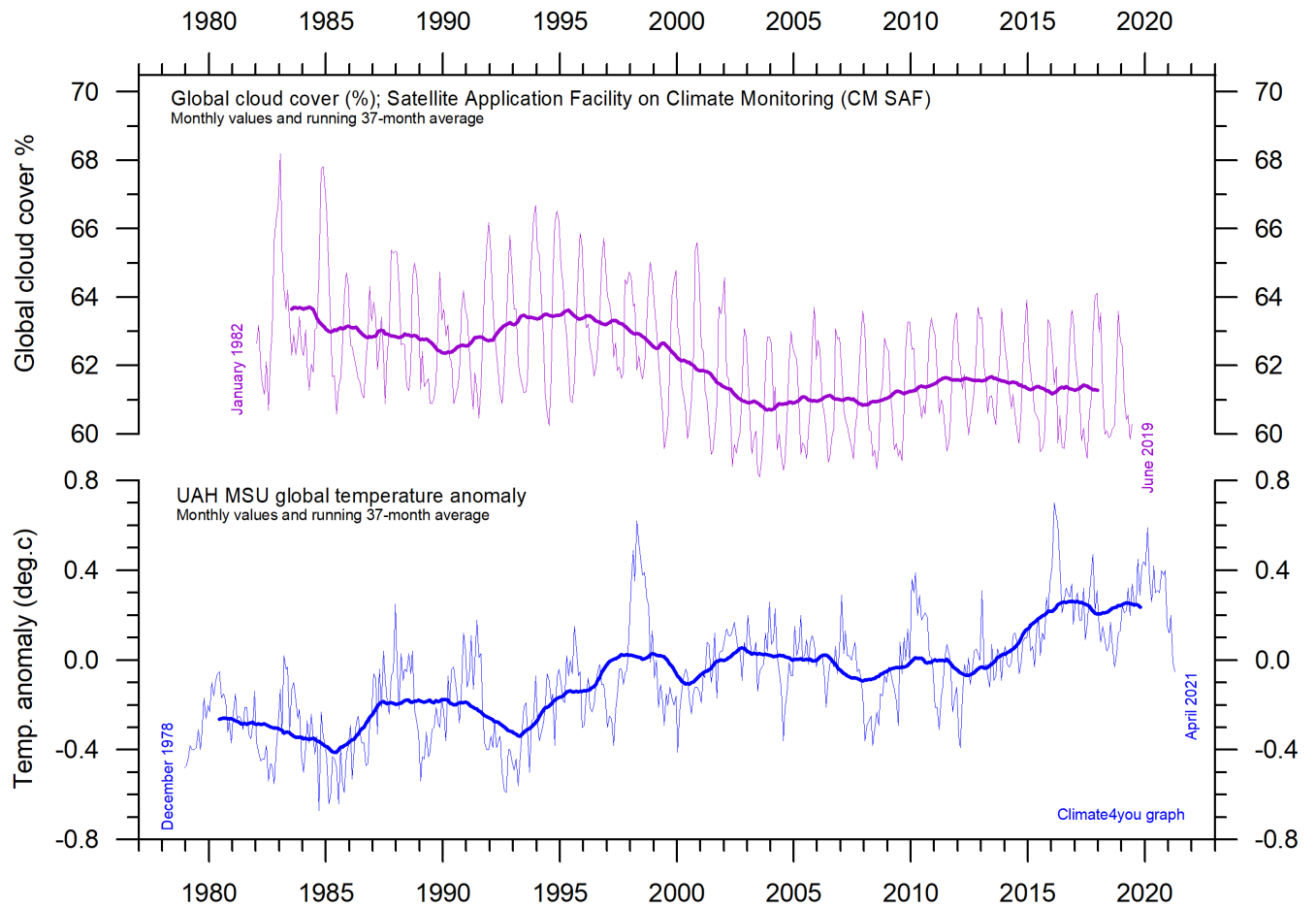


54

Visual association since 1958 between (from bottom to top) Sunspot Number, Oceanic Niño Index (ONI) and annual change rate of atmospheric CO<sub>2</sub> and specific humidity at 300 mb (ca. 9 km altitude). Upper two panels: Annual (12 month) change rate of atmospheric CO<sub>2</sub> and specific humidity at 300 mb since 1959, calculated as the average amount of atmospheric CO<sub>2</sub>/humidity during the last 12 months, minus the average for the preceding 12 months (see also diagrams on page 43+44). Niño index panel: Warm (>+0.5°C) and cold (<-0.5°C) episodes for the Oceanic Niño Index (ONI), defined as 3 month running mean of ERSSTv4 SST anomalies in the Niño 3.4 region (5°N-5°S, 120°-170°W)]. For historical purposes cold and warm episodes are defined when the threshold is met for a minimum of 5 consecutive over-lapping seasons. Anomalies are centred on 30-yr base periods updated every 5 years. Thin vertical stippled lines indicate the visually estimated timing of sunspot minima. The typically sequence following a sunspot minimum appears to be a warm El Niño episode followed by a cold La Niña episode. Effects on change rates of atmospheric CO<sub>2</sub> and atmospheric specific humidity are visually apparent, with ONI variations being followed by changes in first humidity, and then (last) by CO<sub>2</sub>.

The above diagram is inspired by the Leamon et al. 2021 publication: Robert J. Leamon, Scott W. McIntosh, Daniel R. Marsh. Termination of Solar Cycles and Correlated Tropospheric Variability. Earth and Space Science, 2021; 8 (4) DOI: [10.1029/2020EA001223](https://doi.org/10.1029/2020EA001223)

**Monthly lower troposphere temperature (UAH) and global cloud cover, updated to April 2021**



55

*Lower tropospheric air temperature and global cloud cover. Upper panel: Global cloud cover according to Satellite Application Facility on Climate Monitoring. Lower panel: Global monthly average lower troposphere temperature (thin line) since 1979 according to [University of Alabama](https://climate4you.com/) at Huntsville, USA. The thick lines represent the simple running 37-month average. Reference period for UAH is 1991-2020.*

Cloud cover data citation: Karlsson, Karl-Göran; Anttila, Kati; Trentmann, Jörg; Stengel, Martin; Solodovnik, Irina; Meirink, Jan Fokke; Devasthale, Abhay; Kothe, Steffen; Jääskeläinen, Emmihenna; Sedlar, Joseph; Benas, Nikos; van Zadelhoff, Gerd-Jan; Stein, Diana; Finkensieper, Stephan; Håkansson, Nina; Hollmann, Rainer; Kaiser, Johannes; Werscheck, Martin (2020): CLARA-A2.1: CM SAF cCloud, Albedo and surface RAdiation dataset from AVHRR data - Edition 2.1, Satellite Application Facility on Climate Monitoring, DOI:10.5676/EUM\_SAF\_CM/CLARA\_AVHRR/V002\_01, [https://doi.org/10.5676/EUM\\_SAF\\_CM/CLARA\\_AVHRR/V002\\_01](https://doi.org/10.5676/EUM_SAF_CM/CLARA_AVHRR/V002_01).

## Climate and history; one example among many

### Year 101-106 AD: Bridge constructed across the River Danube at the Iron Gate



56

Map showing the location of the [Iron Gate](#) (black arrow) in south-east Europe.

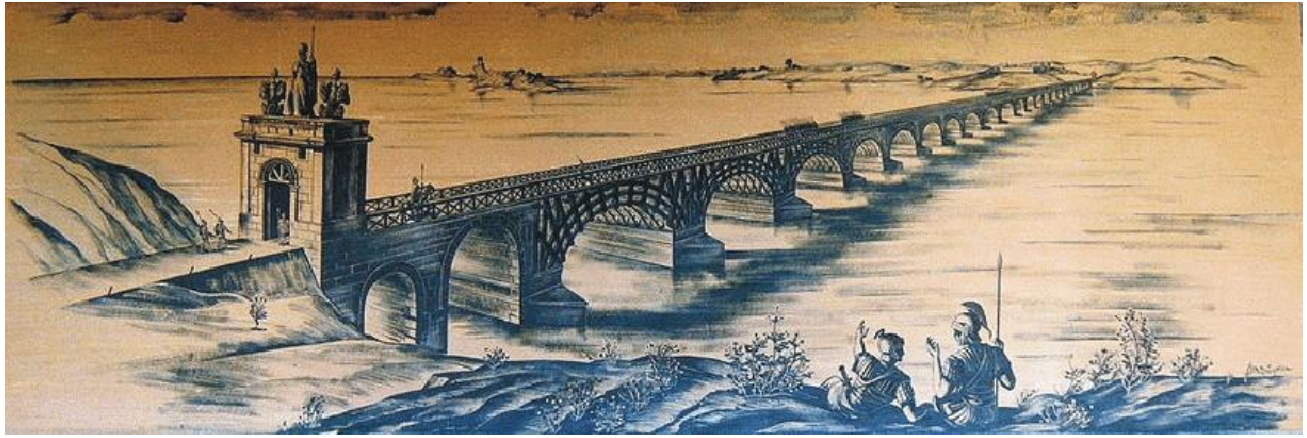
An indication of the benign climate of Roman times with a rather long immunity from cold winters in Europe may be seen in the building between AD 101 and 106 of a bridge with many stone piers across the [River Danube](#) at the [Iron Gate](#) in south-east Europe, between [Serbia](#) and the Transylvanian highlands in [Romania](#) (cf. Lamb 1995).

The bridge was designed by [Appolodorus of Damascus](#) for the [Emperor Trajan](#) for efficient passage of the Roman armies and administration across the Danube, preceding Trajan's subsequent

conquest of [Dacia](#), a large region broadly corresponding to modern [Romania](#) and [Moldova](#).

Trajan's bridge apparently stood for no less than about 170 years Lamb (1977, 1995). This must be considered an amazing fact, as in any recent century such a construction would rapidly have been carried away by river ice during a cold winter. In the end the bridge is said to have been destroyed by the Dacian tribes when the Romans later withdrew from this part of Europe (Lamb 1977, 1995).





Artistic reconstruction of [Trajan's bridge](#) across the river Danube (source: [Wikimedia Commons](#)).

[Trajan's bridge](#) was 1,135 m in length (the Danube is about 800 m wide at the place of crossing), 15 m in width, and 19 m in height above the average water level. At each end of the bridge was a Roman [castrum](#), each built around an entrance to the bridge. In other words, to cross the bridge, you had first to pass through a Roman military camp.

more than 1000 years Trajan's bridge was the longest arch bridge ever constructed, in both total and span length, and it apparently survived for no less than about 170 years (Lamb 1977, 1995), before being demolished by the Dacian people. Although representing an impressive engineering feat, relative mild winters with little river ice presumably contributed to the long survival time of the bridge.

57

For the bridge's construction [Appolodorus of Damascus](#) used wooden arches set on twenty masonry pillars (made of bricks, mortar and [pozzolana cement](#)) that spanned 38 m each. The entire bridge was built quickly within two years only (between 103 and 105 AD), employing the construction of a wooden caisson for each pier. For

A relief on [Trajan's Column](#) shows the Roman bridge across the river Danube (see figure below). Noteworthy on this illustration are the unusually flat segmental arches on high-rising concrete piers; in the foreground of the relief Emperor Trajan sacrificing by the Danube can be seen.



The River Danube and the Kazan gorge at its narrowest point (left), and relief showing the Roman bridge across Danube on [Trajan's Column](#) in Rome (right). Source: [Wikimedia Commons](#).

The Iron Gate gorge(s) lies between Romania in the north and Serbia in the south. At this point, the river separates the southern [Carpathian Mountains](#) from the northwestern foothills of the Balkan Mountains. The Romanian, Hungarian, Slovakian, Turkish, German and Bulgarian names literally mean "Iron Gates" and are used to name the entire range of gorges. The Romanian side of the gorge now constitutes [the Iron Gates natural park](#), whereas the Serbian part constitutes the Đerdap national park.

The Great Kazan (kazan meaning "boiler") is the most famous and the narrowest gorge of the Iron Gate route (photo above): the river here narrows to 150 m and reaches a depth of up to 53 m (174 ft).

Shortly downstream is the site where the Roman Emperor Trajan had the legendary military bridge erected between 103 and 105 AD, preceding his conquest of Dacia. On the right (Serbian) bank of the river a Roman memorial plaque (*Tabula Trajana*) commemorates Emperor Trajan's military road into Dacia. The Tabula was originally located 50 meters lower than now. The original site was flooded with the construction of a major hydroelectric dam in late 1960s and the monument was moved to a new position just above the waterline. On the opposite Romanian bank, at the Small Kazan, a statue of Trajan's Dacian opponent [Decebalus](#) was carved in rock from 1994 through 2004 (see photos below).



Rock carving showing [Decebalus](#) on the Romanian side of the Iron Gate (left), and a plate commemorating the roman [Emperor Trajan](#) on the Serbian bank (right). Source: [Wikimedia Commons](#).

The twenty pillars carrying Trajan's bridge were still visible in 1856, when the level of the Danube hit a record low. In 1906, the [International Commission of the Danube](#) however decided to destroy two of the pillars, to ensure safe navigation on the river. In 1932, there were 16 remaining pillars underwater, but in 1982 archaeologists only manage to find 12 of these. Presumably the missing four had been swept away by river ice following the relative cold period

1960-1980 in Europe. Today, only the entrance pillars are visible on either bank of the Danube.

In 1979, Trajan's Bridge was added to the [Monument of Culture of Exceptional Importance](#), and in 1983 it was added to the [Archaeological Sites of Exceptional Importance list](#), and by that it is protected by Republic of Serbia.

Sources and References:

Lamb, H.H. 1977. Climate, present, past and future. Volume 2. Climatic history and the future. Methuen & Co Ltd., London, 835 pp.

Lamb, H.H. 1995. Climate, History and the Modern World. Routledge, London, 2nd edition, 433 pp.

\*\*\*\*\*

All diagrams in this report, along with any supplementary information, including links to data sources and previous issues of this newsletter, are freely available for download on [www.climate4you.com](http://www.climate4you.com)

Yours sincerely,

Ole Humlum (Ole.Humlum@gmail.com)

Arctic Historical Evaluation and Research Organisation, Longyearbyen, Svalbard

21 October 2022.

Planned publication of next newsletter: around 26 November 2022.

In the past, the present newsletter usually was published around the 20<sup>th</sup> each month. However, as the reporting of monthly air temperatures from various databases today often is delayed somewhat compared to previously, also the planned publication of the present newsletter will be equally later.

Everybody interested in climate science should gratefully acknowledge the efforts put into maintaining the different temperature databases referred to in the present newsletter, no matter how rapid their updated results are published.